U.S.NRC
United States Nuclear Regulatory Commission
Protecting People and the Environment

NUREG-2163

Technical Basis for Regulatory Guidance on the Alternate Pressurized Thermal Shock Rule

Draft Report for Comment

Office of Nuclear Regulatory Research

AVAILABILITY OF REFERENCE MATERIALS IN NRC PUBLICATIONS

NRC Reference Material

As of November 1999, you may electronically access NUREG-series publications and other NRC records at NRC's Public Electronic Reading Room at http://www.nrc.gov/reading-rm.html. Publicly released records include, to name a few, NUREG-series publications; *Federal Register* notices; applicant, licensee, and vendor documents and correspondence; NRC correspondence and internal memoranda; bulletins and information notices; inspection and investigative reports; licensee event reports; and Commission papers and their attachments.

NRC publications in the NUREG series, NRC regulations, and Title 10, "Energy," in the *Code of Federal Regulations* may also be purchased from one of these two sources.

1. The Superintendent of Documents
   U.S. Government Printing Office
   Mail Stop SSOP
   Washington, DC 20402–0001
   Internet: bookstore.gpo.gov
   Telephone: 202-512-1800
   Fax: 202-512-2250
2. The National Technical Information Service
   Springfield, VA 22161–0002
   www.ntis.gov
   1–800–553–6847 or, locally, 703–605–6000

A single copy of each NRC draft report for comment is available free, to the extent of supply, upon written request as follows:
Address: U.S. Nuclear Regulatory Commission
Office of Administration
Publications Branch
Washington, DC 20555-0001
E-mail: DISTRIBUTION.RESOURCE@NRC.GOV
Facsimile: 301–415–2289

Some publications in the NUREG series that are posted at NRC's Web site address http://www.nrc.gov/reading-rm/doc-collections/nuregs are updated periodically and may differ from the last printed version. Although references to material found on a Web site bear the date the material was accessed, the material available on the date cited may subsequently be removed from the site.

Non-NRC Reference Material

Documents available from public and special technical libraries include all open literature items, such as books, journal articles, transactions, *Federal Register* notices, Federal and State legislation, and congressional reports. Such documents as theses, dissertations, foreign reports and translations, and non-NRC conference proceedings may be purchased from their sponsoring organization.

Copies of industry codes and standards used in a substantive manner in the NRC regulatory process are maintained at—
The NRC Technical Library
Two White Flint North
11545 Rockville Pike
Rockville, MD 20852–2738

These standards are available in the library for reference use by the public. Codes and standards are usually copyrighted and may be purchased from the originating organization or, if they are American National Standards, from—
American National Standards Institute
11 West 42nd Street
New York, NY 10036–8002
www.ansi.org
212–642–4900

Legally binding regulatory requirements are stated only in laws; NRC regulations; licenses, including technical specifications; or orders, not in NUREG-series publications. The views expressed in contractor-prepared publications in this series are not necessarily those of the NRC.

The NUREG series comprises (1) technical and administrative reports and books prepared by the staff (NUREG–XXXX) or agency contractors (NUREG/CR–XXXX), (2) proceedings of conferences (NUREG/CP–XXXX), (3) reports resulting from international agreements (NUREG/IA–XXXX), (4) brochures (NUREG/BR–XXXX), and (5) compilations of legal decisions and orders of the Commission and Atomic and Safety Licensing Boards and of Directors' decisions under Section 2.206 of NRC's regulations (NUREG–0750).

NUREG-2163

Technical Basis for Regulatory Guidance on the Alternate Pressurized Thermal Shock Rule

Draft Report for Comment

Manuscript Completed: November 2014
Date Published: February 2015

Prepared by:
Gary L. Stevens, Mark T. Kirk, and Mohammad Modarres*

*University of Maryland

Gary L. Stevens, NRC Project Manager

Office of Nuclear Regulatory Research

COMMENTS ON DRAFT REPORT

Any interested party may submit comments on this report for consideration by the NRC staff. Comments may be accompanied by additional relevant information or supporting data. Please specify the report number **NUREG-2163** in your comments, and send them by the end of the comment period specified in the *Federal Register* notice announcing the availability of this report.

Addresses: You may submit comments by any one of the following methods. Please include Docket ID **NRC-2014-0137** in the subject line of your comments. Comments submitted in writing or in electronic form will be posted on the NRC website and on the Federal rulemaking website http://www.regulations.gov.

Federal Rulemaking Website: Go to http://www.regulations.gov and search for documents filed under Docket ID **NRC-2014-0137**. Address questions about NRC dockets to Carol Gallagher at 301-415-3463 or by e-mail at Carol.Gallagher@nrc.gov.

Mail comments to: Cindy Bladey, Chief, Rules, Announcements, and Directives Branch (RADB), Division of Administrative Services, Office of Administration, Mail Stop: OWFN-12-H08, U.S. Nuclear Regulatory Commission, Washington, DC 20555-0001.

For any questions about the material in this report, please contact: Gary Stevens, Senior Materials Engineer, 301-415-3608, or by e-mail at Gary.Stevens@nrc.gov; or Mark Kirk, Senior Materials Engineer, 301-251-7631 or by e-mail at Mark.Kirk@nrc.gov.

Please be aware that any comments that you submit to the NRC will be considered a public record and entered into the Agencywide Documents Access and Management System (ADAMS). Do not provide information you would not want to be publicly available.

ABSTRACT

During plant operation, the walls of reactor pressure vessels (RPVs) are exposed to neutron radiation, resulting in embrittlement of the vessel steel and weld materials in the area of the RPV adjacent to the core. If an embrittled RPV had a flaw of critical size and certain severe system transients were to occur, the flaw could rapidly propagate through the vessel, resulting in a through-wall crack and, thereby, challenging the integrity of the RPV. The severe transients of concern, known as pressurized thermal shock (PTS), are characterized by a rapid cooling of the internal RPV surface in combination with repressurization of the RPV. Advancements in understanding and knowledge of materials behavior, the ability to realistically model plant systems and operational characteristics, and the ability to better evaluate PTS transients to estimate loads on vessel walls led the U.S. Nuclear Regulatory Commission (NRC) to develop a risk-informed revision of the existing PTS Rule that was published in Section 50.61a, "Alternate Fracture Toughness Requirements for Protection against Pressurized Thermal Shock Events," of Title 10, "Energy," of the *Code of Federal Regulations* (10 CFR 50.61a).

This report explains the basis for the requirements that establish the entry conditions to permit use of 10 CFR 50.61a and describes methods by which the following four requirements can be met: (1) criteria relating to the date of construction and design requirements, (2) criteria relating to evaluation of plant-specific surveillance data, (3) criteria relating to inservice inspection (ISI) data and non-destructive examination (NDE) requirements, and (4) criteria relating to alternate limits on embrittlement.

FOREWORD

The reactor pressure vessel (RPV) is exposed to neutron radiation during normal operation. Over time, the RPV steel becomes progressively more brittle in the region adjacent to the core. If a vessel had a preexisting flaw of critical size and certain severe system transients occurred, this flaw could propagate rapidly through the vessel, resulting in a through-wall crack. The severe transients of concern, known as pressurized thermal shock (PTS), are characterized by rapid cooling (i.e., thermal shock) of the internal RPV surface that may be combined with repressurization. The simultaneous occurrence of critical-size flaws, embrittled steel, and a severe PTS transient is a low-probability event. U.S. pressurized-water reactors (PWRs) are not projected to approach the levels of embrittlement to make them susceptible to PTS failure, even during extended operation beyond the original 40-year design life.

Advancements in understanding and knowledge of materials behavior, the ability to realistically model plant systems and operational characteristics, and the ability to better evaluate PTS transients to estimate loads on vessel walls led to the development of a risk-informed revision of the existing PTS Rule that was published in Section 50.61a, “Alternate Fracture Toughness Requirements for Protection against Pressurized Thermal Shock Events,” of Title 10, “Energy,” of the *Code of Federal Regulations* (10 CFR 50.61a).

The “Alternate PTS Rule” contained in 10 CFR 50.61a provides revised PTS screening criteria in the form of an embrittlement reference temperature, RT_{MAX-X}, which characterizes the RPV material’s resistance to fracture from initiated flaws. The Alternate PTS Rule is based on more comprehensive analysis methods than the existing PTS Rule contained in 10 CFR 50.61, “Fracture Toughness Requirements for Protection against Pressurized Thermal Shock Events.” This alternate rule became desirable because the existing requirements contained in 10 CFR 50.61 are based on unnecessarily conservative assumptions. The Alternate PTS Rule reduces regulatory burden for those PWR licensees who expect to exceed the 10 CFR 50.61 embrittlement requirements before the expiration of their operating licenses, while still maintaining adequate safety margins. PWR licensees may choose to comply with the Alternate PTS Rule as a voluntary alternative to complying with the requirements contained in 10 CFR 50.61.

This document explains the basis for the requirements that establish the entry conditions to permit use of the Alternate PTS Rule. It also describes methods by which the following four requirements can be met:

1. Criteria relating to the date of construction and design requirements;
2. Criteria relating to evaluation of plant-specific surveillance data;
3. Criteria relating to inservice inspection (ISI) data and non-destructive examination (NDE) requirements; and
4. Criteria relating to alternate limits on embrittlement.

Brian W. Sheron, Director
Office of Nuclear Regulatory Research
U.S. Nuclear Regulatory Commission

TABLE OF CONTENTS

LIST OF FIGURES

LIST OF TABLES

EXECUTIVE SUMMARY

In early 2010, the U.S. Nuclear Regulatory Commission (NRC) promulgated the Alternate Pressurized Thermal Shock (PTS) Rule as 10 CFR 50.61a, "Alternate Fracture Toughness Requirements for Protection against Pressurized Thermal Shock Events," which amended existing regulations to provide alternate embrittlement requirements for protection against PTS events for pressurized-water reactor (PWR) pressure vessels. These requirements are based on more comprehensive, accurate, and realistic analysis methods than those used to establish the limits in 10 CFR 50.61, "Fracture Toughness Requirements for Protection against Pressurized Thermal Shock Events." This alternate rule became desirable because the existing requirements, as contained in 10 CFR 50.61, are based on unnecessarily conservative assumptions. The Alternate PTS Rule reduces regulatory burden for those PWR licensees who expect to exceed the 10 CFR 50.61 embrittlement requirements before the expiration of their operating licenses while still maintaining adequate safety margins. PWR licensees may choose to comply with the Alternate PTS Rule as a voluntary alternative to complying with the requirements contained in 10 CFR 50.61.

The Alternate PTS Rule provides revised PTS screening criteria in the form of embrittlement reference temperatures, RT_{MAX-X}, that characterize the RPV material's resistance to fracture initiating from flaws. The RT_{MAX-X} embrittlement limits may be used by licensees provided that the following criteria are met:

1. **<u>Criteria relating to the date of construction and design requirements</u>**: The Alternate PTS Rule is applicable to licensees whose construction permits were issued before February 3, 2010, and whose RPVs were designed and fabricated to the 1998 Edition (or an earlier edition) of the ASME (formerly the American Society of Mechanical Engineers) Boiler and Pressure Vessel Code ("Code"). The reason for this applicability restriction is because the structural and thermal hydraulic analyses that established the basis for the Alternate PTS Rule embrittlement limits only represented plants constructed before this date. It is the responsibility of a licensee to demonstrate that the risk-significant factors controlling PTS for any plant constructed after February 3, 2010, are adequately addressed by the technical-basis calculations developed in support of the Alternate PTS Rule. Chapter 4 of this document describes methods by which licensees can satisfy these criteria and identifies factors to be considered in such an evaluation.
2. **<u>Criteria relating to evaluation of plant-specific surveillance data</u>**: The Alternate PTS Rule includes statistical tests that must be performed on RPV surveillance data to determine whether the surveillance data are sufficiently close to the predictions of an embrittlement trend curve (ETC) that the predictions of the ETC are valid for use. From a regulatory perspective, it is of particular interest to determine whether plant-specific surveillance data deviate significantly from the predictions of the ETC in a manner that suggests that the ETC is likely to underpredict plant-specific data trends. Chapter 5 of this document describes guidance by which licensees can assess the closeness of plant-specific data to the ETC using statistical tests, including:
    - A detailed description of the mathematical procedures to use to assess compliance with the three statistical tests in the Alternative PTS Rule.
    - A list of factors to consider in diagnosing the reason that particular surveillance data sets might fail these statistical tests.
    - A description of certain situations in which adjustments of the ETC predictions can be made.

3. **Criteria relating to inservice inspection (ISI) data and nondestructive examination (NDE) requirements**: The Alternate PTS Rule describes a number of tests of and conditions on the collection and analysis of ISI data that are intended to provide reasonable assurance that the distribution of flaws that was assumed to exist in the probabilistic fracture mechanics (PFM) calculations that provided the basis for the $RT_{MAX\text{-}X}$ limits provide an appropriate, or bounding, model of the population of flaws in the RPV of interest. Chapter 6 of this document provides guidance by which licensees can satisfy these criteria. The guidance discussed in this NUREG includes the following components:
    - Guidance for initial evaluation of NDE data obtained from qualified ISI examinations.
    - Guidance for further evaluation of NDE data obtained from qualified ISI examinations, as follows:
        i. Elements and NDE techniques associated with the qualified ASME Code, Section XI, Mandatory Appendix VIII ISI examinations performed to assess compliance with the requirements of the Alternate PTS Rule.
        ii. A mathematical procedure that can be used to adjust NDE data to account for flaw detection and sizing errors and comparison of the adjusted data to the population of flaws assumed in PFM technical basis for the Alternate PTS Rule.
    - Guidance for plants with RPV flaws that fall outside the applicability of the flaw tables in the Alternate PTS Rule, including:
        i. A mathematical procedure that can be used to preclude brittle fracture based on RT_{NDT} information.
        ii. A mathematical procedure that can be used to combine the NDE data with the population of flaws assumed in the PFM calculations to estimate the total flaw distribution that is predicted to exist in the RPV, and guidance on the use of this total flaw distribution as part of a PFM calculation using the Fracture Analysis of Vessels—Oak Ridge (FAVOR) computer code.
4. **Criteria relating to alternate limits on embrittlement**: Guidance is provided by which licensees can estimate a plant-specific value of through-wall cracking frequency (TWCF) for cases in which the $RT_{MAX\text{-}X}$ limits of the Alternate PTS Rule are not satisfied. Chapter 7 of this document describes these two sets of guidance so that licensees can satisfy embrittlement acceptability criteria.

This document provides guidance and the associated technical basis for methods by which these requirements can be met.

ABBREVIATIONS AND ACRONYMS

Abbreviation	Definition
AP	Advanced Passive
APWR	Advanced Pressurized-Water Reactor
ASME	(Not an abbreviation now; formerly stood for the American Society of Mechanical Engineers)
BWR	boiling-water reactor
CFR	*Code of Federal Regulations*
E	energy
EPR	Evolutionary Power Reactor
EPRI	Electric Power Research Institute
ETC	embrittlement trend curve
FAVOR	Fracture Analysis of Vessels—Oak Ridge
FRN	*Federal Register* Notice
IGSCC	intergranular stress-corrosion cracking
ISI	inservice inspection
MeV	million electron-Volts
MRP	Materials Reliability Program
NDE	non-destructive examination
NRC	United States Nuclear Regulatory Commission
NRR	Office of Nuclear Reactor Regulation
NSSS	Nuclear Steam Supply System
ORNL	Oak Ridge National Laboratory
PDF	probability density function
PDI	Performance Demonstration Initiative
PFM	Probabilistic Fracture Mechanics
PNNL	Pacific Northwest National Laboratory
POD	probability of detection
PRA	probabilistic risk assessment
PTS	pressurized thermal shock
PVRUF	Pressure Vessel Research User Facility
PWR	pressurized-water reactor
RES	Office of Nuclear Regulatory Research
RPV	reactor pressure vessel
TLR	Technical Letter Report
TWCF	through-wall cracking frequency
TWE	through-wall extent
UT	ultrasonic testing

SYMBOLS AND EXPRESSIONS

Symbol	Definition
A	Multiplier for determining ΔT_{30} based on product form
ADJ	An adjustment in the embrittlement prediction to account for a failure of the mean test
B	Multiplier for determining ΔT_{30} based on product form
C_1 and C_2	Critical values of the outlier test
CRP	Intermediate term for determining ΔT_{30} in degrees Fahrenheit or Celsius
Cu	Copper content in weight-percent
Cu_e	Effective copper content in weight-percent
$f(Cu_e,P)$	Intermediate term for determining ΔT_{30} based on effective copper content and phosphorus content
$g(Cu_e,Ni, \phi t_e)$	Intermediate term for determining ΔT_{30} based on effective copper content, nickel content, and effective fluence
m	Slope of ΔT_{30} prediction residuals plotted vs. the base-10 logarithm of fluence
$Max(Cu_e)$	Intermediate term for determining ΔT_{30} based on effective copper content
MD	Intermediate term for determining ΔT_{30} based on degrees Fahrenheit or Celsius
Mn	Manganese content in weight percent
n	Number of ΔT_{30} observations in a plant-specific surveillance dataset
Ni	Nickel content in weight percent
P	Phosphorus content in weight percent
r*	Normalized residual
r^*_1 and r^*_2	Calculated values of residuals for the outlier test
$r_{LIMIT(1)}$ and $r_{LIMIT(2)}$	Critical values of the outlier test (same as C_1 and C_2)
r_{max}	Maximum permissible ΔT_{30} prediction residual
r_{mean}	Mean ΔT_{30} prediction residual for a plant-specific surveillance dataset
$R_{(max1)}$	The largest ΔT_{30} prediction residual for a plant-specific surveillance dataset
$R_{(max2)}$	The second-largest ΔT_{30} prediction residual for a plant-specific surveillance dataset
RT_{MAX-X}	Any or all of the material properties $RT_{MAX–AW}$, $RT_{MAX–PL}$, $RT_{MAX–FO}$, $RT_{MAX–CW}$, or sum of $RT_{MAX–AW}$ and $RT_{MAX–PL}$ for a particular reactor vessel, expressed as a temperature in degrees Fahrenheit (°F) or Celsius (°C)
RT_{MAX-AW}	Material property, expressed as a temperature in degrees Fahrenheit (°F) or Celsius (°C), which characterizes the reactor vessel's resistance to fracture initiating from flaws found along axial weld fusion lines
RT_{MAX-PL}	Material property, expressed as a temperature in degrees Fahrenheit (°F) or Celsius (°C), which characterizes the reactor vessel's resistance to fracture initiating from flaws found in plates remote from welds
RT_{MAX-FO}	Material property, expressed as a temperature in degrees Fahrenheit (°F) or Celsius (°C), which characterizes the reactor vessel's resistance to fracture initiating from flaws in forgings remote from welds
RT_{MAX-CW}	Material property, expressed as a temperature in degrees Fahrenheit (°F) or Celsius (°C), which characterizes the reactor vessel's resistance to fracture initiating from flaws found along circumferential weld fusion lines
RT_{NDT}	Nil ductility transition temperature in degrees Fahrenheit (°F) or Celsius (°C)
$RT_{NDT(u)}$	Unirradiated nil ductility transition temperature in degrees Fahrenheit (°F) or Celsius (°C)
RT_{PTS}	The RT_{NDT} value at end of license, as defined in 10 CFR 50.61, in degrees Fahrenheit (°F) or Celsius (°C)
S	Distance of flaw below surface in inches (in) or millimeters (mm)
se(m)	Standard error of m
t_e	Effective time in seconds
T_C	Irradiated (coolant) temperature in degrees Fahrenheit (°F) or Celsius (°C)

SYMBOLS AND EXPRESSIONS (concluded)

Symbol	Definition
$T_{CRIT(\alpha)}$	Critical value of Student's t-distribution
T_m	T-statistic for m
t, T_{WALL}	Wall thickness in inches (in) or millimeters (mm)
t(...)	Student's t-distribution
TWE	Through-wall extent in inches (in) or millimeters (mm)
TWE_{MAX}	Maximum through-wall extent in inches (in) or millimeters (mm)
TWE_{MIN}	Minimum through-wall extent in inches (in) or millimeters (mm)
α	Statistical significance level
ΔT_{30}	Increase in the Charpy-V notch energy transition temperature, in degrees Fahrenheit (°F) or Celsius (°C), at 30 foot-pounds (ft-lb) or 41 Joules (J) caused by neutron-irradiation embrittlement
$\Delta T_{30(ADJ)}$	An adjusted value of ΔT_{30} in degrees Fahrenheit (°F) or Celsius (°C) that accounts for a failure in the mean slope test
$\Delta T_{30i(measured)}$	A measured value of ΔT_{30} in degrees Fahrenheit (°F) or Celsius (°C)
$\Delta T_{30i(ETC\text{-}mean)}$	A value of ΔT_{30} predicted by Eqn. (1) in degrees Fahrenheit (°F) or Celsius (°C)
ΔYS	Change in yield strength in thousands of pounds per square inch (ksi) or Megapascals (MPa)
ϕ	Flux in neutrons per square centimeter per second (n/cm^2-sec)
ϕt	Fluence in neutrons per square centimeter (n/cm^2)
ϕt_e	Effective fluence in neutrons per square centimeter (n/cm^2)
σ	Standard deviation in degrees Fahrenheit (°F) or Celsius (°C)

1. INTRODUCTION

1.1 Background

The United States Nuclear Regulatory Commission (NRC) promulgated Section 50.61a, “Alternate Fracture Toughness Requirements for Protection against Pressurized Thermal Shock Events,” of Title 10, “Energy,” of the *Code of Federal Regulations* (10 CFR 50.61a) [1] on January 4, 2010, as reported in the *Federal Register* Notice (FRN) 75 FR 13 [2]. 10 CFR 50.61a amended existing regulations to provide alternate fracture toughness requirements for protection against pressurized thermal shock (PTS) events for pressurized-water reactor (PWR) pressure vessels.

The “Alternate PTS Rule” contained in 10 CFR 50.61a provides alternate embrittlement requirements based on more comprehensive analysis methods. This action became desirable because the existing requirements, as contained in 10 CFR 50.61, “Fracture Toughness Requirements for Protection against Pressurized Thermal Shock Events” [3], are based on unnecessarily conservative assumptions. The Alternate PTS Rule reduces regulatory burden for those PWR licensees who expect to exceed the 10 CFR 50.61 embrittlement requirements before the expiration of their operating licenses, while maintaining adequate safety. PWR licensees may choose to comply with the Alternate PTS Rule as a voluntary alternative to complying with the requirements contained in 10 CFR 50.61.

The Alternate PTS Rule provides revised PTS screening criteria in the form of embrittlement reference temperatures, RT_{MAX-X}, that characterize the reactor pressure vessel (RPV) material’s resistance to fracture initiation from flaws. The PTS screening criteria are provided in Table 1 of the Alternate PTS Rule, and are shown in Table 1 of this document. The values shown in Table 1 below are based on up-to-date understandings and models of the many factors affecting the operating safety of PWRs. Further discussion on the provisions and use of the Alternate PTS Rule appear in Chapter 2 of this report.

Table 1. $RT_{MAX\text{-}X}$ PTS Embrittlement Limits from the Alternate PTS Rule

Product form and $RT_{MAX\text{-}X}$ Values	$RT_{MAX\text{-}X}$ limits [°F] for different vessel wall thicknesses[6] (T_{WALL})		
	$T_{WALL} \leq 9.5$ in.	9.5 in. < $T_{WALL} \leq 10.5$ in.	10.5 in. < $T_{WALL} \leq 11.5$ in.
Axial Weld $RT_{MAX\text{-}AW}$	269	230	222
Plate $RT_{MAX\text{-}PL}$	356	305	293
Forging without underclad cracks $RT_{MAX\text{-}FO}$[7]	356	305	293
Axial Weld and Plate $RT_{MAX\text{-}AW} + RT_{MAX\text{-}PL}$	538	476	445
Circumferential Weld $RT_{MAX\text{-}CW}$[8]	312	277	269
Forging with underclad cracks $RT_{MAX\text{-}FO}$[9]	246	241	239

[6] Wall thickness is the beltline wall thickness including the clad thickness.

[7] Forgings without underclad cracks apply to forgings for which no underclad cracks have been detected and that were fabricated in accordance with Regulatory Guide 1.43.

[8] RT_{PTS} limits contribute 1×10^{-8} per reactor year to the reactor vessel TWCF.

[9] Forgings with underclad cracks apply to forgings that have detected underclad cracking or were not fabricated in accordance with Regulatory Guide 1.43.

1.2 Scope of this Report

The RT_{MAX-X} embrittlement limits shown in Table 1 may be used by licensees provided that certain criteria are met, as outlined in the Alternate PTS Rule. This document explains the basis for these requirements (which establish the entry conditions to permit use of the Alternate PTS Rule) and describes methods by which the following four requirements can be met:

1. **<u>Criteria relating to the date of construction and design requirements</u>**: Paragraph (b) of 10 CFR 50.61a restricts the applicability of the Alternate PTS Rule to reactors for which a construction permit was issued before February 3, 2010, and whose RPV was designed and fabricated to the 1998 Edition, or earlier, of the ASME (formerly the American Society of Mechanical Engineers) Boiler and Pressure Vessel Code ("Code"). Chapter 4 of this document describes the criteria related to the date of plant construction by which licensees can make use of the Alternate PTS Rule.

2. **<u>Criteria relating to evaluation of plant-specific surveillance data</u>**: Paragraph (f) of the Alternate PTS Rule requires that the licensee verify that plant-specific surveillance data for the RPV in question satisfy three statistical tests described in the Alternate PTS Rule. These tests assess whether or not the plant-specific surveillance data are adequately predicted by the embrittlement trend curve (ETC) used in the Alternate PTS Rule. If this verification cannot be made, the licensee is required to submit an evaluation of plant-specific surveillance data to the Director of the NRC Office of Nuclear Reactor Regulation (NRR) that proposes a method to account for plant-specific surveillance data when assessing the subject RPV relative to the Alternate PTS Rule limits on RT_{MAX-X}. Chapter 5 of this document describes methods by which licensees can satisfy these criteria.

3. **<u>Criteria relating to inservice inspection (ISI) data and non-destructive examination (NDE) requirements</u>**: Paragraph (e) of the Alternate PTS Rule requires that the licensee verify that the flaw density and size distributions detected within the beltline region of the RPV during a qualified examination under Section XI of the ASME Code [4] are bounded by flaw tables contained within the Alternate PTS Rule. The Alternate PTS Rule requires that any flaws detected within the inner 1 inch or 10 percent of the wall thickness of the vessel base material, whichever is greater, do not exceed the limits shown in Table 2. If this verification cannot be made, the licensee must demonstrate that the RPV will have a through-wall cracking frequency (TWCF) of less than 1×10^{-6} per reactor year. Chapter 6 of this document describes methods by which licensees can satisfy these criteria.

4. **<u>Criteria relating to alternate limits on embrittlement</u>**: Chapter 7 of this document describes criteria by which licensees can assess plant-specific TWCF for cases in which the RT_{MAX-X} limits of the Alternate PTS Rule are not satisfied.

References to the "beltline" region of the RPV throughout this report refer to all regions of the RPV adjacent to the reactor core that are exposed to a fluence of 1×10^{17} n/cm^2 or higher during the operating lifetime of the reactor [25]. Fluence values should be determined in accordance with methodology consistent with that specified in Regulatory Guide 1.190 [27] or using methods otherwise acceptable to the staff.

The NRC solicited input from interested stakeholders regarding an Alternate PTS regulation during three public meetings in 2011 [17]. The Materials Reliability Program (MRP) developed recommended technical methods or approaches in seven areas. Those recommended technical methods are described in MRP-334 [10] and were provided to reduce the resources needed by utilities and the NRC to implement the Alternate PTS Rule, as well as to provide a consistent and acceptable level of safety subsequent to Rule implementation, especially in those instances in which alternate evaluations are required to demonstrate compliance with the Alternate PTS Rule. NRC responses to the recommendations made in MRP-334 are discussed in Chapter 3.

Table 2. Flaw Limit Tables from the Alternate PTS Rule

Through–wall extent, TWE [in.]		Maximum number of flaws per 1000-inches of weld length in the inspection volume that are greater than or equal to TWE_{MIN} and less than TWE_{MAX}
TWE_{MIN}	TWE_{MAX}	
0	0.075	No Limit
0.075	0.475	166.70
0.125	0.475	90.80
0.175	0.475	22.82
0.225	0.475	8.66
0.275	0.475	4.01
0.325	0.475	3.01
0.375	0.475	1.49
0.425	0.475	1.00
0.475	Infinite	0.00

Through-wall extent, TWE [in.]		Maximum number of flaws per 1000 square-inches of inside surface area in the inspection volume that are greater than or equal to TWE_{MIN} and less than TWE_{MAX}. This flaw density does not include underclad cracks in forgings.
TWE_{MIN}	TWE_{MAX}	
0	0.075	No Limit
0.075	0.375	8.05
0.125	0.375	3.15
0.175	0.375	0.85
0.225	0.375	0.29
0.275	0.375	0.08
0.325	0.375	0.01
0.375	Infinite	0.00

2. OVERVIEW OF THE ALTERNATE PTS RULE

2.1 Background

PTS events are system transients in a PWR during which there is a rapid cooldown that results in cold vessel temperatures with or without repressurization of the RPV. The rapid cooling of the inside surface of the RPV causes thermal stresses which can combine with stresses caused by high pressure. The aggregate effect of these stresses is an increase in the potential for fracture if a pre-existing flaw is present in a region of the RPV having significant embrittlement.

The PTS Rule, described in 10 CFR 50.61, establishes screening criteria below which the potential for a RPV to fail because of a PTS event is deemed to be acceptably low. These screening criteria effectively define a limiting level of embrittlement beyond which operation cannot continue without further plant-specific compensatory action or analysis unless the licensee receives an exemption from the requirements of 10 CFR 50.61. Some compensatory actions are neutron-flux reduction, plant modifications to reduce the PTS event probability or severity, and RPV annealing, which are addressed in 10 CFR 50.61(b)(3), (b)(4), and (b)(7) and in 10 CFR 50.66, "Requirements for Thermal Annealing of the Reactor Pressure Vessel" [5].

Currently, no operating PWR RPV is projected to exceed the 10 CFR 50.61 screening criteria before the expiration of its original 40-year operating license. However, several PWR RPVs are approaching the screening criteria, while others are likely to exceed the screening criteria during the period of license renewal.

The NRC developed technical bases that support updating the PTS regulations (see References [6], [7], [8], [9], and [14]). These technical bases concluded that the risk of through-wall cracking because of a PTS event is much lower than previously estimated. This finding indicated that the screening criteria in 10 CFR 50.61 are unnecessarily conservative. Therefore, the NRC developed 10 CFR 50.61a, the Alternate PTS Rule, which provides alternate screening criteria based on the updated technical bases. These technical bases covered the following topics:

a. Applicability of the Alternate PTS Rule;
b. Updated embrittlement correlation;
c. ISI volumetric examination and flaw assessments;
d. NDE-related uncertainties; and
e. Surveillance data.

A brief overview of these topics is provided in the following sections.

In addition, seven subsequent requirements that licensees must satisfy as a part of implementation of the Alternate PTS Rule are defined in paragraph (d) of 10 CFR 50.61a.

2.2 Applicability of the Alternate PTS Rule

The Alternate PTS Rule is based, in part, on analysis of information from three currently operating PWRs. Because the severity of the risk-significant transient classes (e.g., primary-side pipe breaks and stuck-open valves on the primary side that may later reclose) is controlled by factors that are common to PWRs in general, the NRC concluded that the results and screening criteria developed from these analyses could be applied with confidence to the entire fleet of operating PWRs. This conclusion was based on an understanding of the characteristics of the dominant transients that drive their risk significance and on an evaluation of a larger population of high-embrittlement PWRs. This evaluation revealed no design, operational, training, or procedural factors that could credibly increase either the severity of these transients or the frequency of their occurrence in the general PWR population above the severity and frequency characteristic of the three plants that were modeled in detail. The NRC also concluded that PTS events that were insignificant risk contributors in these analyses are not expected to become dominant contributors in other plants.

The Alternate PTS Rule is applicable to licensees whose construction permits were issued before February 3, 2010, and whose RPVs were designed and fabricated to the 1998 Edition or an earlier edition of the ASME Code.

2.3 Updated Embrittlement Correlation

The technical basis for the Alternate PTS Rule used many different models and parameters to estimate the yearly probability that a PWR will develop a through-wall crack as a consequence of PTS loading. One of these models was a revised ETC that uses information on the chemical composition and neutron exposure of low-alloy steels in the RPV beltline region to estimate the fracture-mode transition temperature of these materials. Although the general trends predicted by the embrittlement models in 10 CFR 50.61 and the Alternate PTS Rule are similar, the mathematical form of the revised ETC in the Alternate PTS Rule differs substantially from the ETC in 10 CFR 50.61. The ETC in the Alternate PTS Rule was updated to more accurately represent the substantial amount of RPV surveillance data that has accumulated between the last revision of the 10 CFR 50.61 ETC in the mid-1980s and the database supporting the 10 CFR 50.61a ETC, which was finalized in 2002. The specifics of the updated ETC used in the Alternate PTS Rule are discussed in Section 5.1.

2.4 ISI Volumetric Examination and Flaw Assessments

The Alternate PTS Rule differs from 10 CFR 50.61 in that it requires licensees who choose to follow its requirements to analyze the results from ISI volumetric examinations done in accordance with Section XI, "Inservice Inspection of Nuclear Power Plant Components," of the ASME Code. The analyses of ISI volumetric examinations may be used to determine whether the flaw density and size distribution in the licensee's RPV beltline region are bounded by the flaw density and size distribution used in the development of the Alternate PTS Rule.

The Alternate PTS Rule was developed using a flaw density, spatial distribution, and size distribution determined from experimental data, as well as from physical models and expert judgment. The experimental data were obtained from samples removed from RPV materials from cancelled plants (i.e., from the Shoreham and the Pressure Vessel Research Users Facility (PVRUF) vessels). The NRC considers that comparison of the results from qualified ASME Code Section XI ISI volumetric examination is needed to confirm that the flaw density and size distributions in the RPV to which the Alternate PTS Rule may be applied are consistent with the flaw density and size distribution used in the development of the Alternate PTS Rule.

Paragraph (g)(6)(ii)(C) in 10 CFR 50.55a, "Codes and Standards" [11], requires licensees to implement ISI examinations in accordance with Supplements 4 and 6 [12] to Mandatory Appendix VIII to Section XI of the ASME Code. Supplement 4 contains qualification requirements for the RPV ISI volume from the clad-to-base-metal interface to the inner 15 percent of the RPV base material wall thickness. Supplement 6 contains qualification requirements for RPV weld volumes that lie within the outer 85% of the RPV base material wall thickness.

A simplified representation of the flaw density and size distribution used in the development of the Alternate PTS Rule is summarized by numerical values in Tables 2 and 3 of the Alternate PTS Rule for weld and plate/forging materials, respectively, as duplicated in Table 2. Hereafter, Tables 2 and 3 of the Alternative PTS rule are referred to, collectively, as "the flaw tables." These limits represent the number of flaws in each size range that were evaluated in the underlying technical bases. If a distribution of flaws having size and density greater than that of the flaw tables is found in a RPV, those flaws must be evaluated to ensure that they are not causing the TWCF to exceed a value of 1×10^{-6}.

The technical basis for the Alternate PTS Rule also indicated that flaws buried more deeply than 1 inch from the clad-to-base interface are not as susceptible to brittle fracture as flaws of similar size located closer to the inner surface. Therefore, the Alternate PTS Rule does not require an assessment of the density of these flaws, but still requires large flaws, if discovered, to be evaluated for contributions to TWCF if they are within the inner three-eighths of the vessel base material wall thickness. Section II, "Discussion," of the January 4, 2010, Federal Register Notice [2] for the Alternate PTS Rule indicates that the limitation for flaw acceptance, specified in Table IWB-3510-1 in Section XI of the ASME Code, approximately corresponds to the threshold for the sizes of flaws that can make a significant contribution to TWCF if they are present in RPV material at this depth. Therefore, the Alternate PTS Rule requires that flaws exceeding the size limits in Table IWB-3510-1 be evaluated for contribution to TWCF in addition to the other evaluations for such flaws that are prescribed in the ASME Code.

The Alternate PTS Rule also clarifies that, to be consistent with Mandatory Appendix VIII to Section XI of the ASME Code, the smallest flaws that must be sized are 0.075 inch in through-wall extent (TWE). For each flaw detected that has a TWE equal to or greater than 0.075 inch, the licensee is required to document the dimensions of the flaw, its orientation, its location within the RPV, and its depth from the clad-to-base-metal interface. Those planar flaws for which the major axis of the flaw is identified by a circumferentially-oriented ultrasonic transducer must be categorized as ''axial.'' All other planar flaws may be categorized as ''circumferential.'' If there is uncertainty about which flaw dimension constitutes the major axis for a given flaw identified with an ultrasonic transducer oriented in the circumferential direction, it should be considered as an axial flaw. The NRC may also use this information to evaluate whether plant-specific information gathered suggests that the NRC staff should generically re-examine the technical basis for the Alternate PTS Rule.

Surface cracks that penetrate through the RPV stainless steel clad and more than 0.070 inch into the welds or the adjacent RPV base metal were not included in the technical basis for the Alternate PTS Rule because these types of flaws have not been observed in the beltline of any operating PWR vessel. However, flaws of this type were observed in a boiling-water reactor (BWR) RPV head in 1990 that were attributed to intergranular stress-corrosion cracking (IGSCC) of the stainless steel cladding. BWRs are not susceptible to PTS events and hence are not subject to the requirements of 10 CFR 50.61. However, if similar cracks were found in the beltline region of a PWR, they would be a significant contributor to TWCF because of their size and location. As a result, the Alternate PTS Rule requires licensees to determine whether cracks of this type exist in the beltline weld region as a part of each required ASME Code Section XI ultrasonic examination.

2.5 NDE-Related Uncertainties

The flaw sizes shown in Table 2 represent actual flaw dimensions, while the results from ASME Code Section XI examinations are estimated dimensions. The available information indicates that, for most flaw sizes in Table 2, qualified inspectors will oversize flaws. Comparing oversized flaws to the size and density distributions in Table 2 is conservative, but not necessary.

As a result of stakeholder feedback received during the NRC's solicitation for public comments on a preliminary draft of the Alternate PTS Rule, the final published Alternate PTS Rule permits licensees to adjust the flaw sizes estimated by inspectors qualified under Supplements 4 and 6 to Mandatory Appendix VIII to Section XI of the ASME Code. The NRC also determined that licensees should be allowed to consider other NDE uncertainties, such as probability of detection (POD) and flaw density and location, because these uncertainties may affect the ability of a licensee to demonstrate compliance with the Alternate PTS Rule. As a result, the language in 10 CFR 50.61a(e) allows licensees to account for the effects of NDE-related uncertainties in meeting the flaw size and density requirements of Table 2. The Alternate PTS Rule does not provide specific guidance on a methodology to account for the effects of NDE-related uncertainties, but notes that accounting for such uncertainties may be based on data collected from ASME Code inspector-qualification tests or any other tests that measure the difference between the actual flaw size and the size determined from the ultrasonic examination. Because collecting, evaluating, and using data from ASME Code inspector-qualification tests requires extensive engineering judgment, the Alternate PTS Rule requires that the methodology used to adjust flaw sizes to account for the effects of NDE-related uncertainties be reviewed and approved by the Director of NRR.

2.6 Surveillance Data

Paragraph (f) of the Alternate PTS Rule defines the process for calculating the values for the reference temperature, RT_{MAX-X}, for a particular RPV material. These values may be based on the RPV material's copper (Cu), manganese (Mn), phosphorus (P), and nickel (Ni) weight percentages, reactor cold-leg coolant temperature, and fast neutron flux and fluence values, as well as the unirradiated nil-ductility transition reference temperature, RT_{NDT}.

The Alternate PTS Rule includes a procedure by which the RT_{MAX-X} values, which are predicted for plant-specific RPV materials using an ETC, are compared to heat-specific surveillance data that are collected as part of surveillance programs under Appendix H, "Reactor Vessel Material Surveillance Requirements" [13], to 10 CFR Part 50. The purpose of this comparison is to assess how well the surveillance data are represented by the ETC. If the surveillance data are close (closeness is assessed statistically) to the ETC, the predictions of this ETC are used. This is expected to be the case most often. However, if the heat-specific surveillance data deviate significantly and non-conservatively from the predictions of the ETC, this indicates that alternative methods (i.e., other than the ETC) may be needed to reliably predict the temperature-shift trend (and to estimate RT_{MAX-X}) for the conditions being assessed. Therefore, the Alternate PTS Rule includes three statistical tests to determine the significance of the differences between heat-specific surveillance data and the ETC.

3. RESPONSES TO STAKEHOLDER FEEDBACK

The NRC solicited input from interested stakeholders regarding an Alternate PTS Implementation Regulatory Guide during three of public meetings in 2011 [17]. Based on those meetings, the Electric Power Research Institute's (EPRI's) Materials Reliability Program (MRP) developed recommended technical methods or approaches that would be useful for Alternate PTS Rule implementation in seven areas. Those recommended technical methods are described in MRP-334 [10]. That report provided fifteen specific recommendations that might reduce the resources needed by utilities and the NRC to implement the Alternate PTS Rule. In addition, EPRI stated that the recommendations would provide a consistent and acceptable level of safety subsequent to Alternate PTS Rule implementation, especially in those instances where evaluations are required to demonstrate compliance with the Alternate PTS Rule.

EPRI's recommendations from MRP-334 are included in Table 3. The NRC responses to the recommendations made in MRP-334 are shown in the last column of the table. As indicated by some of the responses to EPRI's recommendations, some of the guidance established in this document was adjusted for further clarification.

Table 3. EPRI Recommendations for Addressing Alternate PTS Rule Requirements [10]

No.	10 CFR 50.61a Paragraph	MRP-334 Recommendation	MRP-334 Justification	NRC Response
1	(f)(6), (a)(10)	Adjustments should not be made to sister-plant ΔT_{30} values for the purposes of performing the surveillance data tests in 10 CFR 50.61a.	The 10 CFR 50.61a ETC directly takes into consideration the material properties and the irradiation temperature in the calculation of ΔT_{30} and the residual for each point of plant or sister-plant data. Additional detail is provided in Section 3.1.	The NRC agrees with the comment. Sister-plant data are used as part of the surveillance data set (see Step (1a) of the surveillance procedure), but no adjustments to the data are made.
2	(f)(6), (a)(10)	Limitations should be placed on the variation in chemistry within a weld heat that must be considered when considering sister-plant data.	An example of a weld heat with significant variation is shown in Appendix A of this report. Additional discussion is provided in Section 3.1.	The NRC agrees that variations in composition should be considered if there is a need to explain/understand deviations identified by the statistical tests that are required for surveillance data. This is pointed out in Step 2(d)(ii)(a) in the section entitled "Factors to Consider when the Statistical Tests of Step 2 are Failed" under the heading "Composition and Exposure Variables." Specific limits are not provided; these should be justified on a case-specific basis.
3	(f)(6)(vi), (a)(11)	If the surveillance data tests cannot be met using exact time weighted average T_C values, a tolerance that is equivalent to plus or minus one half of the range of the operating temperatures over the irradiation time should be considered. If the surveillance data tests can be satisfied by using a temperature within this tolerance range on T_C, adjustment to ΔT_{30} values should not be required.	Large differences in irradiation temperature can also have significant effects on the calculated ΔT_{30} values. 10 CFR 50.61a defines TC as a time-weighted average of the cold-leg temperature under normal full-power operating conditions. However, the values used in the development of the ETC may not have reflected an accurate time-weighted average for each specific plant. This tolerance accounts for the uncertainty in the actual operating temperature when the largest changes in the embrittlement index occurred. Additional discussion is provided in Section 3.1.	The NRC agrees that variations in cold-leg temperature should be considered if there is a need to explain/understand deviations identified by the statistical tests that are required for surveillance data. This is pointed out in Step 2(d)(ii)(a) in the section entitled "Factors to Consider when the Statistical Tests of Step 2 are Failed" under the heading "Composition and Exposure Variables." Specific limits are not provided; these should be justified on a case-specific basis.

No.	10 CFR 50.61a Paragraph	MRP-334 Recommendation	MRP-334 Justification	NRC Response
4	(f)(6)(vi), (f)(6)(v)(A), (f)(6)(v)(C)	A procedure is recommended in Section 3.2 of the report for calculating the ΔT_{30} adjustment to meet the requirements of Paragraph (f)(6)(vi) when either the mean or outlier statistical tests are failed when applying the requirements of Paragraph (f)(6)(v) of 10 CFR 50.61a.	The surveillance capsule data (SCD) statistical tests in (f)(6) can be overly conservative, so any needed adjustments to ΔT_{30} and RT_{MAX} for failing the SCD statistical tests should be minimal. The proposed procedure is simple to implement and addresses the concerns with deviation from the ETC without excessive conservatism. Additional discussion is provided in Section 3.2.	The NRC adopted this recommendation to address failures of the mean test. Refer to Step 2(b)(i). The NRC adopted a different approach to address outlier failures caused by a low fluence datum. Refer to Step 2(b)(ii). The NRC does not disagree with the proposed procedure for outlier failures, but considers that use of this procedure should be justified on a case-specific basis.
5	(f)(6)(vi), (f)(6)(v)(B)	An industry-consensus ETC that addresses irradiation-induced shifts caused by fluence values up to 1×10^{20} n/cm^2 (E > 1 MeV) should be used to calculate the predicted values of ΔT_{30} if the slope test is not satisfied.	Data from several plants, with fluence exposures of up to 8.5×10^{19} n/cm^2, have been evaluated and no slope-test deviations were encountered. It is possible that high-fluence surveillance capsule data could fail the statistical slope test. The industry has developed a Coordinated Surveillance program in order to obtain high fluence data from power reactors. The intent is to use this data to develop an industry-consensus ETC that addresses irradiation-induced shifts caused by fluence values up to 1×10^{20} n/cm^2 (E > 1 MeV). Additional discussion is provided in Section 3.3.	As of the current date, an ETC agreed on by broad consensus between the NRC and industry stakeholders does not exist. Also, the data from the coordinated surveillance program will not be available in large quantities until 2025. The NRC agrees that, in the event of a slope-test failure, the best current understanding of irradiation damage mechanics should be used to help explain the failure and suggest corrective actions. However, because technical consensus on this matter has not been reached, the NRC is not providing guidance on this matter.
6	(f)(6)(vi), (f)(6)(v)(A), (f)(6)(v)(B), (f)(6)(v)(C)	Recommendations for possible criteria for not adjusting ΔT_{30} values in accordance with (f)(6)(vi) when the tests of (f)(6)(v)(A), (B), and (C) cannot be satisfied are provided in Section 3.4.	There are several scenarios where an adjustment to ΔT_{30} values would not be appropriate. These scenarios and criteria are discussed in Section 3.4.	As discussed in Step 2(d) of the Regulatory Guide, the NRC agrees that there are many situations in which adjustment of the ΔT_{30} values is neither needed nor justifiable. Some of these situations are discussed in Step 2(d). However, specific exceptions are not provided; these should be justified on a case-specific basis.

No.	10 CFR 50.61a Paragraph	MRP-334 Recommendation	MRP-334 Justification	NRC Response
7	(d)(4), (c)(3)	A provision should be included in the proposed Regulatory Guide for direct calculation of $TWCF_{95\text{-}TOTAL}$ using the plant-specific $RT_{MAX\text{-}XX}$ values for cases in which the $RT_{MAX\text{-}XX}$ limits in Table 1 of 10 CFR 50.61a cannot be met.	There are some conservatisms in the $RT_{MAX\text{-}XX}$ screening limits. Also, plate and forging limited plants are likely to reach the more restrictive limit for circumferential welds before reaching the plate or forging limits. Additional discussion is provided in Section 3.5	The NRC agrees with this recommendation. Guidance was added to the Regulatory Guide as Position 4 that refers to the appropriate formulae and methods in Section 3.5.1 of NUREG-1874.
8	(e)(1)	Any small flaws detected by ISI within +0.5 inch of the outer boundaries of the ASME Section XI inspection volume can be treated as potential plate flaws. All other flaws within the inspection volume should be treated as weld flaws.	The plate flaw limits in Table 3 of 10 CFR 50.61a should only be evaluated for RPV base metal flaws not affected by welding that are detected by ISI. Additional discussion is provided in Section 3.6.	The NRC agrees with this comment. Guidance for establishing whether the flaws are in the plate or the weld is included in this NUREG (see Step D in Section 6.1).
9	(e)(1)	Plate flaws that have a depth (TWE) of 0.4 inch or more should be evaluated as weld flaws.	This is needed to ensure that the small flaws created during fabrication of the plates and forgings, which is what was simulated in the FAVOR probabilistic fracture mechanics analysis code, have not been expanded to larger-sized flaws by the effects of welding, which were simulated by FAVOR as weld flaws. Additional discussion is provided in Section 3.6.	The NRC disagrees with this recommendation because it is arbitrary. A case-specific justification would need to be developed to demonstrate why a plate flaw should be recategorized as a weld flaw.

No.	10 CFR 50.61a Paragraph	MRP-334 Recommendation	MRP-334 Justification	NRC Response
10	(e)(4)(i)	The proposed Regulatory Guide should provide criteria or methods for determining whether the deviation in flaw limits will have a detrimental effect on the applicability of the PTS Screening Criteria in Table 1 of 10 CFR 50.61a.	Such criteria would reduce burden on both the NRC and industry while providing an acceptable level of safety and quality. Additional discussion is provided in Section 3.7 and Appendix E.	The NRC agrees with this comment. Both simplified and more detailed procedures are given in Step 3(i) of the Regulatory Guide that address evaluations that may be performed when the flaw limits are exceeded. The industry may choose to justify alternatives to these procedures on a case-specific basis.
11	(e)(4)(i)	Deviations to the flaw limits for plants that have low embrittlement should be generically allowed. Low embrittlement can be defined as having RT_{MAX-X} values that are equivalent to or less than a TWCF of 1% of the PTS risk objective, or approximately 1×10^{-8} events per year.	The vessel material at these plants would still have high enough fracture toughness that even large increases in the number of flaws above the 10 CFR 50.61a limits would not result in reaching the PTS risk objective of 1×10^{-6} events per year. Additional discussion is provided in Section 3.7.	The NRC disagrees with this recommendation and the associated justification. If the flaw limits are failed, it would be inappropriate to use the relationships between TWCF and RT_{MAX-X} that depend on these limits being correct to address the issue. Simplified criteria for assessing brittle fracture are provided in the Regulatory Guide that may be used in this situation or, alternatively, another valid case-specific solution may be proposed.

No.	10 CFR 50.61a Paragraph	MRP-334 Recommendation	MRP-334 Justification	NRC Response
12	(e)(1)	The flaw limits in Tables 2 and 3 of 10 CFR 50.61a should be applied to axial flaws only.	This proposed approach addresses what the real technical concern should be; that is, the maximum number of axial flaws that could lead to potential vessel failure. Additional discussion is provided in the flaw-orientation discussion in Section 3.7.1.	The NRC disagrees with this comment. All flaws, whether axial or circumferential, are considered in the comparison to Tables 2 and 3 of 10 CFR 50.61a because under subpart (e), "Examination and Flaw Assessment Requirements," paragraph (e)(1)(iii) states: "(iii) For each flaw detected in the inspection volume described in paragraph (e)(1) with a through-wall extent equal to or greater than 0.075 inches, the licensee shall document the dimensions of the flaw, including through-wall extent and length, whether the flaw is axial or circumferential in orientation and its location within the reactor vessel, including its azimuthal and axial positions and its depth embedded from the clad-to-base-metal interface." Paragraph (e)(4) states, in part: "(4) The licensee shall perform analyses to demonstrate that the reactor vessel will have a TWCF of less than 1×10^{-6} per reactor year if the ASME Code, Section XI volumetric examination required by paragraph (c)(2) or (d)(2) of this section indicates any of the following: "(i) The flaw density and size in the inspection volume described in paragraph (e)(1) exceed the limits in Tables 2 or 3 of this section. […]"

No.	10 CFR 50.61a Paragraph	MRP-334 Recommendation	MRP-334 Justification	NRC Response
13	(e)(1), (e)(4)	A qualitative assessment process should be provided for addressing a flaw that exceeds the maximum size allowed in the flaw limit tables but is less than 0.875" in through-wall extent.	A qualitative process that considers flaw orientation, flaw location, flaw size, and material properties is proposed in Section 3.7.1.	The NRC agrees with this comment. The recommendation is addressed in Step I of the Regulatory Guide.
14	(e)(1), (e)(4), (e)(5)	A quantitative assessment process should be provided (a) for instances in which multiple flaws exceed the flaw limit tables or (b) if the requirements of the qualitative process cannot be satisfied.	A quantitative process that considers the contribution of individual flaws to the total vessel TWCF is provided in Section 3.7.2. If needed, an additional process that reduces some of the conservatisms in the Section 3.7.2 process is provided in Appendix F.	The NRC agrees with this comment. The recommendation is addressed in Step I of the Regulatory Guide.
15	(e)(1)	When assessing the flaw-limit tables, multiple flaws that are combined into one flaw in accordance with the ASME Section XI proximity rules should not be counted as multiple ISI flaws.	The ASME Section XI proximity rules were considered in the development of the flaw distributions used in the technical basis for 10 CFR 50.61a. Additional discussion is provided in Section 3.7.2.	The NRC agrees with this comment. Flaw proximity is considered in the Regulatory Guide, as indicated in Figure 3.

4. GUIDANCE FOR CRITERIA RELATING TO THE DATE OF CONSTRUCTION AND DESIGN REQUIREMENTS

The Alternate PTS Rule is applicable to plants with construction permits issued before February 3, 2010, and with RPVs designed and fabricated in accordance with the 1998 Edition or an earlier edition of the ASME Code. This chapter provides guidelines and supporting bases for this requirement.

4.1 Requirements in the Alternate PTS Rule

Paragraph (b), "Applicability," of the Alternate PTS Rule identifies that the Alternate PTS Rule is applicable for plants for which a construction permit was issued after February 3, 2010. Section II, "Discussion," of the January 4, 2010, Federal Register Notice [2] includes the following:

> *...The final rule is applicable to licensees whose construction permits were issued before February 3, 2010 and whose reactor vessels were designed and fabricated to the American Society of Mechanical Engineers Boiler and Pressure Vessel Code (ASME Code), 1998 Edition or earlier. This would include applicants for plants such as Watts Bar Unit 2 who have not yet received an operating license. However, it cannot be demonstrated, a priori, that reactor vessels that were not designed and fabricated to the specified ASME Code editions will have material properties, operating characteristics, PTS event sequences and thermal hydraulic responses consistent with those evaluated as part of the technical basis for this rule. Therefore, the NRC determined that it would not be prudent at this time to extend the use of the rule to future PWR plants and plant designs such as the Advanced Passive (AP) 1000, Evolutionary Power Reactor (EPR) and U.S. Advanced Pressurized Water Reactor (US–APWR). These designs have different reactor vessels than those in the currently operating plants, and the fabrication of the vessels based on these designs may differ from the vessels evaluated in the analyses that form the bases for the final rule. Licensees of reactors who commence commercial power operation after the effective date of this rule or licensees with reactor vessels that were not designed and fabricated to the 1998 Edition or earlier of the ASME Code may, under the provisions of § 50.12, seek an exemption from § 50.61a(b) to apply this rule if a plant-specific basis analyzing their plant operating characteristics, materials of fabrication, and welding methods is provided....*

Regulatory guidance for the above requirements is discussed in the next section.

4.2 Regulatory Guidance

The purpose of the restriction given in Section 4.1 on the applicability of the Alternate PTS Rule embrittlement limits is that the structural and thermal hydraulic analyses that established the basis for the Alternate PTS Rule only represented plants constructed before February 3, 2010. A licensee that applies the Alternate PTS Rule to a plant with a construction permit issued after February 3, 2010, must demonstrate that the risk-significant factors controlling PTS for the plant in question are adequately addressed by the technical-bases calculations, which are detailed in NUREG-1806 [6] and its supporting technical references. Factors to be considered in this evaluation should include, but might not be limited to, the following:

- the event sequences that may lead to overcooling of the RPV;

- the thermal-hydraulic response of the nuclear steam supply system (NSSS) in response to such sequences;

- Characteristics of the RPV design (e.g., vessel diameter, vessel wall thickness, and operating pressure) that influence the stresses that develop in the beltline region of the vessel (as defined in Section 1.2) in response to the event sequences; and

- Characteristics of the RPV materials and their embrittlement behavior.

5. GUIDANCE FOR CRITERIA RELATING TO THE EVALUATION OF PLANT-SPECIFIC SURVEILLANCE DATA

The information in this chapter was developed and published in support of the development of the Alternate PTS Rule. Relevant information from this work is repeated here for completeness and clarity [14]. In some cases, the information in Reference [14] is further clarified here compared to the technical bases supporting the Alternate PTS Rule. Additionally, the information presented in this chapter adds to that from Reference [14] in two respects: in Section 5.2 procedures for data grouping (e.g., treatment of "sister plant" data) before performing the statistical tests are described, and Section 5.6.2 describes procedures that can be used if the statistical tests are failed.

In this chapter, procedures are described by which the plant-specific surveillance data that are collected as part of surveillance programs (in accordance with Appendix H to 10 CFR 50) can be analyzed to assess how well they are represented by the ETC for ΔT_{30} adopted in the Alternate PTS Rule. If the surveillance data are "close" (closeness is assessed statistically) to the prediction of the ETC, the predictions of the ETC are used. Statistically significant differences between plant-specific data sets and the ETC prediction identify situations in which more focused attention is warranted, and are taken as an indication that methods other than, or in addition to, the ETC may be needed to predict ΔT_{30} trends. While standard statistical procedures exist to assess the significance of differences between individual data sets and ETC predictions, similarly standard procedures are not as commonly available to assess the practical importance of such differences, or to adjust the data to account for these differences. This chapter concludes with discussions of (1) factors that may be considered if the statistical tests are failed and (2) procedures that could be used to adjust the predictions of the ETC in certain circumstances.

The remainder of this chapter is divided into six sections, as follows:

- Section 5.1 describes the ΔT_{30} ETC. Details on the development of this ETC appear in ORNL/TM-2006/530 [9].

- Section 5.2 describes entry conditions that need to be met to use the proposed surveillance assessment procedure.

- Section 5.3 describes different types of deviations between plant-specific surveillance data and the trends represented by the ΔT_{30} ETC from Reference [9].

- Section 5.4 describes procedures that statistically assess the deviations described in Section 5.3.

- Section 5.5 applies the procedures of Section 5.4 to the surveillance database that supported the development of the ETC [9].

- Section 5.6 discusses factors that should be considered if the statistical tests of Section 5.4 are failed; it also describes procedures that could be used to adjust the predictions of the ETC in certain circumstances.

5.1 Embrittlement Trend Curve

As detailed in ORNL/TM-2006/530 [9], the numerical coefficients in the following equations were determined by fitting them to the ΔT_{30} data collected in 10 CFR 50 Appendix H surveillance programs that have been reported to the NRC through approximately 2002. This ΔT_{30} ETC, which is used in the Alternate PTS Rule, has the following form:

$$\Delta T_{30} = MD + CRP \tag{1}$$

$$MD = A \times (1 - 0.001718 \times T_C) \times (1 + 6.13 \times P \times Mn^{2.471}) \times \varphi t_e^{\,0.5} \tag{2}$$

$$A = \begin{cases} 1.140 \text{x} 10^{-7} & \text{for forgings} \\ 1.561 \text{x} 10^{-7} & \text{for plates} \\ 1.417 \text{x} 10^{-7} & \text{for welds} \end{cases} \tag{3}$$

$$CRP = B \times \left(1 + 3.77 \times Ni^{1.191}\right) \times f\left(Cu_e, P\right) \times g\left(Cu_e, Ni, \varphi t_e\right) \tag{4}$$

$$B = \begin{cases} 102.3 & \text{for forgings} \\ 102.5 & \text{for plates in vessels not manufactured by Combustion Engineering} \\ 135.2 & \text{for plates in vessels manufactured by Combustion Engineering} \\ 155.0 & \text{for welds} \end{cases} \tag{5}$$

$$Cu_e = \begin{cases} 0 & \text{for } Cu \le 0.072 \text{ wt\%} \\ MIN[Cu, MAX(Cu_e)] & \text{for } Cu > 0.072 \text{ wt\%} \end{cases} \tag{6}$$

$$MAX(Cu_e) = \begin{cases} 0.243 & \text{for Linde 80 welds} \\ 0.301 & \text{for all other materials} \end{cases} \tag{7}$$

$$f\left(Cu_e, P\right) = \begin{cases} 0 & \text{for } Cu \le 0.072 \\ \left[Cu_e - 0.072\right]^{0.668} & \text{for } Cu > 0.072 \text{ and } P \le 0.008 \\ \left[Cu_e - 0.072 + 1.359 \times (P - 0.008)\right]^{0.668} & \text{for } Cu > 0.072 \text{ and } P > 0.008 \end{cases} \tag{8}$$

$$g\left(Cu_e, Ni, \varphi t_e\right) = 0.5 + (0.5 \text{ x } \tanh\left\{\frac{[\log_{10}\left(\varphi t_e\right) + (1.1390 \times Cu_e) - (0.448 \times Ni) - 18.120]}{0.629}\right\} \tag{9}$$

$$\varphi t_e = \begin{cases} \varphi t & \text{for } \varphi \ge 4.39 \times 10^{10} \text{ n/cm}^2\text{/sec} \\ \varphi t \times \left(\dfrac{4.39 \times 10^{10}}{\varphi}\right)^{0.2595} & \text{for } \varphi < 4.39 \times 10^{10} \text{ n/cm}^2\text{/sec} \end{cases} \tag{10}$$

The dependent variable, ΔT_{30}, is estimated by Eqn. (1) in degrees Fahrenheit. The standard deviation of residuals about Eqn. (1) for different product forms and copper contents appears in

Table 4. The units and descriptions of independent variables in these equations are given in Table 5. As with any equation calibrated to empirical data, inaccuracies have a greater tendency to occur at the extremes of, or beyond this limits of, the calibration dataset. Users of Eqn. (1) should therefore exercise caution when applying it to conditions near to or beyond the extremes of its calibration dataset, which appear in Table 5. For example, for materials having copper contents below 0.072 weight percent, Eqn. (1) predicts negative ΔT_{30} values when the irradiation temperature exceeds 582.1°F; clearly, negative shift values are incorrect.

Table 4. Standard Deviation of Residuals about Eqn. (1)

<table>
<tr><th rowspan="2">Product Form</th><th colspan="2">Standard Deviation, σ (°F)</th></tr>
<tr><th>Cu ≤ 0.072 wt %</th><th>Cu > 0.072 wt %</th></tr>
<tr><td>Weld</td><td rowspan="3">18.6</td><td>26.4</td></tr>
<tr><td>Plate</td><td>21.2 [(a)]</td></tr>
<tr><td>Forging</td><td>19.6</td></tr>
</table>

a. Includes the standard reference materials.

Table 5. Independent Variables in the Eqn. (1) ETC and the Ranges and Mean Values of the Calibration Dataset

Variable	Symbol	Units	Values of Surveillance Database			
			Average	Standard Deviation	Minimum	Maximum
Neutron Fluence (E > 1 MeV)	ϕt	n/cm^2	1.24E+19	1.19E+19	9.26E+15	1.07E+20
Neutron Flux (E > 1 MeV)	ϕ	$n/cm^2/sec$	8.69E+10	9.96E+10	2.62E+08	1.63E+12
Irradiation Temperature	T_C	°F	545	11	522	570
Copper Content	*Cu*	weight %	0.140	0.084	0.010	0.410
Nickel Content	*Ni*	weight %	0.56	0.23	0.04	1.26
Manganese Content	*Mn*	weight %	1.31	0.26	0.58	1.96
Phosphorus Content	*P*	weight %	0.012	0.004	0.003	0.031

5.2 Data Used in Statistical Tests

Surveillance data used to perform the statistical tests outlined in this chapter should be as follows:

1. Materials Evaluated (i.e., the Meaning of "Plant-Specific")
   a) When performing the statistical tests required by the Alternate PTS Rule, each shell and weld material in the RPV beltline region for which 10 CFR 50 Appendix H surveillance data exist should be evaluated. The statistical tests should be performed separately for each heat.
   b) For each heat for which data are available, the ΔT_{30} values used in the statistical tests should include data from both of the following sources:
      - Data obtained for the heat of material in question as part of a 10 CFR 50 Appendix H surveillance program conducted for the plant in question; and
      - Data obtained for the heat of material in question as part of a 10 CFR 50 Appendix H surveillance program conducted for any other plant that is operating, or has operated, under a license issued by the NRC. Data from this source is often referred to as having come from a "Sister Plant." Such data may have different best-estimate chemistry values and different irradiation temperatures (e.g., the Cu and T values for Heat "123" at Plant "XYZ" may be 0.23 and 553°F, respectively, whereas the Cu and T values for Heat "123" at Plant "ABC" may be 0.21 and 544°F, respectively). The statistical tests described in Sections 5.3 and 5.4 operate on the residuals (i.e., the difference between the surveillance measurement of ΔT_{30} and the prediction of the ETC). In so doing, the ETC takes account of these plant-specific variations in chemistry and/or temperature, so there is no need to make further adjustments to account for so-called "Sister Plant" data (see Reference [10]).
2. Data-Quantity Requirements: To perform these statistical tests, at least three plant-specific ΔT_{30} values measured at three different fluence levels should be available. If this condition is not met, the ETC described in the Alternate PTS Rule should be used to estimate ΔT_{30}.
3. Data-Binning Requirements
   a) As discussed in Item 1, data obtained for the heat of material in question as part of a 10 CFR 50 Appendix H surveillance program conducted for any plant that is operating, or has operated, under a license issued by the NRC should be binned together and considered in these statistical evaluations.
   b) For plates and forgings, Charpy data is often obtained for different orientations of the notch relative to the primary working direction of the plate or forging. For the purpose of these statistical tests, ΔT_{30} values for a particular plate or forging should be computed from unirradiated specimens having the same notch orientation. Once ΔT_{30} values are calculated, different notch orientation data from the same heat of material should be binned together for the purpose of the statistical tests described in Sections 5.3 and 5.4. This is appropriate because the differences in unirradiated transition temperature caused by notch orientation will be subtracted out when ΔT_{30} values are calculated.
4. Data-Characterization Requirements: For all materials meeting the requirements of the three preceding items, the following information is needed:
      - heat identification
      - plant identification
      - capsule identification

- product form
- notch orientation
- the unirradiated reference temperature, $RT_{NDT(U)}$
- ΔT_{30}
- Charpy V-notch energy data used to estimate ΔT_{30}
- fluence
- operating time
- cold-leg temperature under normal full-power operating conditions (T_c)
    - Note: T_c (°F) is determined as the time-weighted average coolant temperature of the cold leg of the reactor coolant system covering the time period from the start of full-power operation through the end of licensed operation.
- copper (Cu) content
- nickel (Ni) content
- phosphorus (P) content
- manganese (Mn) content
- citation

The values of Cu, Ni, P, and Mn are the best-estimate values for the material. For a plate or forging, the best-estimate value is normally the mean of the measured values for that plate or forging. For a weld, the best-estimate value is normally the mean of the measured values for a weld deposit made using the same weld wire heat number as the critical vessel weld. If these values are not available, either the upper limiting values given in the material specifications to which the vessel material was fabricated, or conservative estimates (i.e., mean plus one standard deviation) based on generic data should be used. Table 4 of 10 CFR 50.61a provides upper-bound estimates for P and Mn. Similarly, upper bound estimates for Cu and Ni are provided in 10 CFR 50.61.

5.3 Statistical Evaluation of Surveillance Data

In developing this surveillance assessment procedure, consideration was given to the development of statistical tests capable of detecting the four types of deviations between heat-specific surveillance data and the ΔT_{30} ETC expressed by Eqns. (1) through (10). These deviations are illustrated in Figure 1 and are identified as Types A, B, C, and D. The potential origins and implications of these types of statistical deviations are described briefly in the following sections. Only situations in which the data suggest that the ΔT_{30} ETC may provide a non-conservative prediction (i.e., situations in which the data exceed the ETC prediction) are illustrated in Figure 1. The opposite situation is also possible; i.e., situations in which the data are underestimated by the ETC. However, from a regulatory standpoint, only non-conservative predictions are important.

- Type A Deviations: For Type A deviations, measurements differ from the mean ETC prediction more or less uniformly at all fluence levels. Additionally, the magnitude of this deviation is larger than would be expected based on the population of data used to calibrate the ETC. Potential origins of Type A deviations may include, but are not limited to, errors in the chemical composition values or errors in the unirradiated ΔT_{30} value associated with the surveillance sample. The implication of a statistically significant Type A deviation (procedures for evaluating statistical significance are described in Section 5.4.1) is that the ETC may systematically underestimate the value of ΔT_{30} for the heat of steel being evaluated.

- Type B Deviations: For Type B deviations, measurements differ from the mean ETC prediction by an amount that increases as fluence increases. Additionally, the magnitude of this deviation is larger than would be expected based on the population of data used to calibrate the ETC. Potential origins of Type B deviations may include, but are not limited to, (1) errors in the temperature value associated with the surveillance sample or (2) the existence in the surveillance sample of an embrittlement mechanism that is not represented in the ETC calibration dataset. A recent review of high-fluence data has revealed the possible existence of Type B deviations in a large empirical database (see Figure 2 and Reference [15]). The implications of a statistically significant Type B deviation (procedures for evaluating statistical significance are described in Section 5.4.2) are that the ETC may systematically underestimate the value of ΔT_{30} for the heat of steel being evaluated and that the magnitude of this underestimation will increase as the plant operation continues.

- Type C Deviations: For Type C deviations, measurements differ from the mean ETC by exhibiting more scatter than would be expected based on the population of data used to calibrate the ETC. Potential origins of Type C deviations may include, but are not limited to, errors made in testing, labeling, or controlling the notch orientation of surveillance specimens. The implication of statistically significant Type C deviations is not that the ETC may systematically underpredict the true embrittlement, but rather that the ability of the surveillance data to provide insight into embrittlement trends is called into question for a specific heat of material.

- Type D Deviations: For Type D deviations, one or more of the ΔT_{30} measurements differ significantly from the mean ETC prediction even though all other measurements for the heat of steel being evaluated agree well with that prediction. The magnitude of the deviation of these outliers is larger than would be expected based on the population of data used to calibrate the ETC. Potential origins of Type D deviations may include, but are not limited to, (1) a large measurement error in the single datum or (2) the rapid emergence in the surveillance sample of an embrittlement mechanism that is not represented in the calibration dataset (e.g., rapid emergence of a Type B deviation). The implication of a statistically significant Type D deviation (procedures for evaluating statistical significance are described in Section 5.4.3) is that the ETC may systematically underestimate the value of ΔT_{30} for the heat of steel being evaluated.

If they are statistically significant, Type A, B, and D deviations all give rise to concerns that the embrittlement trends predicted by the ETC may produce non-conservative estimates of the embrittlement experienced by materials used to construct the RPV that is being evaluated. For this reason, methods to assess the statistical significance of these deviations are described in Sections 5.4.1 through 5.4.3. Type C deviations, if they are statistically significant, suggest that the surveillance program for the material in question may not provide a reliable indication of embrittlement trends for that material. Because Appendix H to 10 CFR 50 requires the performance of surveillance on the “limiting” (meaning “most irradiation-sensitive”) materials used to construct the RPV beltline, the existence of a Type C deviation is important from a regulatory viewpoint, but not in the context of indicating a potential non-conservatism in the predictions of the ΔT_{30} ETC adopted in the Alternate PTS Rule. For this reason, statistical procedures to detect Type C deviations were not included in the Alternate PTS Rule (see Reference [1]) and, therefore, are not described in Section 5.4.

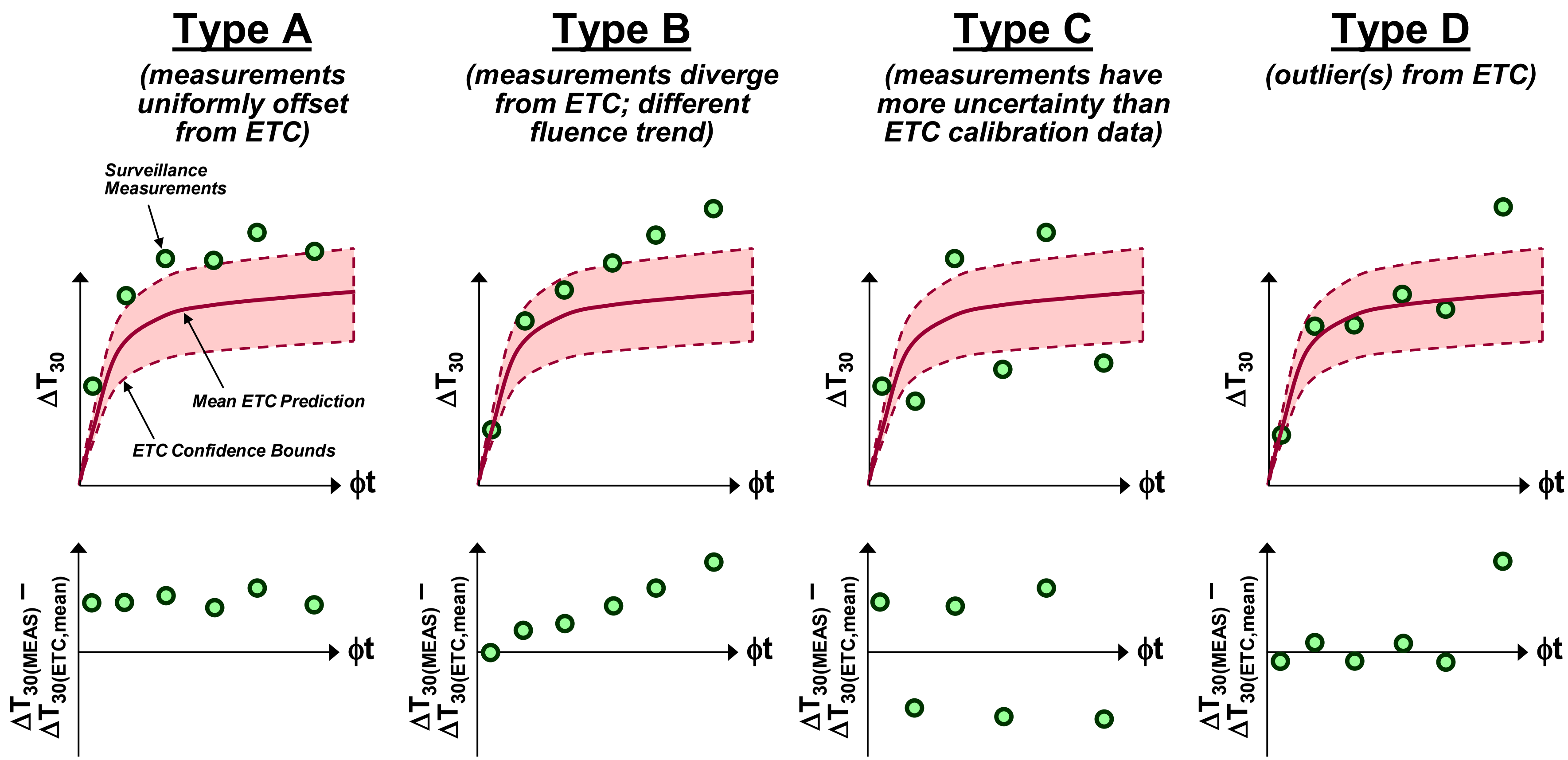

Figure 1. Four Types of Deviation between Heat-Specific Surveillance Data and a ΔT_{30} ETC.

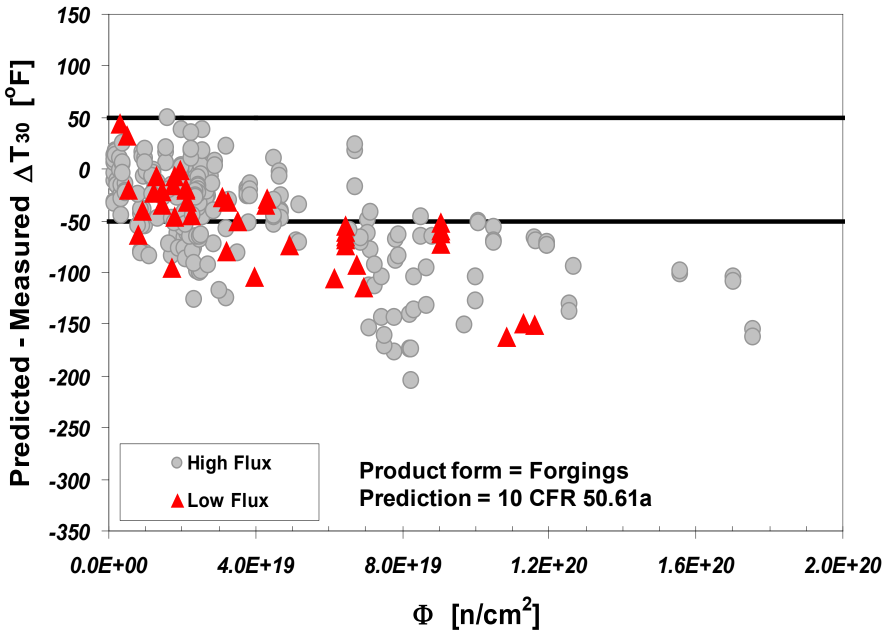

Figure 2. ΔT_{30} Prediction Residuals Based on Eqn. (1). Low flux points are from power reactors while high flux points are from test reactors. Similar trends exist for both plates and welds [15].

5.4 How to Perform Statistical Tests of Surveillance Data

This section describes how to perform the Type A (mean test), Type B (slope test), and Type D (outlier test) assessments of surveillance data that are required by the Alternate PTS Rule.

5.4.1 Type A Deviations

As illustrated by Figure 1, Type A deviations are characterized by measurements that differ from the mean ETC prediction more or less uniformly at all fluence levels. The following procedure can be used to detect Type A deviations when the ΔT_{30} measurements for a specific heat of material are uniformly underpredicted by Eqn. (1). A statistical significance level of α = 1% (i.e., 2.33 standard deviations) is recommended for this one-sided test; Section 5.4.4 discusses the rationale for this selection.

A-1. Ensure that the entry conditions of Section 5.2 have been met.

A-2. Estimate the residual for each datum using the following formula:

$$r = \Delta T_{30(measured)} - \Delta T_{30(predicted)} \qquad (11)$$

where $\Delta T_{30(measured)}$ represents each individual measurement, and $\Delta T_{30(predicted)}$ is the value of ΔT_{30} predicted using Eqn. (1) and best-estimate composition and exposure values for the plant from which the companion $\Delta T_{30(measured)}$ value was obtained.

A-3. Estimate the mean residual (r_{mean}) for the ΔT_{30} dataset using the following formula:

$$r_{mean} = \frac{1}{n}\sum_{i=1}^{n}\{r_i\} \qquad (12)$$

where n is the number of ΔT_{30} measurements for the specific heat of material being assessed.

A-4. Estimate the maximum allowable residual (r_{max}) using the following formula:

$$r_{max} = \frac{2.33\sigma}{\sqrt{n}} \qquad (13)$$

where n is the number of ΔT_{30} measurements for the specific heat of material being assessed and σ is the population standard deviation, which is taken from Table 4.

A-5. If r_{mean} exceeds r_{max}, the subject dataset is judged to show a Type A deviation.

5.4.2 Type B Deviations

As illustrated by Figure 1, Type B deviations are characterized by measurements that differ from the ETC prediction by an amount that increases as fluence increases. The following procedure is used to detect Type B deviations. Similarly to the test for Type A deviations, a statistical significance level of α = 1% is recommended for this one-sided test; Section 5.4.4 discusses the rationale for this selection.

B-1. Ensure that the entry conditions of Section 5.2 have been met.

B-2. For each measured ΔT_{30} value, calculate the difference between the measured and predicted value of ΔT_{30} using Eqn. (11). As illustrated in Figure 3, plot r vs. the $\log_{10}$ value of fluence. The abscissa is expressed in this way because embrittlement, as quantified by ΔT_{30}, increases approximately linearly with the logarithm of fluence.

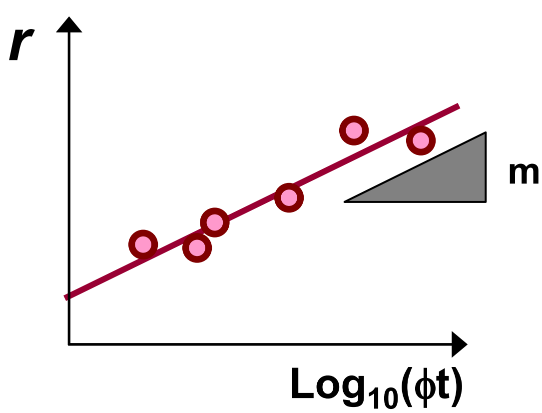

Figure 3. Procedure to Assess Type B Deviations.

B-3. Using the method of least squares, estimate the slope (m) of the data plotted as shown in Figure 3. Also estimate the standard error of the estimated value of the slope, se(m).

B-4. Estimate the T-statistic for the slope as follows:

$$T_m = \frac{m}{se(m)} \quad (14)$$

B-5. Establish the critical T-value as follows:

$$T_{CRIT(\alpha)} \equiv t(\alpha, n-2) \quad (15)$$

where t(…) represents Student's t-distribution, α is the selected significance level, and n is the number of $\Delta T_{30(Measured)}$ values. Adoption of α = 1% is recommended for regulatory implementation of this procedure (Section 5.4.4 discusses the rationale for this selection). Table 6 provides values of $T_{CRIT(1\%)}$.

Table 6. α = 1% Student's t-Values

Number of ΔT_{30} Values, n	n-2	One-Tailed T_{CRIT} (1%, n-2)
3	1	31.82
4	2	6.96
5	3	4.54
6	4	3.75
7	5	3.36
8	6	3.14
9	7	3.00
10	8	2.90
11	9	2.82
12	10	2.76
13	11	2.72
14	12	2.68
15	13	2.65

B-6. If T_m exceeds $T_{CRIT(\alpha)}$,the subject dataset is judged to show a Type B deviation.

5.4.3 Type D Deviations

As illustrated by Figure 1, Type D deviations are characterized by one or more of the ΔT_{30} measurements differing significantly from the mean ETC prediction even though all other measurements for the heat of steel being evaluated agree well with the ETC. Similarly to the tests for both Type A and Type B deviations, a statistical significance level of α = 1% is recommended for this one-sided test; Section 5.4.4 discusses the rationale for this selection.

D-1. Ensure that the entry conditions of Section 5.2 have been met.

D-2. Estimate the normalized residual, *r**, for each or the n observations in the ΔT_{30} dataset using the following formula:

$$r^* = \frac{r}{\sigma} \quad (16)$$

where *r* is defined from Eqn. (11) and σ is the population standard deviation taken from Table 4.

D-3. Find the largest and second largest *r** values from Step D-2; designate these r^*_1 and r^*_2 respectively.

D-4. Find the limit values $r_{LIMIT(1)}$ and $r_{LIMIT(2)}$ corresponding to n in Table 7. These threshold values correspond to a significance level of α = 1%. Appendix A of this document describes how the values of C_1 and C_2 that appear in Table 7 were derived.

D-5. If $r^*_1 \leq r_{LIMIT(1)}$ and $r^*_2 \leq r_{LIMIT(2)}$, the dataset is judged to not show a Type D deviation. Otherwise the surveillance dataset is judged to show a Type D deviation.

Table 7. α = 1% Threshold Value for the Outlier Test

n	$r_{LIMIT(2)}$	$r_{LIMIT(1)}$
3	1.55	2.71
4	1.73	2.81
5	1.84	2.88
6	1.93	2.93
7	2.00	2.98
8	2.05	3.02
9	2.11	3.06
10	2.16	3.09
11	2.19	3.12
12	2.23	3.14
13	2.26	3.17
14	2.29	3.19
15	2.32	3.21
17	2.37	3.24
26	2.53	3.36
64	2.83	3.62
Note: In Appendix A, $r_{LIMIT(1)}$ is referred to as C_2 and $r_{LIMIT(2)}$ is referred to as C_1. The notation is changed here to improve clarity.		

5.4.4 Comments on the Statistical Tests

The significance level recommended for regulatory implementation of the Type A, B, and D tests is α = 1%. At this significance level, there is less than a 1% chance that the underlying cause of the detected difference (Type A, B, or D) between the plant-specific surveillance data and the value of ΔT_{30} predicted by Eqn. (1) has occurred as a result of chance alone. The following considerations informed this recommendation:

- A 1% significance level makes it more difficult for plant-specific surveillance data to be declared “different” from the predictions of the ETC than has traditionally been the case. For example, both 10 CFR 50.61 [3] and Revision 2 of Regulatory Guide 1.99 [16] use a “2σ” criterion which, for a one-sided test, implies an α = 2.5% significance level. The staff views this change in significance level from 2.5% to 1% as appropriate in view of the greater physical and empirical support of Eqn. (1) than was available at the time both 10 CFR 50.61 and Revision 2 of Regulatory Guide 1.99 were adopted.
- The selection of the α = 1% significance level represents a conscious tradeoff between the competing goals of providing high confidence in the determination of a statistically significant difference between plant-specific surveillance data and the predictions of Eqn. (1) versus limiting the risk of judging that a particular set of plant-specific

surveillance data are similar to the ΔT_{30} ETC when, in fact, they are not. The former goal is achieved by adopting a small value for α, whereas the latter goal is achieved by increasing the α value.

- If a plant-specific data set is determined by these statistical tests to be “different” from the predictions of Eqn. (1), the alternatives that are available to licensees to either troubleshoot the cause of the difference or develop new/replacement data are limited, expensive, or have long lead times. Consequently, while the NRC recognizes that it is important to compare plant-specific data to generic trends and to take action when such comparisons show differences, the NRC believes it is technically justified to reserve such actions for those cases in which the differences are the most clear and are the most practically significant.

Considering all of these factors, a significance level for Type A, B, and D deviations of α = 1% was adopted in the Alternative PTS Rule.

5.5 Evaluation of Plant Data Relative to the Statistical Tests

The information presented in this section appeared previously in Reference [14]. It is repeated here for clarity and completeness.

The plant surveillance data used in ORNL/TM-2006/530 [9] to calibrate Eqn. (1) were evaluated according to the statistical tests detailed in Section 5.4. After filtering to remove heats having less than three ΔT_{30} observations at three different fluence values, 159 data sets remained for evaluation. These sets included data from both PWRs and BWRs, as well as from plants that are no longer in operation. While the BWR and ex-plant data are not directly pertinent to the Alternate PTS Rule, they were retained in this analysis for information. The detailed results of these analyses appear in Appendix B.

Table 8 summarizes the 14 heats of material from 12 plants that show a statistically significant deviation of Type A, B, or D, while Table 9 summarizes the proportion of heats in the surveillance database that exhibit statistically significant deviations at the α = 1% level. The information in Table 9 demonstrates that both the mean and the outlier tests exhibit a rate of deviation above the expected value for a population of 159 data sets (i.e., 1% of 159, or 1.59), while the deviation rate of the slope test is close to this expected value. These observations suggest that, for the mean and outlier tests, the assumption that the residuals are distributed normally about the ETC (Eqn. (1)) may be incorrect. One possible explanation for this situation could be the presence of systematic biases in some of the unirradiated T_{30} values (arising from, for example, measurement error or imprecision). Such biases, if present, would have no effect on the detection rate of the slope test because it operates on the differences between ΔT_{30} residuals, not on their absolute values. Thus, any systematic biases in the unirradiated ΔT_{30} values would be subtracted out of the ΔT_{30} difference values that are used to perform the slope test and, consequently, could not affect the outcome of the test. Conversely, the mean and outlier tests both operate on the absolute values of ΔT_{30} residuals. Consequently, systematic biases in the unirradiated values of ΔT_{30} could affect the normalcy of the ΔT_{30} residuals and, thereby, the detection rate of the mean and outlier tests.

Table 8. Heats of Material that Exhibit Statistically Significant Deviations (α = 1%) of Type A, B, or D

Plant Name	Heat ID	Product Form	Population σ (°F)	Number of ΔT_{30} Values	Test Results		
					A - Mean Test	B - Slope Test	D - Outlier Test
Operating PWRs							
San Onofre Unit 3	PSO301	Plate	18.6	3	FAIL	PASS	FAIL
D.C. Cook 2	PCK201	Plate	21.2	8	FAIL	PASS	PASS
Beaver Valley 1	PBV101	Plate	21.2	8	FAIL	PASS	FAIL
Callaway	WCL101	Weld	18.6	4	FAIL	PASS	FAIL
Surry 1	WSU101	Weld	26.4	3	FAIL	PASS	FAIL
Indian Point 2	PIP203	Plate	21.2	3	FAIL	PASS	PASS
Sequoyah 1	FSQ101	Forging	19.6	8	FAIL	PASS	PASS
Sequoyah 1	WSQ101	Weld	26.4	4	FAIL	PASS	PASS
Sequoyah 2	WSQ201	Weld	26.4	4	PASS	PASS	FAIL
Operating BWRs							
River Bend 1 and Oyster Creek	WRB01	Weld	18.6	3	FAIL	PASS	FAIL
Decommissioned PWRs							
Maine Yankee	PMY01	Plate	21.2	6	FAIL	PASS	PASS
Zion 1	WZN101	Weld	18.6	5	PASS	FAIL	PASS
Decommissioned BWRs							
Big Rock Point	PBR01	Plate	21.2	5	FAIL	FAIL	FAIL

Table 9. Proportion of Material Heats in the Current Surveillance Database that Exhibit Statistically Significant Deviations (α = 1%) of Type A, B, or D

Test Type		Data Sets that Show Statistically Significant (α = 1%) Deviation	
		Count	Percent
A	Mean Test	11	6.9%
B	Slope Test	2	1.3%
D	Outlier Test	7	4.4%

5.6 Considerations When Statistical Tests Are Failed

Failure of plant-specific surveillance data to pass any of these statistical tests indicates a situation in which Eqn. (1) may underestimate the embrittlement magnitude; use of Eqn. (1) in such situations without additional justification is not advised. Such failures suggest that more focused assessment of the surveillance data is warranted, and are taken as an indication that methods other than, or in addition to, the ETC may be needed to reliably predict ΔT_{30} trends. However, the most appropriate approach may not be a heat-specific adjustment of the ETC predictions in all cases. For example, statistically significant differences may indicate situations in which the available data (i.e., the ΔT_{30} measurements and/or the composition and exposure values associated with the ΔT_{30} measurements) are incorrect, making adjustment of the ETC predictions to match these data unwise.

The discussion of this section is divided into two parts. First, a list of factors is provided that could be helpful in diagnosing the reason that the surveillance data failed the statistical tests. This is followed by a discussion of situations in which adjustments of the ETC predictions may be made using simple procedures.

5.6.1 Factors to Consider When Statistical Tests Are Failed

Before adjustments of the ETC predictions to match surveillance data are considered, a detailed assessment of the accuracy and appropriateness of the ΔT_{30} data is suggested. Such an assessment should consider, but not be limited to, the following factors:

- Unirradiated RT_{NDT} value: As noted in Section 5.5, the occurrence of mean and outlier failures in the available surveillance data exceeds the statistically expected value. Both of these tests are sensitive to the accuracy of the unirradiated RT_{NDT} value. In these cases, a records investigation of the unirradiated RT_{NDT} value, and/or the performance of additional testing of archival material may provide a more accurate estimate of RT_{NDT}, which may explain the reason for failure of the mean and/or outlier tests.
- Irradiated ΔT_{30} values: While most CVN energy vs. temperature curves from which ΔT_{30} values are estimated are based on 8 to 12 individual measurements, some data sets are more limited, which can increase uncertainty in the ΔT_{30} estimate. If any of the statistical tests are not satisfied, a review of the individual CVN energy vs. temperature curves may help to reveal the cause of the failure.
- Composition and exposure variables: The input variables to Eqn. (1) are subject to variability and are often based on limited data. However, the predictions of Eqn. (1) depend on these input variables, particularly Cu content, fluence, temperature, and Ni content. If a sensitivity analysis reveals that small variations of the values input to Eqn. (1) rationalize the failure of the statistical tests, this might indicate that more refined information concerning input values (e.g., additional measurements) could explain the reason for the failure of the statistical tests.
- Notch orientation: The ΔT_{30} value for plate and forging materials is sensitive to the orientation of the notch in the CVN specimen relative to the primary working direction of the plate or forging. Differences in notch orientation between the unirradiated ΔT_{30} value and the ΔT_{30} value of all the irradiated specimens could help to explain why the mean test is not satisfied. Similarly, differences in notch orientation between the unirradiated ΔT_{30} value and the ΔT_{30} value of the irradiated specimens in a single capsule could help to explain why the outlier test is not satisfied. In these situations, the outcome of a

records search or metallurgical investigation of the tested specimens might be useful to explain the reason for the failure of the statistical tests.

- Comparative trends analysis: In addition to CVN specimens, surveillance capsules also contain tensile specimens that are part of the capsule testing program. Like ΔT_{30}, the increase in yield strength with irradiation (ΔYS) also follows certain trends. If the ΔYS data for a particular material that failed the statistical tests follows the trends exhibited by ΔYS data for a similar composition, this information might indicate that the CVN specimens were taken from the wrong material, or have been somehow mislabeled.

5.6.2 Specific Procedures

If a statistical test is failed, it is permissible to use any of the following procedures:

1. Mean Test (Type A) Failure: A procedure to adjust ETC predictions to account for a failure of the mean test is illustrated in Figure 4 (left side). This procedure is as follows:

   a. Calculate the value *ADJ* as follows:

   $$ADJ = r_{mean} - r_{\max} \qquad (17)$$

   b. Adjust the prediction of Eqn. (1) as follows:

   $$\Delta T_{30(ADJ)} = MD + CRP + ADJ \qquad (18)$$

   c. Use the value $\Delta T_{30(ADJ)}$ in place of ΔT_{30} in all calculations required by the Alternate PTS Rule for the material that failed the mean test.

2. Slope Test (Type B) Failure: One procedure for adjusting ETC predictions to account for a failure of the slope test is to adjust the ETC predictions, Eqn. (1), based on the greater increase of embrittlement with fluence suggested by the plant-specific data. The specific procedure used should be technically justified and documented.

3. Outlier Test (Type D) Failure (Not Satisfied at Low Fluence): Figure 4 (right side) illustrates a situation in which a ΔT_{30} value measured at low fluence is the cause of failing the outlier test. Such a failure is not considered structurally relevant to a PTS evaluation, and may therefore be ignored, provided both of the following conditions are satisfied:
   a. The fluence of the datum that caused the outlier test failure, ϕt_{LOW}, is less than 10% of the fluence at which the PTS evaluation is being performed, ϕt_{EVAL}, and
   b. After elimination of the datum measured at ϕt_{LOW}, the entry conditions for the surveillance tests are still met (i.e., at least three data points measured at three different fluence levels remain) and all three statistical tests are satisfied with the reduced data set.

Other approaches to assessment of surveillance data in which all surveillance measurements are bounded are subject to review and approval by the NRC.

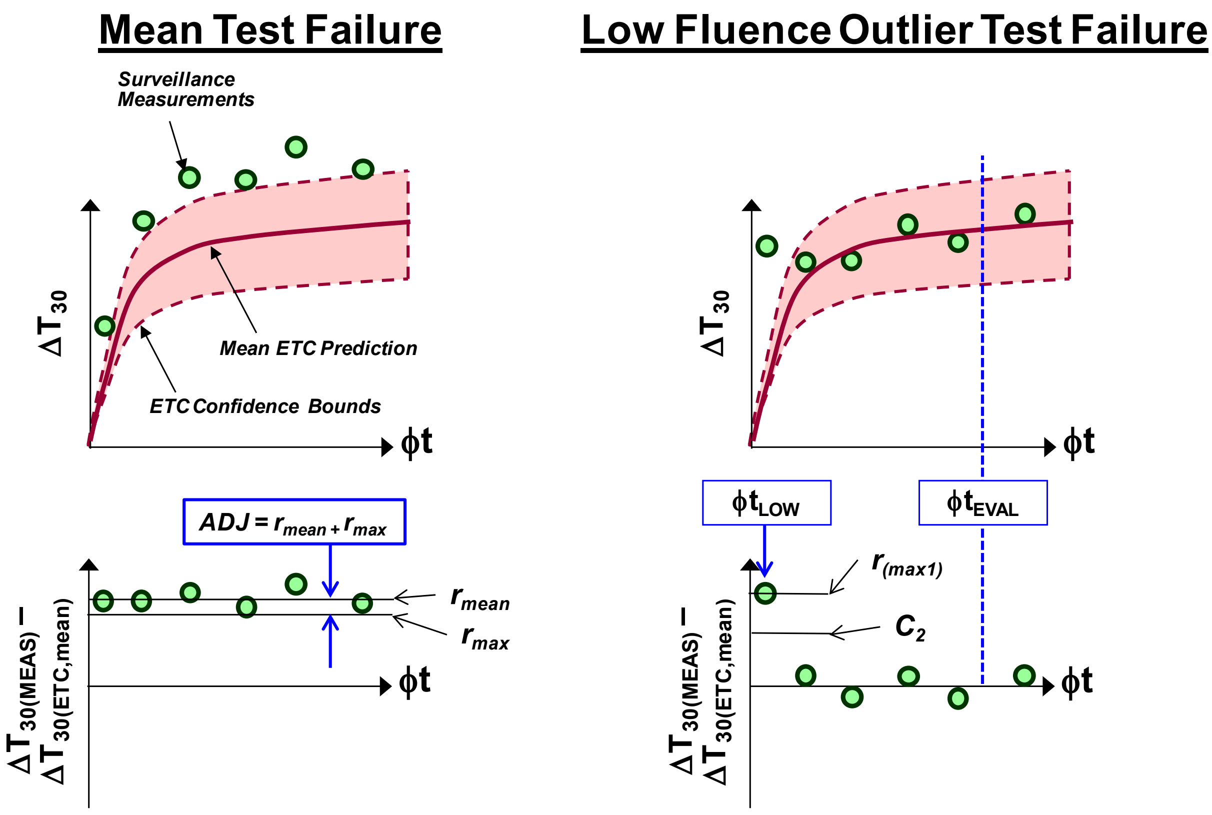

Figure 4. Specific Procedures to Account for Failure of the Mean Test (left) or Low Fluence Outlier Statistical Test (right).

5.7 Summary and Conclusions

This chapter discusses the three statistical tests required by the Alternate PTS Rule and methods by which data can be evaluated relative to these tests. The aim of performing these tests is to determine whether the surveillance data are sufficiently "close" to the predictions of the ETC that the predictions of the ETC may be used. From a regulatory perspective, it is of particular interest to determine whether plant-specific surveillance data deviate significantly from the predictions of the ETC in a manner that suggests that the ETC is likely to underpredict plant-specific trends. To this end, a statistical significance level of α = 1% was adopted, which represents a conscious tradeoff between the competing goals of providing high confidence in the determination of a statistically significant difference between plant-specific surveillance data and the ΔT_{30} ETC versus limiting the risk of judging that a particular set of plant-specific surveillance data are similar to the ETC when, in fact, they are not. The α = 1% tests will show fewer statistically significant deviations than did either 10 CFR 50.61 or Revision 2 of Regulatory Guide 1.99, both of which use a "2σ" criterion that, for a one-sided test, implies an α = 2.5% significance level. The staff views this change in significance level (from 2.5% to 1%) as appropriate in view of the greater empirical support for the ETC used in the Alternate PTS Rule than was available at the time either 10 CFR 50.61 or Regulatory Guide 1.99 (Revision 2) were adopted.

Three tests were adopted in the Alternate PTS Rule because they collectively indicate when an underprediction of embrittlement magnitude by the ETC may have occurred. In Appendix B, these statistical tests are applied to the operating plant surveillance database assembled through (approximately) 2002. Of the heats of material considered, only 14 heats from 12 plants fail one or more of the three statistical tests. Failure of plant-specific surveillance data to pass any of the statistical tests indicates a situation in which the ETC may underestimate the embrittlement magnitude; use of Eqn. (1) in such situations without additional justification is not advised. Such failures suggest that more focused assessment of the surveillance data is warranted, and are taken as an indication that methods other than, or in addition to, the ETC may be needed to reliably predict ΔT_{30} trends. However, the most appropriate approach may not be a heat-specific adjustment of the ETC predictions in all cases. For example, statistically significant differences may indicate situations in which the available data (i.e., the ΔT_{30} measurements and/or the composition and exposure values associated with the ΔT_{30} measurements) are incorrect, making adjustment of the ETC predictions to match these data unwise. This chapter includes both a list of factors that could be helpful in diagnosing the reason that the surveillance data fail the statistical tests and a discussion of certain situations for which adjustments of the ETC predictions can be made.

6. GUIDANCE RELATING TO ISI DATA AND NDE REQUIREMENTS

6.1 Background

The technical basis for the Alternate PTS Rule concludes that flaws as small as 0.1 inch in through-wall extent contribute to the TWCF, and nearly all of the contributions come from flaws buried less than 1 inch below the inner diameter surface of the reactor vessel wall. Therefore, the Alternate PTS Rule specifies flaw limits for such flaws as indicated in Table 2 in this document. For weld flaws that exceed the sizes prescribed in Table 2, the risk analyses indicated that a single flaw contributes a significant fraction of the 1×10^{-6} per reactor year limit on TWCF. Therefore, if a flaw that exceeds the sizes and quantities described in the flaw tables is found in a reactor vessel, it is important to assess it individually.

The technical basis for the Alternate PTS Rule also indicated that flaws buried deeper than 1 inch from the clad-to-base interface did not contribute as significantly to total risk as flaws of similar size located closer to the inner surface. Therefore, the Alternate PTS Rule does not require the comparison of the density of these flaws, but still requires large flaws, if any are discovered, to be evaluated for contributions to TWCF if they are within the inner three-eighths of the vessel wall's thickness. Because flaws greater than three-eighths of the vessel wall's thickness from the inside surface do not contribute to TWCF, flaws greater than three-eighths of the vessel wall's thickness from the inside surface need not be analyzed.

The limitation for flaw acceptance, specified in Table IWB-3510-1 in Section XI of the ASME Code, approximately corresponds to the threshold for flaw sizes that can make a significant contribution to TWCF if flaws of such sizes are present in reactor vessel material at this depth. Therefore, the final rule requires that flaws exceeding the size limits in Table IWB-3510-1 be evaluated for their contribution to TWCF in addition to the other evaluations for such flaws that are prescribed in the ASME Code.

Paragraph (e) of the Alternate PTS Rule describes a number of tests and conditions on the collection and analysis of NDE data that are intended to provide reasonable assurance that the distribution of flaws assumed to exist in the probabilistic fracture mechanics (PFM) calculations that provided the basis for the RT_{MAX-X} limits in Table 1 in this document provide an appropriate, or bounding, model of the population of flaws in the RPV of interest. These tests and conditions, the totality of which are illustrated by the diagram in Figure 5 in this document, go beyond a simple comparison of the NDE data to the flaw table limits in Table 2.

A summary of the process depicted in Figure 5 is as follows:

Step A: All plant-specific recordable flaw data (see Figure 6) should be collected for the inner three-eighths of the wall thickness (3/8t) for the base material and weld metal examination volumes[†] within the RPV beltline region by performing ultrasonic test (UT) volumetric examinations and by using procedures, equipment, and personnel required by Supplements 4 and 6 to Mandatory Appendix VIII to Section XI of the ASME Code.

[†] Any flaws that are detected within the ultrasonic transducer scan paths but are located outside the examination volume required by Section XI of the ASME Code should also be included in the flaw table evaluation.

Step B: The plant-specific flaw data from Step A should be evaluated for axial flaw surface connection. Any flaws with a through-wall extent greater than or equal to 0.075 inch, axially oriented and located at the clad-to-base-metal interface, should be verified to not be connected to the RPV inner surface using surface-examination techniques capable of detecting and characterizing service-induced cracking of the RPV cladding. Eddy current and visual examination methods are acceptable to the staff for detection of cladding cracks. An appropriate quality standard shall be implemented to ensure that these examinations are effective at identification of surface cracking as required by Criterion IX, "Control of Special Processes," in Appendix B to 10 CFR 50. This requires, in part, that measures are established to assure that special processes, including nondestructive testing, are controlled and accomplished by qualified personnel using qualified procedures in accordance with applicable codes, standards, specifications, criteria, and other special requirements. Appropriate quality standards for implementation of surface examinations are identified in Section V, "Nondestructive Examination," and Section XI of the ASME Code.

Step C: If the results of Step B are acceptable, the plant-specific flaw data should be evaluated for acceptability in accordance with the flaw-acceptance standards in Table IWB-3510-1 in Section XI of the ASME Code.

Step D: If the results of Step C are satisfactory, or if the results of Step F (if applicable) are acceptable, the plant-specific flaw data should be compared to Tables 2 and 3 of the Alternate PTS Rule. A specific example of how this step may be performed is shown in Section 6.3.

Step E: If the results of Step B indicate that any axial flaw with a TWE greater than 0.075 inch are connected to the RPV inner surface, or if the results of Step F (if applicable) are not acceptable, other plant-specific assessment is required and the provisions of the Alternate PTS Rule may not be used.

Step F: If the evaluation associated with Step C is not successful (i.e., if any flaws exceed the flaw-acceptance standards in Table IWB-3510-1), the flaws must be evaluated and found to be acceptable in accordance with the flaw-evaluation methods in Section XI of the ASME Code, and the flaws must be evaluated for acceptability according to 10 CFR 50.61a (see Step I).

Step G: If the results of Step D are not acceptable, NDE uncertainties may be accounted for in the evaluation. Appendix C describes the development and application of one methodology acceptable to the staff that accounts for uncertainties in NDE data. This method may be used for the purpose of developing more realistic vessel-specific flaw depth and density distributions for comparison to Tables 2 and 3 of the Alternate PTS Rule, as well as for use in a plant-specific PFM analysis. The methodology considers flaw-sizing error, a flaw-detection threshold, POD, and a prior flaw-distribution assumption. It uses a Bayesian updating methodology to combine the observed NDE data with the available flaw data and models used as part of the PTS re-evaluation effort. The licensee must submit the adjustments made to the volumetric test data to account for NDE-related uncertainties as described in 10 CFR 50.61a(c)(2).

Step H: The revised flaw distribution results of Step G should be used to compare the revised plant-specific flaw data to Tables 2 and 3 of the Alternate PTS Rule.

Step I: If the results of Step H are not acceptable, all flaws should be evaluated for acceptability using one of the following approaches:

1. *Preclusion of brittle fracture*. Satisfactory demonstration of upper shelf behavior, which precludes brittle fracture, can be based on keeping temperature above RT_{NDT} + 60°F using the following steps:
    i. Compute the irradiated RT_{NDT} for all flaws as follows:
        - Determine the unirradiated value of RT_{NDT} and $RT_{NDT(u)}$ for the material at each flaw location.
        - Determine the fluence at each flaw location.
        - Compute ΔT_{30} for each flaw using Eqn. (1) and the fluence at each flaw location.
        - Compute the flaw-specific value of RT_{NDT} as $RT_{NDT(u)} + \Delta T_{30}$ for each flaw.

    ii. Assuming a lower-bound PTS transient temperature of 75°F, upper shelf behavior is assured if $RT_{NDT} + 60 \leq 75$°F. Therefore, the flaw-specific value of RT_{NDT} should be less than or equal to 15°F.

    iii. The evaluation associated with Step I is acceptable if the flaw-specific value of RT_{NDT} is less than or equal to 15°F for all flaws.

2. *Calculate the plant-specific TWCF using a plant-specific PFM analysis*. A plant-specific PFM analysis to calculate TWCF is complex, and there are many variations of inputs possible for such an analysis. Therefore, specific guidance for plant-specific PFM analysis to calculate TWCF is not included in this document. General considerations to include in a plant-specific PFM analysis are provided in Section 6.2.2. A discussion of the methodology that was used in performing TWCF calculations for PTS may be found in NUREG-1806 [6], NUREG-1807 [21], and NUREG/CR-6854 [22]. The steps associated with conducting a plant-specific PFM calculation are as follows:
    i. Perform a Bayesian update of the flaw distribution:
        - Apply the procedures of Appendix C and obtain revised flaw-depth and flaw-density parameters (similar to those shown in Table 16).

    ii. Calculate the TWCF using a PFM computer code (e.g., the code in ORNL/TM-2012/567, "Fracture Analysis of Vessels – Oak Ridge FAVOR, v12.1, Computer Code: Theory and Implementation of Algorithms, Methods, and Correlations" [20]):
        - Run the generalized procedure for generating flaw-related inputs for the FAVOR Code described in NUREG/CR-6817 [19] using the revised flaw-depth and flaw-density parameters.
        - Develop necessary plant-specific input using the guidance in NUREG-1806 [6], NUREG-1807 [21], and NUREG/CR-6854 [22].
        - Run a plant-specific PFM analysis.
        - Calculate the TWCF.

    iii. Compare the plant-specific TWCF to the TWCF limit specified in the Alternate PTS Rule:
        - The evaluation associated with Step I is acceptable if the calculated TWCF is less than or equal to the limit of 1×10^{-6} events per reactor year specified in the Alternate PTS Rule.

Step J: If the results of Step I are not acceptable, the licensee must perform a plant-specific assessment for PTS and submit the assessment to the Director of the Office of Nuclear Reactor Regulation for review and approval.

Step K: If the results of Step D or (if applicable) Step H or (if applicable) Step I are satisfactory, the screening criteria contained in Table 1 of the Alternate PTS Rule may be applied to the plant in question. The plant-specific assessment, including explicit details and results, must be submitted to the Director of the Office of Nuclear Reactor Regulation for review and approval in the form of a license amendment at least three years before RT_{MAX-X} is projected to exceed the Alternate PTS Rule screening criteria.

Based on this process, the guidelines discussed in this chapter include the following components:

1. Guidance for plants for the case in which RPV flaws fall outside the applicability of the flaw tables in the Alternate PTS Rule, including:
   i. Guidance on a procedure to preclude brittle fracture.
   ii. Guidance on considerations to include in a plant-specific PFM analysis.
2. Guidance for initial evaluation of NDE data obtained from qualified ISI examinations.
3. Guidance on methods for further evaluation of NDE data obtained from qualified ISI examinations, including:
   i. Guidance on the elements and NDE techniques associated with the qualified ISI examinations performed in accordance with Mandatory Appendix VIII to Section XI of the ASME Code to assess compliance with the requirements of the Alternate PTS Rule.
   ii. Guidance on a mathematical procedure that can be used to adjust NDE data to account for flaw-detection and sizing errors, as well as guidance on comparison of the adjusted data to the population of flaws assumed in the PFM analysis used to develop the Alternate PTS Rule.

Guidance for these topics is described in detail in the following sections.

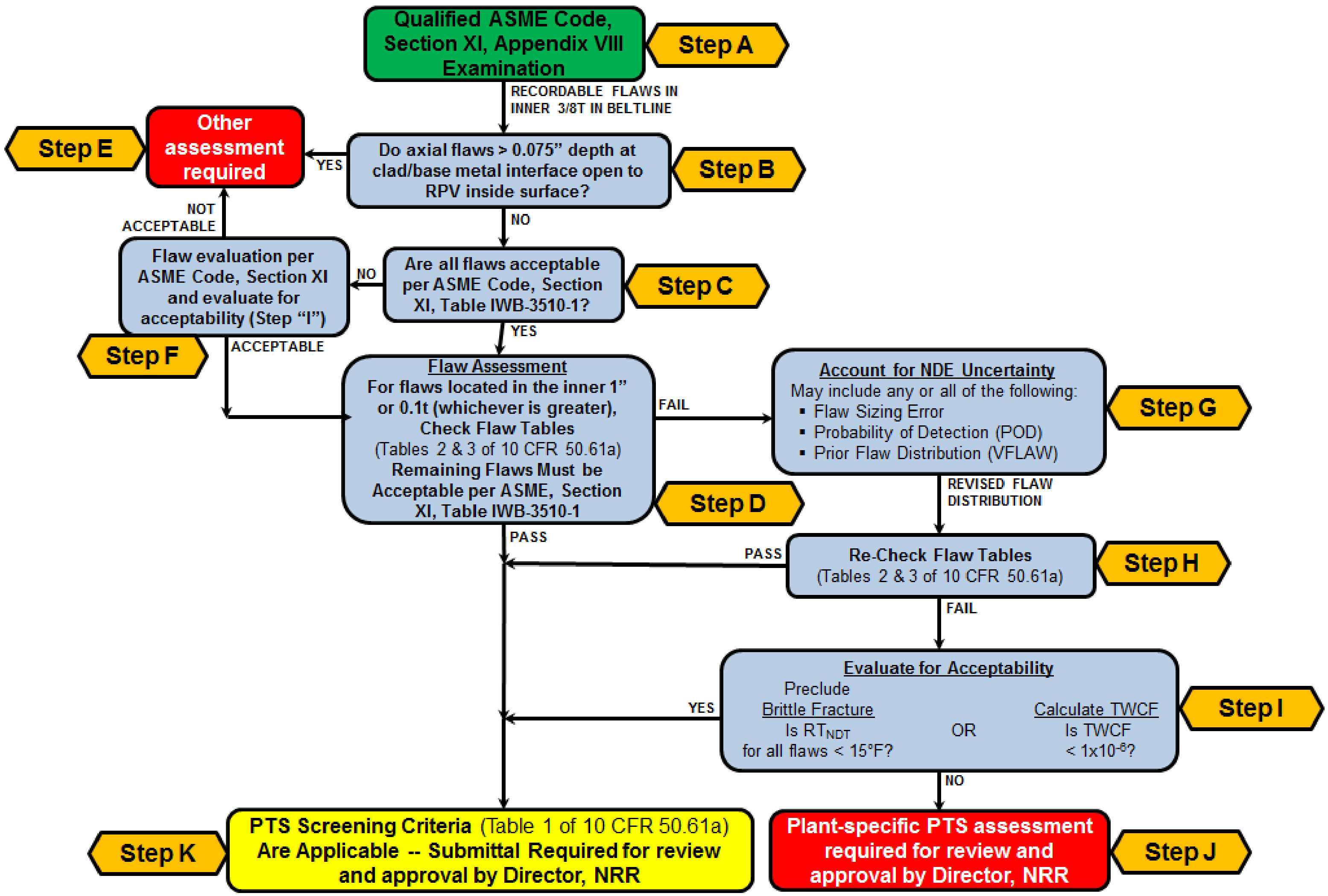

Figure 5. Flow Diagram with Recommendations for Meeting the Requirements of the Alternate PTS Rule.

6.2 Guidance on Criteria Relating to Alternate Limits on Embrittlement

This section describes guidance for situations in which plant-specific NDE results do not meet the acceptance standards of Table IWB-3510-1 in Section XI of the ASME Code or are not within the limits prescribed by the flaw tables in the Alternate PTS Rule. In such situations, additional efforts beyond those described in Section 6.1 may still allow application of the PTS Screening Criteria shown in Table 1 in this document.

The guidelines discussed in this section include the following components:

- Guidance on a procedure that can be used to preclude brittle fracture based on RT_{NDT} information for RPV flaws that fall outside the applicability of the Alternate PTS Rule flaw tables.
- Guidance on a procedure that can be used to combine the NDE data with the population of flaws assumed in the TWCF calculations to estimate a total flaw distribution that is predicted to exist in the RPV, as well as guidance on the use of the total flaw distribution if a licensee chooses to conduct a PFM calculation.

These topics are described in detail in the following sections.

6.2.1 Guidance on a Procedure to Preclude Brittle Fracture

Guidance on a mathematical procedure to preclude brittle fracture for flaws that exceed the acceptance standards of Table IWB-3510-1, as identified by Step I in Figure 5 in this document, is provided in this section. Such guidance is based on Section II, "Discussion," provided in the Supplemental Information section of the Federal Register Notice for the Alternate PTS Rule [2], which includes the following discussion with respect to ISI Volumetric Examination and Flaw Assessments:

> *The technical basis for the final rule also indicates that flaws buried deeper than 1 inch from the clad-to-base interface are not as susceptible to brittle fracture as similar size flaws located closer to the inner surface. Therefore, the final rule does not require the comparison of the density of these flaws, but still requires large flaws, if discovered, to be evaluated for contributions to TWCF if they are within the inner three-eighths of the vessel thickness. The limitation for flaw acceptance, specified in ASME Code, Section XI, Table IWB-3510-1, approximately corresponds to the threshold for flaw sizes that can make a significant contribution to TWCF if present in reactor vessel material at this depth. Therefore, the final rule requires that flaws exceeding the size limits in ASME Code, Section XI, Table IWB-3510-1 be evaluated for contribution to TWCF in addition to the other evaluations for such flaws that are prescribed in the ASME Code.*

A simplified procedure is described here for the situation in which the as-found NDE data for a plant reveals that one or more flaws fall outside the maximum range of the Alternate PTS Rule flaw tables, and that the flaws do not satisfy ASME Code Section XI flaw-acceptance criteria. Therefore, the following situation results:

- The NDE data was obtained using a qualified examination in accordance with Appendix VIII of Section XI of the ASME Code, thereby satisfying Step A in Figure 5.

- All recordable flaws are located away from the clad-to-base-metal interface. Therefore, Step B is satisfied with a result of “NO” in Figure 5.
- Some of the recordable flaws do not meet ASME Code Section XI flaw-acceptance criteria. Therefore, Step C is not satisfied with a result of “NO” in Figure 5.

Thus, based on the above, Step F in Figure 5 requires that flaw evaluation be performed with acceptable results in accordance with ASME Code Section XI for those recordable flaws that do not meet ASME Code Section XI flaw-acceptance criteria. In addition, further evaluation for acceptability using Step I is required. For the purposes of this example, it is assumed that flaw evaluation in accordance with ASME Code Section XI is successful and is not described in the assessment that follows.

For the further evaluation required by Step I in Figure 5, one approach is to determine whether brittle fracture can be precluded. For this situation, a recommended evaluation could be as follows:

- <u>Step I - Preclude Brittle Fracture Option</u>:
  - Satisfactory demonstration of upper shelf behavior, which precludes brittle fracture, can be based on maintaining temperature above RT_{NDT} + 60°F [23].
  - Compute the irradiated RT_{NDT} for all flaws as follows:
    - Determine the unirradiated value of RT_{NDT} and $RT_{NDT(u)}$ for the material at each flaw location.
    - Determine the fluence at each flaw location.
    - Compute ΔT_{30} for each flaw using Eqn. (1) and the fluence at each flaw location.
    - Compute the flaw-specific value of RT_{NDT} as $RT_{NDT(u)} + \Delta T_{30}$ for each flaw.
  - Assuming a lower-bound PTS transient temperature of 75°F, upper shelf behavior is assured if $RT_{NDT} + 60 \leq 75$°F. Therefore, the flaw-specific value of RT_{NDT} should be less than or equal to 15°F.
  - Flaws are acceptable if the flaw-specific value of RT_{NDT} is less than or equal to 15°F. For this situation, the decision at Step F is “ACCEPTABLE” in Figure 5.
  - Flaws are not acceptable if the flaw-specific value of RT_{NDT} is greater than 15°F. For this situation, the decision at Step F is “NOT ACCEPTABLE” in Figure 5, other assessment is required (Step E in Figure 5), and the provisions of the Alternate PTS Rule may not be used.
- For the case in which Step F is “ACCEPTABLE”, all recordable flaws less than the maximum of 0.1t or 1.0" must be checked against the flaw tables (Step D in Figure 5).
- If the result of Step D is “PASS,” the RT_{MAX-X} limits of the Alternate PTS Rule may be used (Step K in Figure 5).

A sample calculation demonstrating acceptability by the “Preclude Brittle Fracture” option in Step I is demonstrated in Table 10.

Table 10. Sample Brittle Fracture Assessment

STEP D: Preclude Brittle Fracture for J-2 Flaws

Flaw No.	Flaw Position			Fluence at Clad/Base Metal Interface at Flaw Location (n/cm^2)[a]	Attenuation Factor, $e^{-0.24x}$	Attenuated Fluence at Flaw Location (n/cm^2)	End-of-Life Effective Full Power Years (EFPY)	Attenuated Flux at Flaw Location (n/cm^2-sec)
	Height on RPV (inches)	RPV Circumferential Position (°)	Depth Below Clad, x (inches)					
X	235.00	150.1	1.66	1.02E+19	0.6714	6.85E+18	54.0	4.02E+09
Y	235.14	157.7	2.70	1.02E+19	0.5231	5.34E+18	54.0	3.13E+09

Flaw No.	LINDE 80 Weld Chemistry[b]				
	$RT_{NDT(u)}$ (°F)	Cu (wt %)	Ni (wt %)	Mn (wt%)	P (wt%)
X	-40	0.09	0.48	1.300	0.004
Y	-40	0.09	0.48	1.300	0.004

Flaw No.	Temperature (°F)	ϕt_e Effective Fluence (n/cm^2)	A	B	Max(Cu_e)	Cu_e	f(Cu_e,P)	g(Cu_e,Ni,ϕt_e)	Mfterm (°F)	CRPterm (°F)	ΔT_{30} (°F)	RT_{NDT} (°F)
X	550.0	1.272E+19	1.417E-07	155.0	0.2430	0.0900	0.0683	9.412E-01	29.2	25.6	54.8	14.8
Y	550.0	1.057E+19	1.417E-07	155.0	0.2430	0.0900	0.0683	9.253E-01	26.6	25.2	51.8	11.8

Notes: a. Determined from a plant-specific fluence map.
b. From RPV surveillance program.

6.2.2 Guidance on Considerations to Include in a Plant-Specific PFM Analysis

Guidance on the key considerations that should be included in a plant-specific PFM analysis to calculate TWCF, as identified by Step I in Figure 5, is provided in this section. Such guidance includes a mathematical procedure to combine NDE data with the PFM flaw distribution used to develop the Alternate PTS Rule. A plant-specific TWCF analysis might be necessary based on Section d(4) of the Alternate PTS Rule [1], where the following is stated:

> *(4) If the analysis required by paragraph (d)(3) of this section indicates that no reasonably practicable flux reduction program will prevent the RT_{MAX-X} value for one or more reactor vessel beltline materials from exceeding the PTS screening criteria, then the licensee shall perform a safety analysis to determine what, if any, modifications to equipment, systems, and operation are necessary to prevent the potential for an unacceptably high probability of failure of the reactor vessel as a result of postulated PTS events. In the analysis, the licensee may determine the properties of the reactor vessel materials based on available information, research results and plant surveillance data, and may use probabilistic fracture mechanics techniques...*

The PFM computer code, FAVOR [20], was developed by Oak Ridge National Laboratory (ORNL) under NRC funding to predict failure probabilities for embrittled vessels subject to PTS transients. FAVOR was used in the underlying TWCF analyses performed as a part of the development of the Alternate PTS Rule. Critical inputs to FAVOR are the number and sizes of fabrication flaws in the RPVs of interest and the characteristics of cooldown scenarios. The TWCF analysis further requires the expected frequencies of the cooldown scenarios. Work on flaw distributions was coordinated with another NRC research program conducted by PNNL to perform examinations of RPV materials to detect and measure the numbers and sizes of fabrication flaws in welds and base metal. To supplement the limited data from flaw detection and measurements, PNNL applied an expert judgment elicitation process and the PRODIGAL flaw simulation model developed in the United Kingdom by Rolls-Royce and Associates. PNNL's experimental work on flaw distributions provided fabrication flaw data from nondestructive and destructive examinations, which were used to develop statistical distributions to characterize the numbers and sizes of flaws in the various regions of RPVs. Based on these statistical distributions, PNNL developed a computer program, VFLAW, which generated flaw distributions that were used as inputs to the FAVOR computer code [19]. These input files for FAVOR describe flaw distributions based on PNNL's research activities. The VFLAW program and the incorporation of plant-specific NDE data are therefore critical input elements for performing plant-specific TWCF analyses.

A recommended methodology for combining plant-specific NDE data with the PFM flaw distribution used to develop the Alternate PTS Rule is provided in Appendix C. For the sample application to Beaver Valley 2 discussed in Appendix C (Table C-4), the results of which are repeated in this section in Table 11, revised flaw parameters that represent a plant-specific flaw distribution are shown. The revised parameters on the flaw uncertainty distribution may be used to generate a revised flaw distribution for Beaver Valley 2 that is consistent with the flaw distribution used in the PTS FAVOR analyses. The revised parameters will lead to revised flaw distributions that may be input to a FAVOR PFM analysis. These parameters have been customized using the Appendix C procedure based on Beaver Valley 2's specific geometry and as-found NDE data. The revised flaw distributions may be generated and used as input to FAVOR by re-running the VFLAW program with the revised parameters shown in Table 11. Re-running the VFLAW program allows adjustment of the generic VFLAW flaw distribution used to develop the Alternate PTS Rule into a plant-specific flaw distribution based on the updated knowledge of flaws obtained from plant-specific ISI. As shown in Table 11, this yields a Bayesian updated flaw distribution for use in the plant-specific PFM required at Step I in Figure 5.

As described in Appendix C, it is important to note that the VFLAW data, while representing generic values of flaw characteristics (based on expert judgment and the PVRUF and Shoreham RPVs), should be specialized to a specific RPV by using RPV-specific weld length, weld bead thickness, geometry, and other weld characteristics. Therefore, the specialized VFLAW data that results from this evaluation is the most representative information that can be used to describe a prior distribution of flaw depth and flaw density for a plant-specific PFM assessment. If other prior information is available, such information may also be used instead of, or in addition to, the specialized VFLAW data.

A PFM analysis that calculates TWCF also requires (1) the thermal-hydraulic characteristics of the cooldown scenarios as input to FAVOR and (2) the frequency of those scenarios as input to the TWCF calculation. The characteristics and frequency of excessive cooldown scenarios are not developed by existing probabilistic risk assessments (PRAs), which only model the end states of core damage and containment failure. The PTS rulemaking relied on extensive PRA analyses to explore, identify, and characterize excessive cooldown end states.

A plant-specific PFM analysis that calculates TWCF is complex, and there are many variations of inputs possible for such an analysis. Therefore, guidance for plant-specific PFM analysis to calculate TWCF is not included in this report. A discussion of the methodology that was used in performing a PFM analysis to calculate TWCF for PTS may be found in NUREG-1806 [6], NUREG-1807 [21], and NUREG/CR-6854 [22]. As indicated in the Alternate PTS Rule, plant-specific PFM analysis to calculate TWCF and the description of the modifications made to the plant-specific inputs must be submitted to the Director of NRR in the form of a license amendment at least three years before RT_{MAX-X} is projected to exceed the PTS screening criteria.

The steps associated with conducting a plant-specific PFM evaluation are as follows:

- <u>Bayesian Update of Flaw Distribution:</u>
    - Apply the procedures of Appendix C and obtain revised flaw depth and flaw density parameters (similar to those shown in Table 11).
- <u>Calculate TWCF Using FAVOR:</u>
    - Run VFLAW using the revised flaw depth and flaw density parameters.
    - Develop necessary plant-specific input using the guidance in NUREG-1806, NUREG-1807, and NUREG/CR-6854.
    - Run plant-specific FAVOR analysis.
    - Calculate the TWCF.
- <u>Compare Plant-Specific TWCF from FAVOR Analysis to Limit:</u>
    - If the calculated TWCF value is less than or equal to the limit of 1×10^{-6} per reactor year specified in the Alternate PTS Rule, the NDE data are acceptable and the PTS Screening Criteria in Table 1 may be used (Step K in Figure 5).
    - If the TWCF value is greater than the limit of 1×10^{-6} per reactor year specified in the Alternate PTS Rule, the NDE data are unacceptable and the PTS Screening Criteria in Table 1 may not be used. Alternate actions are required to resolve PTS embrittlement issues, which may include changes to the facility to reduce the likelihood and/or severity of the cooldown transients. Plant-specific PTS assessment is required for review and approval by the Director of NRR (Step J in Figure 5).

Table 11. Summary of the Revised Flaw Depth and Flaw Density VFLAW Parameters to be Used in a Revised PFM Analysis for Beaver Valley 2 (from Appendix C)

Case	**Flaw Size Category**	**Original VFLAW Parameters of Uncertainty Distribution Used in PTS Work** **(Flaw Depth Parameters Specialized to Beaver Valley 2)**	**Revised Parameters of Uncertainty Distribution Based on Beaver Valley 2 NDE Data**
1	Small ($a \le \Delta$)	$\alpha_3 = 0.180$ $\alpha_4 = 1419$	$\alpha'_3 = 0.230$ $\alpha'_4 = 1909$
2	Large ($a > \Delta$)	$\alpha_3 = 0.180$ $\alpha_4 = 4$	$\alpha'_3 = 0.230$ $\alpha'_4 = 5$
3	Small ($a \le \Delta$)	$U_1 = 34$ $U_2 = 8$ $U_3 = 1$	$U'_1 = 513.75$ $U'_2 = 17.71$ $U'_3 = 1.54$
4	Large ($a > \Delta$)	$\alpha_1 = 4.615$ $\alpha_2 = 4$	$\alpha'_1 = 4.563$ $\alpha'_2 = 5$

6.3 Guidance for Initial Evaluation of NDE Data

Guidance for initial evaluation of NDE data obtained from qualified ISI examinations, as identified in Steps A through F in Figure 5, are provided in this section. These steps are expected to be the most common use of the Alternate PTS Rule, and they represent a comparison of the as-reported NDE results with the flaw tables. Successful comparison of the NDE data to the flaw tables provides reasonable assurance that the plant-specific flaw distribution is bounded by the flaw distribution used in the development of the Alternate PTS Rule, therefore justifying application of the alternate PTS screening limits given in Table 1 to the plant in question.

As indicated under Item (e), "Examination and Flaw Assessment Requirements," of the Alternate PTS Rule, the volumetric examination results evaluated under paragraphs (e)(1), (e)(2), and (e)(3) must be acquired using procedures, equipment, and personnel that have been qualified under Supplements 4 and 6 to Mandatory Appendix VIII to Section XI of the ASME Code, as specified in 10 CFR 50.55a(b)(2)(xv). Paragraph (g)(6)(ii)(C) of 10 CFR 50.55a requires licensees to implement Supplements 4 and 6 to Appendix VIII to Section XI of the ASME Code. Supplement 4 contains qualification requirements for the RPV ISI volume from the clad-to-base-metal interface to the inner 15 percent of the RPV base-metal wall thickness. Supplement 6 contains qualification requirements for RPV weld volumes that lie within the outer 85% of the RPV base-metal wall thickness.

Figure 6 shows the ASME Code Section XI examination and flaw-evaluation process and identifies the flaws from that process that should be used for comparison to the Alternate PTS Rule flaw tables. As noted in the figure, the process used to identify flaws for comparison to the flaw tables is a subset of the process outlined in the ASME Code. All recordable flaws, subsequent to application of the flaw proximity rules of Subarticle IWA-3300 in Section XI of the ASME Code, are used for comparison to the Alternate PTS Rule flaw tables [17b].

A sampling of RPV weld examinations (done in accordance with Appendix VIII to Section XI of the ASME Code) from thirteen PWR RPVs is included in Reference [18]. This sampling is a compilation of several RPV beltline weld examinations performed since 2000 that were provided by Westinghouse in response to a request from the NRC. These results form the basis for the example comparison to the flaw tables that is shown in Figure 7 and in Table 12 through Table 15 in this document. A discussion of this figure and these tables is provided in the following paragraphs.

In the example shown in Figure 7 and in Table 12 through Table 15, the following evaluation process was used (Steps A through D and K in Figure 5):

<u>Step A - Qualified Examination in Accordance with Appendix VIII to Section XI of the ASME Code</u>

- The Appendix VIII examination results are shown for Plant J in Figure 7.
- Eleven welds (two girth welds and nine intersecting axial welds) were examined in the RPV beltline region. A total of eight combined recordable flaws (as defined by the process shown in Figure 6) were detected.

<u>Step B - Do Axial Flaws > 0.075" in Depth at the Clad-to-Base-Metal Interface Open to the RPV Inside Surface?</u>

- Based on the S dimension (distance of flaw below the clad-to-base-metal interface) shown in Figure 7 for all flaws, no flaws at the clad-to-base-metal interface require supplemental examination to confirm that they are not connected to the RPV inside surface.
- If supplemental examination is required, perform a demonstrated surface or visual examination of the clad surface within the required ASME Code Section XI

examination volume (e.g., Figures IWB-2500-1 and IWB-2500-2) to identify potential axial indications in the cladding surface that may extend into the base metal. A demonstrated visual or surface examination is one that has been shown to be capable of detecting and characterizing inservice cracking in a clad surface representative of the reactor vessel cladding process. Eddy current test is one examination method acceptable to the staff for performing this verification.

- A method for determining the uncertainty in locating the position of axial flaws identified by surface or visual examination and the location of axial flaws identified by UT examination shall be documented. Any axial flaws located by UT within the uncertainty bounds of an axial crack shall be considered to be the same axial flaw.
- If it is confirmed that no axial flaws are connected to the RPV inside surface, Step B = "NO" in Figure 5.

<u>Step C - Are All Flaws Acceptable According to Table IWB-3510-1 in Section XI of the ASME Code?</u>

- As indicated in Figure 7 (in the column titled "ASME Code Disposition" in the second table), all recordable flaws are acceptable for meeting the requirements of Table IWB-3510-1 in Section XI of the ASME Code. The details of this determination are not shown.
- Therefore, Step C = "YES" in Figure 5.

<u>Step D - For Flaws Located in the Inner 1.0" or 0.1t (Whichever Is Greater), Check Flaw Tables</u>

- *Compute the Total Weld Length Examined*. The total weld examination length is determined in Table 12 based on the circumference of the RPV and the percentage of the weld examined (i.e., the coverage amount) for each of the eleven welds.
- *Compute the Total Plate Surface Area Examined.* The total plate surface area examined is determined in Table 13 based on the surface area of the ASME Code Section XI examination volume less the surface area of the weld for each of the eleven welds examined.
- *Determine the Position of Flaws*. The position of all flaws is determined in Table 14 as follows:
  - Determine whether the flaw resides in plate or weld material. This determination is based on the flaw position with respect to the weld centerline and the maximum crown width[‡] on either surface of the inspected weld; if the flaw position resides within the span of the weld centerline ± one-half of the weld crown width, the flaw was considered to be a WELD flaw. Otherwise, it was treated as a PLATE flaw.
  - Determine whether the flaw resides within the inner one inch or 10% of the base-metal wall thickness, whichever is greater, for comparison to the Alternate PTS Rule flaw tables.
  - Determine whether the flaw resides between the inner one inch or 10% of the base-metal thickness, whichever is greater, and the inner 37.5% of the base-metal wall thickness (3/8t), for potential evaluation of brittle fracture.

[‡] The weld crown width was used in this example for the entire RPV base-metal wall thickness, which can potentially classify flaws located mid-wall as weld flaws rather than plate flaws in single-groove or double-V-groove weld configurations. This approach is conservative with respect to the flaw limits in Table 2. Consideration should also be given to the proximity of the flaw to the weld's heat-affected zone (HAZ). An example might be that any flaw located in the plate material, but within some technically justified minimum distance from the edge of the weld, should be considered to be affected by the HAZ and therefore also considered to be a weld flaw. In addition, if there are any weld-repair areas located within the examination volume, any flaws detected within those areas should be classified as WELD flaws.

    - Based on the results shown in Table 14, two flaws should be compared to the Weld Flaw Table (Table 2) of the Alternate PTS Rule and one flaw should be compared to the Plate/Forging Flaw Table (Table 3) of the Alternate PTS Rule. Although two flaws reside between the inner one inch or 10% of the base-metal thickness, whichever is greater, and the inner 37.5% of the base-metal wall thickness (3/8t) from the clad/base-metal interface, they do not require further assessment for acceptability because they were found to be acceptable in accordance with Table IWB-3510-1.
  - *Flaw Assessment:*
    - The flaws determined in the previous step to be located in the inner 1.0" or 0.1t (whichever is greater) are compared to the flaw tables from the Alternate PTS Rule in Table 15 and found to be acceptable.
    - The remaining two flaws located between the inner one inch or 10% of the base-metal thickness, whichever is greater, and the inner 37.5% of the base-metal wall thickness (3/8t) from the clad/base-metal interface are acceptable in accordance with Table IWB-3510-1.
    - Therefore, Step D = "PASS" in Figure 5.

<u>Step K - PTS Screening Criteria (Table 1 of 10 CFR 50.61a) Is Applicable - Submittal Required</u>

  - Plant J is allowed to use the PTS Screening Criteria shown in Table 1. The licensee must submit their PTS evaluation to the NRC for review and approval.

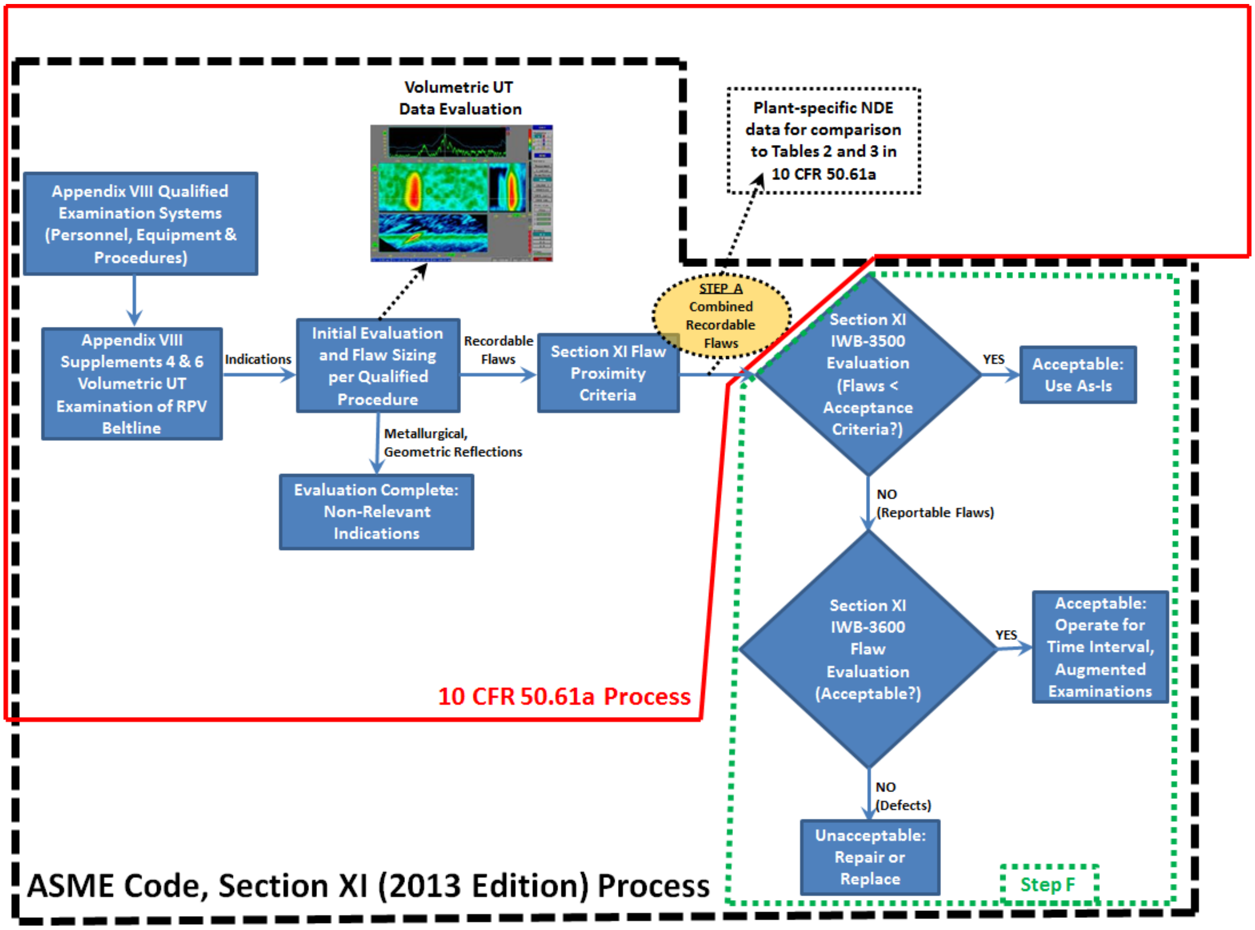

Figure 6. ASME Code Section XI Examination and Flaw Evaluation Process and Identification of Flaws for Comparison to Alternate PTS Rule.

Step A: Plant J Examination Results: (see Westinghouse Letter LTR-AMLRS-11-71 [18])

Reactor Vessel ISI History for Plant J Beltline Materials					
Weld ID	**Description**	**Date Last Inspected**	**Percent Coverage Obtained**	**Number of Recordable Indications**	**Number of Reportable Indications**
J-1	Nozzle Shell to Intermediate Shell Circ. Weld	2004	100	None	None
J-2	Intermediate Shell to Lower Shell Circ.	2004	100	4	None
J-3	Nozzle Shell Longitudinal Seam	2004	100	None	None
J-4	Nozzle Shell Longitudinal Seam	2004	100	None	None
J-5	Nozzle Shell Longitudinal Seam	2004	100	None	None
J-6	Intermediate Shell Longitudinal Seam	2004	100	None	None
J-7	Intermediate Shell Longitudinal Seam	2004	100	1	None
J-8	Intermediate Shell Longitudinal Seam	2004	100	None	None
J-9	Lower Shell Longitudinal Seam	2004	77.80[1]	2	None
J-10	Lower Shell Longitudinal Seam	2004	77.80[1]	None	None
J-11	Lower Shell Longitudinal Seam	2004	77.80[1]	1	None

Note 1: Limitations exist due to core support lugs at bottom of lower shell longitudinal welds.

Reactor Vessel ISI Information for Potential Beltline Flaws Plant J																
Weld Number	Indication No.	Beam Direction	Weld Centerline (in.) or (º)	Weld width (in)	x (in)	θ (°)	2a (in)	a (in)	L (in)	t (in)	S (in)	a/L	AR	a/t (%)	Code Allowable a/t (%)	ASME Code Disposition
J-2	1	DN	235.00 in.	1.65	235.00	150.1	0.16	0.08	2.10	8.60	1.66	0.04	25.0	0.9	2.0	Allowable
	2	UP		1.65	235.14	157.7	0.12	0.06	1.25	8.60	2.70	0.05	20.0	0.7	2.2	Allowable
	3	UP		1.65	235.80	129.3	N/A	0.25	1.00	8.60	0.00[1]	.25	4	2.9	3.3	Allowable
	4	UP		1.65	235.50	332.1	0.24	0.12	1.75	8.60	4.49	0.07	14.3	1.4	2.2	Allowable
J-7	1	CCW	120°	1.38	123.6	123.6	0.22	0.11	2.10	8.60	0.63	0.05	20.0	1.3	7.6	Allowable
J-9	1	DN	60°	1.38	256.50	60.3	0.25	0.13	1.60	8.60	0.11	0.08	12.5	1.5	1.87	Allowable
	2	CCW		1.38	240.30	60.4	0.34	0.17	1.60	8.60	0.79	0.11	9.1	2.0	2.5	Allowable
J-11	1	CCW	300°	1.38	312.61	300.3	0.27	0.14	1.75	8.60	3.60	0.08	12.5	1.6	2.2	Allowable

Note 1: S dimension is from outside diameter surface so this is an OD surface flaw.

Top of core position x=149.1 in.
Bottom of core position x=292.6 in.
Reactor Vessel Inner Diameter (without cladding)= 173 in.
Cladding Thickness= 0.156 in.

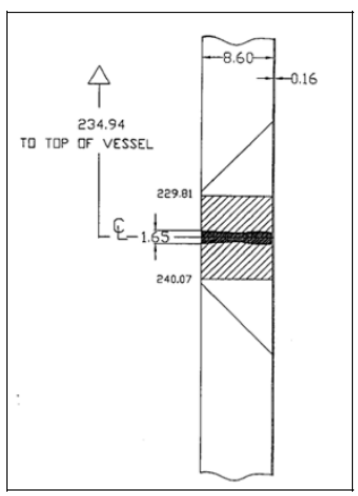

Circumferential Weld

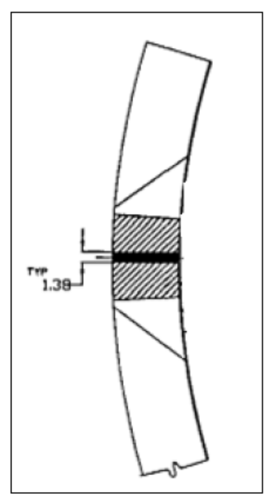

Axial Weld

Figure 7. Sample Appendix VIII Examination Results for Plant J.

Table 12. Determination of Total Weld Length Examined for Plant J

STEP D: Compute Total Weld Length Examined

Weld ID	Direction	Radius, R_i (inches)	Length (inches)	Comments	Examination Coverage	Examined Length, L = Length * Coverage (inches)
J-1	Circumferential	86.5	543.5	Length computed as $2\pi R_i$	100%	543.5
J-2	Circumferential	86.5	543.5	Length computed as $2\pi R_i$	100%	543.5
J-3	Axial	N/A	70	Length assumed	100%	70.0
J-4	Axial	N/A	70	Length assumed	100%	70.0
J-5	Axial	N/A	70	Length assumed	100%	70.0
J-6	Axial	N/A	70	Length assumed	100%	70.0
J-7	Axial	N/A	70	Length assumed	100%	70.0
J-8	Axial	N/A	70	Length assumed	100%	70.0
J-9	Axial	N/A	70	Length assumed	77.8%	54.5
J-10	Axial	N/A	70	Length assumed	77.8%	54.5
J-11	Axial	N/A	70	Length assumed	77.8%	54.5
					Total, L =	**1,670.4**

Table 13. Determination of Total Plate Surface Area Examined for Plant J

STEP D: Compute Total Plate Surface Area Examined

Weld ID	Examined Length, L	Weld Width, W_W (1) (inches)	Examination Width, W_E (2) (inches)	Comments	Plate Surface Area (inches^2)
J-1	543.5	1.65	8.60	Plate surface area computed as L x (W_E - W_W)	3,777.29
J-2	543.5	1.65	8.60	Plate surface area computed as L x (W_E - W_W)	3,777.29
J-3	70.0	1.38	8.60	Plate surface area computed as L x (W_E - W_W)	505.40
J-4	70.0	1.38	8.60	Plate surface area computed as L x (W_E - W_W)	505.40
J-5	70.0	1.38	8.60	Plate surface area computed as L x (W_E - W_W)	505.40
J-6	70.0	1.38	8.60	Plate surface area computed as L x (W_E - W_W)	505.40
J-7	70.0	1.38	8.60	Plate surface area computed as L x (W_E - W_W)	505.40
J-8	70.0	1.38	8.60	Plate surface area computed as L x (W_E - W_W)	505.40
J-9	54.5	1.38	8.60	Plate surface area computed as L x (W_E - W_W)	393.20
J-10	54.5	1.38	8.60	Plate surface area computed as L x (W_E - W_W)	393.20
J-11	54.5	1.38	8.60	Plate surface area computed as L x (W_E - W_W)	393.20
				Total, A =	**11,766.6**

Notes: (1) The weld width, W_W, is defined as the maximum weld crown width from both sides of the RPV wall. From Figure 7, W_W is 1.65" for circumferential welds and 1.38" for axial welds.

(2) The examination width, W_E, is defined as the ASME Code Section XI examination volume width, which is one-half of the wall thickness on both sides of the weld. From Figure 7, the RPV base-metal wall thickness, which is equal to W_E, is 8.60".

Table 14. Determination of the Flaw Positions for Plant J

STEP D: Determine Position of Flaws

Weld No.	Indication No.	Weld Centerline		Weld Width (inches)	Flaw Position: Height on RPV (inches)	Flaw Position: RPV Circumferential Position (°)	Flaw Position: Depth Below Clad (inches)	Weld or Plate Flaw?	Is Flaw Within First 1.0" or 0.10t?	Is Flaw Within First 3/8t?	Through Wall Extent (TWE) = 2a (inches)	Evaluation Required
J-2	1	235	in	1.65	235.00	150.1	1.66	WELD	NO	YES	0.16	Acceptable per ASME XI Table IWB-3510-1
	2	235	in	1.65	235.14	157.7	2.70	WELD	NO	YES	0.12	Acceptable per ASME XI Table IWB-3510-1
	3	235	in	1.65	235.80	129.3	8.60	WELD	NO	NO	0.50	No evaluation for 50.61a required
	4	235	in	1.65	235.50	332.1	4.49	WELD	NO	NO	0.24	No evaluation for 50.61a required
J-7	1	120	°	1.38	123.60	123.6	0.63	PLATE	YES	N/A	0.22	Compare to Plate Flaw Table
J-9	1	60	°	1.38	256.50	60.3	0.11	WELD	YES	N/A	0.25	Compare to Weld Flaw Table
	2	60	°	1.38	240.30	60.4	0.79	WELD	YES	N/A	0.34	Compare to Weld Flaw Table
J-11	1	300	°	1.38	312.61	300.3	3.60	WELD	NO	NO	0.27	No evaluation for 50.61a required

Table 15. Comparison of Flaws to Alternate PTS Rule Flaw Tables for Plant J

STEP D: Compare Flaws to 10 CFR 50.61a Flaw Tables

Table 2 Comparison = Weld Flaws

Bin No.	Minimum TWE (inches)	Maximum TWE (inches)	(Allowable) Max. # of Flaws per 1,000 inches	(Cumulative) # of Flaws Detected	# of Flaws / L x 1,000	Acceptable?	Flaws
1	0	0.075	No limit	0	0.00	YES	
2	0.075	0.475	166.70	2	1.20	YES	J-9-1, J-9-2
3	0.125	0.475	90.80	2	1.20	YES	J-9-1, J-9-2
4	0.175	0.475	22.82	2	1.20	YES	J-9-1, J-9-2
5	0.225	0.475	8.66	2	1.20	YES	J-9-1, J-9-2
6	0.275	0.475	4.01	2	1.20	YES	J-9-1, J-9-2
7	0.325	0.475	3.01	1	0.60	YES	J-9-1
8	0.375	0.475	1.49	0	0.00	YES	
9	0.425	0.475	1.00	0	0.00	YES	
10	0.475	Infinite	0.00	0	0.00	YES	

Table 3 Comparison = Plate/Forging Flaws

Bin No.	Minimum TWE (inches)	Maximum TWE (inches)	(Allowable) Max. # of Flaws per 1,000 inches	(Cumulative) # of Flaws Detected	# of Flaws / A x 1,000	Acceptable?	Flaws
1	0	0.075	No limit	0	0.00	YES	
2	0.075	0.375	8.05	1	0.08	YES	J-7-1
3	0.125	0.375	3.15	1	0.08	YES	J-7-1
4	0.175	0.375	0.85	1	0.08	YES	J-7-1
5	0.225	0.375	0.29	0	0.00	YES	
6	0.275	0.375	0.08	0	0.00	YES	
7	0.325	0.375	0.01	0	0.00	YES	
8	0.375	Infinite	0.00	0	0.00	YES	

6.4 Guidance for Further Evaluation of NDE Data

Guidance for further evaluation of NDE data (Steps G through I in Figure 5) is provided in this section. Such guidance is based on Section II, "Discussion," provided in the Supplemental Information section of the Federal Register Notice for the Alternate PTS Rule [2], where the following discussion is included with respect to NDE-Related Uncertainties:

> *The flaw sizes in Tables 2 and 3 represent actual flaw dimensions while the results from the ASME Code examinations are estimated dimensions. The available information indicates that, for most flaw sizes in Tables 2 and 3, qualified inspectors will oversize flaws. Comparing oversized flaws to the size and density distributions in Tables 2 and 3 is conservative and acceptable, but not necessary.*
>
> *As a result of stakeholder feedback received on the NRC solicitation for comments published in the August 2008 supplemental proposed rule, the final rule will permit licenses to adjust the flaw sizes estimated by inspectors qualified under the ASME Code, Section XI, Appendix VIII, Supplement 4 and Supplement 6.*
>
> *The NRC determined that, in addition to the NDE sizing uncertainties, licensees should be allowed to consider other NDE uncertainties, such as probability of detection and flaw density and location, because these uncertainties may affect the ability of a licensee to demonstrate compliance with the rule. As a result, the language in § 50.61a(e) will allow licensees to account for the effects of NDE-related uncertainties in meeting the flaw size and density requirements of Tables 2 and 3. The methodology to account for the effects of NDE-related uncertainties must be based on statistical data collected from ASME Code inspector qualification tests or any other tests that measure the difference between the actual flaw size and the size determined from the ultrasonic examination…*

Specific guidance on various elements of NDE data evaluation is provided in the following sections.

6.4.1 Guidance on the Elements and NDE Techniques Associated with ASME Code Examinations

The Alternate PTS Rule was developed using a flaw density, spatial distribution, and size distribution determined from experimental data, as well as from physical models and expert judgment. To implement the Alternate PTS Rule, actual flaw densities and distributions need to be estimated from the results of periodic ISI performed on RPV welds and adjacent base material. The method for these examinations is ultrasonic testing (UT). As discussed in Section 6.3, the data used for evaluation of the Alternate PTS Rule must be acquired using procedures, equipment and personnel that are qualified under Supplements 4 and 6 to Appendix VIII to Section XI of the ASME Code. Appendix VIII provides requirements for performance demonstration for UT examination procedures, equipment, and personnel used to detect and size flaws. Supplement 4 specifies qualification requirements for examination of the inner 15% of clad ferritic reactor vessels, and may also be applied to the inner 15% of unclad ferritic reactor vessels. Supplement 6 specifies qualification requirements for examination of unclad ferritic components and the outer 85% of clad ferritic components.

Supplement 4 provides performance-demonstration rules intended to produce effective procedures, personnel, and equipment for detection and sizing of flaws typical of those that might be expected to form as a result of service conditions. These rules result in targeting flaws that are primarily planar in orientation and emanate from the inside surface (clad-to-base-metal interface) of the RPV specimens that are used for the qualification process. The aspect ratio of flaws used for performance demonstration also closely follows the acceptance criteria of Article IWB-3000 in Section XI of the ASME Code. These flaws are the focus of the performance demonstration because they are of structural significance under standard operating conditions. Therefore, the objective of Supplement 4 qualification is to demonstrate UT capabilities on planar flaws. Examinations using Appendix VIII qualification may also detect larger fabrication flaws; this is often the case in practice because no known credible subcritical cracking mechanisms affect the RPV material for the current fleet of U.S. reactors.

The PFM analyses supporting the Alternate PTS Rule assumed all flaws were planar in nature. Because the empirical evidence on which the flaw distribution used in these analyses was based included both planar flaws and fabrication flaws [19], this assumption was viewed as being conservative because it produced a higher density of planar flaws than typically exist in nuclear RPVs. Fabrication flaws are considerably smaller than would be expected to exist within current Supplement 4 qualification specimens and are not typically connected to the clad-to-base-metal interface. Nevertheless, it is probable that parameters associated with qualified UT methods may be optimized to enhance the method's capability to detect and size small fabrication flaws in the inner one inch of RPV base material. Therefore, licensees should consider enhancements to Appendix-VIII-qualified procedures to ensure accurate detection and sizing of the flaws inferred by the Alternate PTS Rule while maintaining the essential variables for which the procedure was qualified.

Within the context of a qualified Appendix VIII RPV examination, various elements and NDE techniques associated with the examination might be able to be varied to provide better NDE data for comparison with the flaw limits included in Tables 2 and 3 of the Alternate PTS Rule. Such elements and techniques may include, but are not be limited to, the following:

- Reducing the scan index;
- Use of an ultrasonic straight-beam examination technique; or
- Use of an enhanced recording criterion (lower threshold).

NRC staff have been working with UT/NDE experts at Pacific Northwest National Laboratory (PNNL) to assess RPV examination and implementation of the Alternative PTS Rule. The assessment, including enhancements to procedures and examination techniques, is addressed in a Technical Letter Report (TLR) [24]. Due consideration of the above elements should be given when establishing the protocols and procedures for Appendix VIII examinations used by licensees who choose to apply the Alternate PTS Rule in order to maximize the usefulness of the resulting NDE data and provide reasonable assurance of the acceptability of the NDE data comparisons required by the Alternate PTS Rule.

6.4.2 Guidance on a Procedure to Adjust NDE Data and Comparison to Flaws Assumed in PFM Calculations

Guidance on a mathematical procedure that can be used to adjust NDE data to account for flaw-detection and -sizing errors, as identified by Step G in Figure 5, is provided in this section. This evaluation adjusts the as-found NDE data by taking into account flaw-sizing errors, POD uncertainties, and prior flaw distributions such as those used in the development of the Alternate PTS Rule (i.e., VFLAW [19]). Any or all of these uncertainties may be considered, depending on the level of detail needed for flaw assessment. After such adjustment, the adjusted NDE results may be compared with the flaw tables again (Step H in Figure 5) because NDE techniques tend to oversize smaller flaws, thereby distributing detected flaws into larger bins where the allowed number of flaws is smaller. In such cases, adjustment for NDE flaw-detection and -sizing uncertainties may result in a less conservative distribution of flaw sizes, possibly allowing a comparison of the adjusted NDE data to the flaw tables to be successful. A successful comparison of the revised NDE data to the flaw tables would be viewed by the staff as providing reasonable assurance that the plant-specific flaw distribution is bounded by the flaw distribution used in the development of the Alternate PTS Rule, indicating that it is appropriate to apply the alternate PTS screening limits (Step K in Figure 5).

Appendix C describes the development and application of a methodology to account for uncertainties in NDE data and for analyzing such data for the purpose of developing more realistic vessel-specific flaw depth and density distributions for comparison to the flaw tables, as well as for plant-specific PFM analysis (discussed in Section 6.2.2). The methodology considers POD, flaw-measurement error, and flaw-detection threshold in its application and uses Bayesian updating to combine the observed NDE data with the available flaw data and models used as part of the PTS re-evaluation effort. The Bayesian framework used by this methodology is described in Appendix C, followed by application details of the NDE data uncertainties (i.e., POD and measurement/sizing error) and the Bayesian updating procedure. Application of the methodology is demonstrated in Appendix C using the ultrasonic NDE data obtained from a previous ISI examination of the Beaver Valley 2 RPV and a MATLAB software routine that uses the Bayesian equations developed in Appendix C. The MATLAB software listing is also included in Appendix C.

As an example of this procedure, assume that Plant J performs an initial NDE assessment using the guidance of Section 6.3 with the results shown in Table 16. These results indicate that Plant J fails the Alternate PTS Rule flaw-table check based on violating the flaw-acceptance limit for Flaw Bin #2, i.e., 170.10 actual flaws per 1,000 inches of weld *vs*. 166.70 allowed flaws per 1,000 inches of weld. Therefore, Step D in Figure 5 yields a “FAIL” decision, thereby necessitating the evaluations associated with Step G in Figure 5. As a result, procedures similar to those described in Appendix C should be applied.

A key input for this procedure is a POD and associated sizing error data appropriate to the methods and techniques used to examine the RPV. Example PODs and flaw-sizing error data have been previously developed by the Electric Power Research Institute (EPRI) based on Performance Demonstration Initiative (PDI) qualification data [26]. Similar information should be obtained for the examination technique being applied and technically justified for use as a part of applying the procedures described in Appendix C.

Table 16. Example for Plant J After Applying an Initial Alternate PTS Rule Flaw Table Check Using the Procedure in Section 6.3.

Flaw Bin #	Flaw Depth (inch)	Observed (Detected) Number of Flaws from NDE ISI	10 CFR 50.61a Flaw Limits (# of Flaws per 1,000" of Weld)	Acceptable? (Is No. of Flaws < Limit?)
1	0.000 < a ≤ 0.075	234.45	No limit	Yes
2	0.075 < a ≤ 0.475	170.10	166.70	No
3	0.125 < a ≤ 0.475	11.23	90.80	Yes
4	0.175 < a ≤ 0.475	0.90	22.82	Yes
5	0.225 < a ≤ 0.475	0.05	8.66	Yes
6	0.275 < a ≤ 0.475	0.01	4.01	Yes
7	0.325 < a ≤ 0.475	0.00	3.01	Yes
8	0.375 < a ≤ 0.475	0.00	1.49	Yes
9	0.425 < a ≤ 0.475	0.00	1.00	Yes

6.4.2.1 Guidance on Application of NDE Uncertainties

Appendix D discusses the results of sensitivity analyses that apply the Appendix C Bayesian updating methodology to systematically assess the effect of NDE uncertainties such as POD and measurement (sizing) error on the estimated flaw populations. The sensitivity analyses were performed for a base case and twelve sensitivity cases that investigated variations in observed NDE data and application of prior probability density functions (PDFs), POD, and flaw-sizing error.

As a part of the sensitivity studies, lower NDE detection limits of 0.04" and 0.075" were also evaluated and found to have no significant impact on the observed data.

The results obtained from the twelve sensitivity cases consistently show that small (i.e., 10%) overpopulation of flaws in Bins 2 and 3 of the Alternate PTS Rule flaw tables, as might be expected from actual plant inspections because of oversizing of small flaws, would be shifted to Bins 1 and 2 after accounting for the measurement error in the Bayesian inference. When POD was also considered, the effects of small flaws that might be missed by NDE methods were clearly seen in Bins 1 and 2, with an additional number of flaws in the posterior estimates as compared to the observed flaws. However, the results are sensitive to the POD used, especially the portion of the POD for smaller flaw sizes. It is therefore important that, if a POD is used, the POD must be sufficiently justified.

The effects of the consideration and choice of the prior distributions of flaw density and depth were significant. When no prior information was used to describe the flaw-density and flaw-depth distributions, POD and measurement error were very sensitive, and significantly amplified the number of flaws that resulted in Bins 1 and 2. However, when prior PDFs were used, the posteriors were significantly moderated by the existence of the prior PDFs, and the POD and measurement errors played less significant roles.

The results of the sensitivity analysis documented in Appendix D reveal the following:

- Neglecting consideration of prior PDFs in the evaluation provides a conservative assessment.
- Neglecting consideration of flaw-sizing error in the evaluation provides a conservative assessment.
- POD has a significant impact in the evaluation and should be included for the case in which PDFs are not considered. For the case in which PDFs are evaluated, the impact of POD is relatively small and may be neglected.
- Consideration of flaw-sizing error, POD, or prior PDFs (identified as “NDE uncertainties” in the Alternate PTS Rule) using methods similar to those shown in Appendix C is successful in removing conservatisms that may unnecessarily prevent a licensee from passing the Alternate PTS Rule flaw tables.

7. GUIDANCE ON CRITERIA RELATING TO ALTERNATE LIMITS ON EMBRITTLEMENT

Paragraph (c)(3) of 10 CFR 50.61a states the following:

> *Each licensee shall compare the projected RT_{MAX-X} values for plates, forgings, axial welds, and circumferential welds to the PTS screening criteria in Table 1 of this section, for the purpose of evaluating a reactor vessel's susceptibility to fracture due to a PTS event.* ***If any of the projected RT_{MAX-X} values are greater than the PTS screening criteria in Table 1*** *of this section, then* ***the licensee may propose*** *the compensatory actions or* ***plant-specific analyses*** *as required in paragraphs (d)(3) through (d)(7) of this section, as applicable, to justify operation beyond the PTS screening criteria in Table 1 of this section.*

This section describes one method by which licensees could perform the plant-specific analyses indicated by the ***highlighted text***. This method is acceptable to the staff provided that the requirements of 10 CFR 50.61a concerning flaw evaluations and surveillance assessment are satisfied.

The RT_{MAX-X} limits in Table 1 of 10 CFR 50.61a were established in NUREG-1874 to ensure that the TWCF remains below 1×10^{-6} per reactor year. As described in NUREG-1874, the RT_{MAX-X} limits are based on the results of PFM analyses; they account for the combined TWCF contributions from various flaw populations in the RPV. Some simplifications of the PFM data underlying these limits were necessary to permit their expression in a tabular form. As an example, the TWCF attributable to circumferentially-oriented flaws occurring in circumferential welds was held below 1×10^{-8} per reactor year rather than 1×10^{-6} per reactor year. This simplification was made for expedience and was not intended to address a safety concern. Therefore, the following procedure, which eliminates similar simplifying assumptions, can be used to demonstrate compliance with the RT_{MAX-X} limits in Table 1 of 10 CFR 50.61a. This procedure was originally described in Section 3.5.1 of NUREG-1874:

1. Determine RT_{MAX-X} for all axial welds (RT_{MAX-AW}), plates (RT_{MAX-PL}), circumferential welds (RT_{MAX-CW}), and forgings (RT_{MAX-FO}) in the RPV beltline region according to the requirements of 10 CFR 50.61a. These RT_{MAX-X} values must be expressed in units of Rankine (R) (degrees Fahrenheit (°F) plus 459.69).
2. Use the RT_{MAX-X} values from Step 1 to estimate the 95th percentile TWCF contribution from each component in the beltline using the following formulas:

$$TWCF_{95-AW} = \exp\{5.5198 \cdot \ln(RT_{MAX-AW} - 616) - 40.542\} \cdot \beta \quad (19)$$

$$TWCF_{95-PL} = \exp\{23.737 \cdot \ln(RT_{MAX-PL} - 300) - 162.38\} \cdot \beta \quad (20)$$

$$TWCF_{95-CW} = \exp\{9.1363 \cdot \ln(RT_{MAX-CW} - 616) - 65.066\} \cdot \beta \quad (21)$$

$$\begin{aligned} TWCF_{95-FO} &= \exp\{23.737 \cdot \ln(RT_{MAX-FO} - 300) - 162.38\} \cdot \beta \\ &\quad + \eta \cdot \{1.3 \times 10^{-137} \cdot 10^{0.185 \cdot RT_{MAX-FO}}\} \cdot \beta \end{aligned} \quad (22)$$

where:

η = 0 if the forging is compliant with Regulatory Guide 1.43; otherwise η = 1.

$\beta = 1$ if $T_{WALL} \leq 9.5$ inches
$\beta = 1 + 8 \times (T_{WALL} - 9.5)$ if $9.5 < T_{WALL} < 11.5$ inches
$\beta = 17$ if $T_{WALL} \geq 11.5$ inches

3. Estimate the total 95th percentile TWCF for the RPV using the following formulae (noting that, depending on the type of vessel in question, certain terms in the following formula will be zero).

$$TWCF_{95-TOTAL} = \begin{bmatrix} \alpha_{AW} \cdot TWCF_{95-AW} + \\ \alpha_{PL} \cdot TWCF_{95-PL} + \\ \alpha_{CW} \cdot TWCF_{95-CW} + \\ \alpha_{FO} \cdot TWCF_{95-FO} \end{bmatrix} \qquad (23)$$

where:

$\alpha = 2.5$ if $RT_{MAX-xx} \leq 625$ R
$\alpha = 2.5 - \frac{1.5}{250}\left(RT_{MAX-xx} - 625\right)$ if 625 R < RT_{MAX-xx} < 875 R
$\alpha = 1$ if $RT_{MAX-xx} \geq 875$ R

4. If $TWCF_{95\text{-}TOTAL}$ from Step 3 is less than 1×10^{-6} per reactor year, the requirements of Table 1 of 10 CFR 50.61a are met.

8. SUMMARY

In early 2010, the NRC promulgated the Alternate PTS Rule in 10 CFR 50.61a, which amended existing regulations to provide alternate embrittlement requirements for protection against PTS events for PWR RPVs. These requirements are based on more comprehensive, accurate, and realistic analysis methods than those used to establish the limits in 10 CFR 50.61. This action became desirable because the existing requirements, as contained in 10 CFR 50.61, are based on unnecessarily conservative assumptions. While still maintaining adequate safety margins, the Alternate PTS Rule reduces regulatory burden for those PWR licensees who expect to exceed the 10 CFR 50.61 embrittlement requirements before the expiration of their operating licenses. PWR licensees may choose to comply with the Alternate PTS Rule as a voluntary alternative to complying with the requirements contained in 10 CFR 50.61.

The Alternate PTS Rule provides revised PTS screening criteria in the form of embrittlement reference temperatures, RT_{MAX-X}, that characterize the RPV material's resistance to fracture initiating from flaws. The RT_{MAX-X} embrittlement limits may be used by licensees provided that the following criteria are met:

1. **<u>Criteria relating to the date of construction and design requirements</u>**: The Alternate PTS Rule is applicable to licensees whose construction permits were issued before February 3, 2010, and whose RPVs were designed and fabricated to the 1998 Edition or an earlier edition of the ASME Code. The reason for this applicability restriction is that the structural and thermal hydraulic analyses that established the basis for the Alternate PTS Rule's embrittlement limits only represented plants constructed before this date. It is the responsibility of a licensee to demonstrate that the risk-significant factors controlling PTS for any plant constructed after February 3, 2010, are adequately addressed by the technical basis calculations developed in support of the Alternate PTS Rule. Chapter 4 of this document describes methods by which licensees can satisfy these criteria and identifies factors to be considered in such an evaluation.

2. **<u>Criteria relating to plant-specific surveillance data</u>**: The Alternate PTS Rule includes statistical tests that must be performed on RPV surveillance data to determine whether the surveillance data are sufficiently "close" to the predictions of an ETC that the predictions of the ETC are valid for use. From a regulatory perspective, it is of particular interest to determine whether plant-specific surveillance data deviate significantly from the predictions of the ETC in a manner that suggests that the ETC is very likely to underpredict plant-specific data trends. Chapter 5 of this document describes guidance by which licensees can assess the closeness of plant-specific data to the ETC using statistical tests. This guidance includes the following, including:
    - A detailed description of the mathematical procedures to use to assess compliance with the three statistical tests in the Alternative PTS Rule.
    - A list of factors to consider in diagnosing the reason that particular surveillance data sets may fail these statistical tests.
    - A description of certain situations in which routine adjustments of the ETC predictions can be made.

3. **<u>Criteria relating to ISI data and NDE requirements</u>**: The Alternate PTS Rule describes a number of tests of and conditions on the collection and analysis of ISI data that are intended to provide reasonable assurance that the distribution of flaws that was

assumed to exist in the PFM calculations that provide the basis for the RT_{MAX-X} limits provide an appropriate, or bounding, model of the population of flaws in the RPV of interest. Chapter 6 of this NUREG includes guidance by which licensees can satisfy these criteria. The guidance discussed in this chapter includes the following components:

- Guidance for plants for the case in which RPV flaws fall outside the applicability of the flaw tables in the Alternate PTS Rule, including:
    i. A mathematical procedure that can be used to preclude brittle fracture based on RT_{NDT} information.
    ii. A mathematical procedure that can be used to combine the NDE data with the population of flaws assumed in the PFM calculations to estimate the total flaw distribution that is predicted to exist in the RPV, as well as guidance on the use of this total flaw distribution as part of a PFM calculation using the FAVOR computer code.
- Guidance for initial evaluation of NDE data obtained from qualified ISI examinations.
- Guidance for further evaluation of NDE data obtained from qualified ISI examinations, as follows:
    i. The elements and NDE techniques associated with the qualified ISI examinations performed in accordance with Mandatory Appendix VIII to Section XI of the ASME Code to assess compliance with the requirements of the Alternate PTS Rule.
    ii. A mathematical procedure that can be used to adjust NDE data to account for flaw-detection and -sizing errors and comparison of the adjusted data to the population of flaws assumed in the PFM technical basis for the Alternate PTS Rule.

4. **Criteria relating to alternate limits on embrittlement**: Guidance is provided by which licensees can estimate a plant-specific value of TWCF for cases in which the RT_{MAX-X} limits of the Alternate PTS Rule are not satisfied. Chapter 7 of this document describes these two sets of guidance so that licensees can satisfy embrittlement acceptability criteria.

This document provides guidance and the associated technical basis for methods by which the above criteria can be satisfied.

9. REFERENCES

[1] *U.S. Code of Federal Regulations*, Title 10, “Energy,” Chapter I, Section 50.61a, “Alternate Fracture Toughness Requirements for Protection Against Pressurized Thermal Shock Events” (10 CFR 50.61a).

[2] U.S. Nuclear Regulatory Commission, “Alternate Fracture Toughness Requirements for Protection Against Pressurized Thermal Shock Events,” *Federal Register*, Vol. 75, No. 1, January 4, 2010, pp. 13–29 (75 FR 13).

[3] *U.S. Code of Federal Regulations*, Title 10, “Energy,” Chapter I, Section 50.61, “Fracture Toughness Requirements for Protection Against Pressurized Thermal Shock Events” (10 CFR 50.61).

[4] American Society of Mechanical Engineers, *Boiler and Pressure Vessel Code*, 2013 edition, Section XI, “Rules for Inservice Inspection of Nuclear Power Plant Components,” New York, NY.

[5] *U.S. Code of Federal Regulations*, Title 10, “Energy,” Chapter I, Section 50.66, “Requirements for Thermal Annealing of the Reactor Pressure Vessel” (10 CFR 50.66).

[6] U.S. Nuclear Regulatory Commission, “Technical Basis for Revision of the Pressurized Thermal Shock (PTS) Screening Limit in the PTS Rule (10 CFR 50.61): Summary Report,” NUREG-1806, August 2007.

[7] U.S. Nuclear Regulatory Commission, “Recommended Screening Limits for Pressurized Thermal Shock (PTS),” NUREG-1874, March 2010.

[8] Elliot, B.J., Senior Materials Engineer, U.S. Nuclear Regulatory Commission, memorandum to M.A. Mitchell, Branch Chief, U.S. Nuclear Regulatory Commission, ‘‘Development of Flaw Size Distribution Tables for Draft Proposed Title 10 of the Code of Federal Regulations (10 CFR) 50.61a,’’ April 3, 2007, Agencywide Documents Access and Management System (ADAMS) Accession No. ML070950392.

[9] Eason, E.D., et al., “A Physically Based Correlation of Irradiation-Induced Transition Temperature Shifts for RPV Steels,” ORNL/TM-2006/530, November 2007, Oak Ridge National Laboratory, Oak Ridge, TN, ADAMS Accession No. ML081000630.

[10] Electric Power Research Institute (EPRI), “Materials Reliability Program: Proposed Resolutions to the Analytical Challenges of Alternate PTS Rule (10 CFR 50.61a) Implementation (MRP-334),” Technical Update No. 1024811, January 2012, Palo Alto, CA.

[11] *U.S. Code of Federal Regulations*, Title 10, “Energy,” Chapter I, Section 50.55a, “Codes and Standards” (10 CFR 50.55a).

[12] ASME, *Boiler and Pressure Vessel Code*, Mandatory Appendix VIII, “Performance Demonstration for Ultrasonic Examination Systems,” to Section XI, “Rules for Inservice Inspection of Nuclear Power Plant Components,” New York, NY, 2013 edition.

[13] *U.S. Code of Federal Regulations*, Title 10, "Energy," Chapter I, Part 50, "Domestic Licensing of Production and Utilization Facilities," Appendix H, "Reactor Vessel Material Surveillance Program Requirements."

[14] U.S. Nuclear Regulatory Commission, ''Statistical Procedures for Assessing Surveillance Data for 10 CFR Part 50.61a,'' June 9, 2008, ADAMS Accession No. ML081290654.

[15] U.S. Nuclear Regulatory Commission, ''Technical Basis for Revision of Regulatory Guide 1.99: NRC Guidance on Methods to Estimate the Effects of Radiation Embrittlement on the Charpy V-Notch Impact Toughness of Reactor Vessel Materials,'' draft NUREG report, October 1, 2007, ADAMS Accession No. ML081120289.

[16] U.S. Nuclear Regulatory Commission, "Radiation Embrittlement of Reactor Vessel Materials," Regulatory Guide 1.99, Rev. 2, May 1988, ADAMS Accession No. ML003740284.

[17] NRC Public Meeting Summary Reports:

a. U.S. Nuclear Regulatory Commission, "Category 2 Public Meeting - Discussion of Reactor Pressure Vessel Integrity Issues for Operating Nuclear Power Plants," August 5, 2011, ADAMS Accession No. ML112170262.

b. U.S. Nuclear Regulatory Commission, "Category 2 Public Meeting - Discussion of Nondestructive Examination Aspects of Reactor Pressure Vessel Integrity Issues for Operating Nuclear Power Plants," October 6, 2011, ADAMS Accession No. ML112790501.

c. U.S. Nuclear Regulatory Commission, "Category 2 Public Meeting - Discussion of Reactor Pressure Vessel Integrity Issues for Operating Nuclear Power Plants," November 18, 2011, ADAMS Accession No. ML113220295.

[18] Palm, Nathan A., Fellow Engineer, and Michael G. Semmler, Acting Manager, Westinghouse Electric Company, letter to Dr. Aladar Csontos, Branch Chief, U.S. Nuclear Regulatory Commission, "Inspection Data for Use in Development of Alternate Pressurized Thermal Shock (PTS) Rule Implementation Regulatory Guide," LTR-AMLRS-11-71, September 7, 2011, ADAMS Accession No. ML112560145.

[19] U.S. Nuclear Regulatory Commission, "A Generalized Procedure for Generating Flaw-Related Inputs for the FAVOR Code," NUREG/CR-6817 (PNNL-14268), March 2004, ADAMS Accession No. ML040830499.

[20] Oak Ridge National Laboratory, "Fracture Analysis of Vessels - Oak Ridge FAVOR, v12.1, Computer Code: Theory and Implementation of Algorithms, Methods, and Correlations," ORNL/TM-2012/567, November 2012, Oak Ridge, TN, ADAMS Accession No. ML13008A015.

[21] U.S. Nuclear Regulatory Commission, "Probabilistic Fracture Mechanics - Models, Parameters, and Uncertainty Treatment Used in FAVOR Version 04.1," NUREG-1807, June 2007.

[22] U.S. Nuclear Regulatory Commission, "Fracture Analysis of Vessels - Oak Ridge FAVOR, v04.1, Computer Code: Theory and Implementation of Algorithms,

Methods, and Correlations," NUREG/CR-6854 (ORNL/TM-2004/244), August 2007.

[23] Pellini, W.S., and P.P. Puzak, "Fracture Analysis Diagram Procedures for the Fracture-Safe Engineering Design of Steel Structures," Bulletin 88, May 1963, Welding Research Council, Shaker Heights, OH.

[24] Pacific Northwest National Laboratory, "Evaluation on the Feasibility of Using Ultrasonic Testing of Reactor Pressure Vessel Welds for Assessing Flaw Density/Distribution per 10 CFR 50.61a, Alternate Fracture Toughness Requirements for Protection Against Pressurized Thermal Shock," PNNL-19666, June 2014, ADAMS Accession No. ML14162A001.

[25] U.S. Nuclear Regulatory Commission, "Evaluation of the Beltline Region for Nuclear Reactor Pressure Vessels," NRC Technical Letter Report TLR-RES/DE/CIB-2013-01, November 14, 2014, ADAMS Accession No. ML14318A177.

[26] EPRI, "Nondestructive Evaluation: Probabilistic Analysis of Performance Demonstration Ultrasonic Flaw Detection and Through-Wall Sizing Results for Reactor Pressure Vessel Inspections," EPRI Report 1025787, September 2012, Palo Alto, CA.

[27] U.S. Nuclear Regulatory Commission, "Calculational and Dosimetry Methods for Determining Pressure Vessel Neutron Fluence," Regulatory Guide 1.190, March 2001, ADAMS Accession No. ML010890301.

APPENDIX A: DERIVATION OF THE STATISTICAL TEST FOR TYPE D DEVIATIONS

C_2 is defined so that the probability that all the normalized residuals are less than C_2 is $1 - \alpha = 0.99$, assuming the embrittlement shift model is correct. Under this assumption, the normalized residuals all have a standard normal distribution with a mean of 0 and standard deviation of 1. The cumulative distribution function of the standard normal distribution, denoted by F, is then:

$$C_2 = F^{-1}\,(0.99)^{1/n} \qquad \text{Eqn. A-1}$$

For any n and C_2 as determined above, define:

$$p = \text{Prob}\,\{C_1 < X \leq C_2\} \qquad \text{Eqn. A-2}$$

for any $C_1 < C_2$ and where X has a standard normal distribution. Then:

$$1\text{-}p = \text{Prob}\,\{X \leq C_1\} + \text{Prob}\,\{X > C_2\} \qquad \text{Eqn. A-3}$$

However, the second term in (1-p) is negligible compared to the first term. In fact, from Table 7 in the main body of the text, $C_2 \geq 2.71$ for $n \geq 3$ and therefore Prob $\{X > C_2\} < 0.0034$ for $n \geq 3$. Thus:

$$1\text{-}p \approx \text{Prob}\,\{X \leq C_1\} \qquad \text{Eqn. A-4}$$

The probability that the subject dataset does not show a Type D deviation can be expressed in terms of p. Because all of the n normalized residuals should be less than or equal to C_1 to pass the Outlier Test, the following may be written:

$$\text{Prob}\,\{x_{[1]} \leq C_1\} = (1\text{-}p)^n \qquad \text{Eqn. A-5}$$

Also, the Outlier test states that it is acceptable to have a single normalized residual between C_1 and C_2 while the other (n – 1) normalized residuals are all less than C_1. Therefore:

$$\text{Prob}\,\{x_{[2]} < C_1 \leq x_{[1]} \leq C_2\} = np\,(1\text{-}p)^{n-1} \qquad \text{Eqn. A-6}$$

Because Eqn. A-5 and Eqn. A-6 are mutually exclusive, the sum of their probabilities is the probability of a Type D deviation, or $1 - \alpha = 0.99$. This sum, denoted by G(p), is:

$$G(p) = (1\text{-}p)^n + np\,(1\text{-}p)^{n-1} = (1\text{-}p)^{n-1}\,[1 + (n\text{-}1)p] \qquad \text{Eqn. A-7}$$

By iteration, the value p_0 may be found that yields $G(p_0) = 0.99$. To calculate C_1 in Table 7, Prob $\{X \leq C_1\}$ is set to 1-p_0. Then:

$$C_1 = F^{-1}\,(1\text{-}p_0) \qquad \text{Eqn. A-8}$$

APPENDIX B: REGULATORY ASSESSMENT OF STATISTICAL SURVEILLANCE TESTS

Table B-1. Type A Deviations (Mean Test)

General Information							Type A Deviation (Mean Test)		
Plant Name	Unit	Reactor Type	Heat	Product Form	n	σ [°F]	r_{mean} [°F]	r_{max} [°F]	Fails Test?
Arkansas Nuclear	1	PWR	PAN101	P	6	21	-13	20	No
Arkansas Nuclear	1	PWR	WAN101	W	3	26	6	36	No
Arkansas Nuclear	2	PWR	PAN201	P	3	21	-3	29	No
Beaver Valley	1	PWR	PBV101	P	8	21	23.0	17.5	Yes
Beaver Valley	1	PWR	WBV101	W	4	26	-3	31	No
Beaver Valley	2	PWR	PBV201	P	6	19	-7	18	No
Beaver Valley	2	PWR	WBV201	W	3	26	-37	36	No
Braidwood	1	PWR	FBD101	F	6	19	-7	18	No
Braidwood	1	PWR	WBD101	W	3	19	3	25	No
Braidwood	2	PWR	FBD201	F	6	19	-9	18	No
Braidwood	2	PWR	WBD201	W	3	19	-8	25	No
Brunswick	1	BWR	PBR_01	P	5	21	31.3	22.1	Yes
Brunswick	1	BWR	WBR_01	W	3	26	35	36	No
Byron	1	PWR	FBY101	F	6	19	15	18	No
Byron	1	PWR	WBY101	W	3	19	0	25	No
Byron	2	PWR	FBY201	F	6	19	-5	18	No
Byron	2	PWR	WBY201	W	3	19	-1	25	No
Callaway		PWR	PCL101	P	8	19	-2	15	No
Callaway		PWR	WCL101	W	4	19	27.0	21.7	Yes
Calvert Cliffs	1	PWR	PCC103	P	3	21	-6	29	No
Calvert Cliffs	1	PWR	WCC101	W	3	26	-17	36	No
Calvert Cliffs	2	PWR	PCC202	P	3	21	-7	29	No
Catawba	1	PWR	FCB101	F	6	20	-16	19	No
Catawba	1	PWR	WCB101	W	3	19	-8	25	No
Catawba	2	PWR	PCB201	P	6	21	-1	20	No
Catawba	2	PWR	WCB201	W	3	19	1	25	No
Commanche Peak	1	PWR	PCP101	P	4	19	-5	22	No
Connecticut Yankee		ex-PWR	PCTY04	P	3	21	-4	29	No

General Information							Type A Deviation (Mean Test)		
Plant Name	Unit	Reactor Type	Heat	Product Form	n	σ [°F]	r_{mean} [°F]	r_{max} [°F]	Fails Test?
Connecticut Yankee		ex-PWR	PCTY02	P	3	21	-13	29	No
Crystal River	3	PWR	PCR301	P	4	21	17	25	No
Crystal River	3	PWR	WCR301	W	4	26	12	31	No
Crystal River	3	PWR	WHSS66	W	4	26	-20	31	No
Crystal River	3	PWR	WHSSCR	W	3	26	-6	36	No
Crystal River & Surry	3 & 2	PWR	WHSS65	W	3	26	3	36	No
D.C. Cook	1	PWR	PCK101	P	8	21	-4	17	No
D.C. Cook	1	PWR	WCK101	W	3	26	-103	36	No
D.C. Cook	2	PWR	PCK201	P	8	21	24.6	17.5	Yes
D.C. Cook	2	PWR	WCK201	W	4	19	17	22	No
Davis Besse		PWR	FDB102	F	4	19	-7	22	No
Davis Besse		PWR	WDB101	W	5	26	1	28	No
Davis Besse		PWR	PRS101	P	3	21	-6	29	No
Davis Besse		PWR	WRS101	W	3	26	-14	36	No
Diablo Canyon	1	PWR	PDC103	P	3	21	-24	29	No
Diablo Canyon	1	PWR	WDC101	W	3	26	-2	36	No
Diablo Canyon	2	PWR	PDC201	P	8	21	-5	17	No
Diablo Canyon	2	PWR	WDC201	W	4	26	-3	31	No
Dresden	3	BWR	WDR302	W	3	26	-17	36	No
Dresden	2	BWR	PDR201	P	5	21	-32	22	No
Dresden	3	BWR	PDR301	P	6	21	-10	20	No
Dresden	3	BWR	WDR301	W	5	26	-5	28	No
Duane Arnold		BWR	PDAC01	P	3	21	10	29	No
Duane Arnold		BWR	WDAC01	W	3	19	-4	25	No
Farley	1	PWR	PFA101	P	8	21	13	17	No
Farley	1	PWR	WFA101	W	4	26	-7	31	No
Farley	2	PWR	PFA201	P	8	21	15	17	No
Farley	2	PWR	WFA201	W	4	19	-51	22	No
FitzPatrick		BWR	PFTZ01	P	6	21	-11	20	No
Fort Calhoun		PWR	PFC101	P	5	21	-10	22	No
Fort Calhoun		PWR	WFC101	W	4	26	-1	31	No
Ginna		PWR	FGIN02	F	4	19	-18	22	No

General Information							Type A Deviation (Mean Test)		
Plant Name	Unit	Reactor Type	Heat	Product Form	n	σ [°F]	r_{mean} [°F]	r_{max} [°F]	Fails Test?
Ginna		PWR	FGIN01	F	4	19	17	22	No
Ginna		PWR	WGIN01	W	4	26	13	31	No
H.B. Robinson	2	PWR	WHB201	W	3	26	6	36	No
Indian Point	2	PWR	PIP202	P	3	21	-1	29	No
Indian Point	2	PWR	PIP203	P	3	21	32.6	28.5	Yes
Indian Point	3	PWR	PIP304	P	5	21	13	22	No
Indian Point	3	PWR	WIP301	W	3	26	33	36	No
Kewaunee		PWR	FKWE02	F	4	19	-7	22	No
Kewaunee		PWR	FKWE01	F	4	19	-9	22	No
Kewaunee		PWR	WKWE01	W	4	26	16	31	No
Maine Yankee		ex-PWR	PMY_01	P	6	21	28.5	20.2	Yes
Maine Yankee		ex-PWR	SHSS01	SRM	17	21	1	12	No
Maine Yankee		ex-PWR	WMY_01	W	4	26	-8	31	No
McGuire	1	PWR	PMC101	P	8	21	13	17	No
McGuire	1	PWR	WMC101	W	4	26	-11	31	No
McGuire	2	PWR	FMC201	F	8	20	1	16	No
McGuire	2	PWR	WMC201	W	4	19	3	22	No
Millstone	1	ex-BWR	PML101	P	4	21	-6	25	No
Millstone	2	PWR	PML201	P	5	21	13	22	No
Millstone	2	PWR	WML201	W	3	26	-27	36	No
Nine Mile Point	1	BWR	PNM101	P	5	21	-10	22	No
North Anna	1	PWR	FNA101	F	6	20	-14	19	No
North Anna	1	PWR	WNA101	W	3	26	21	36	No
North Anna	2	PWR	FNA201	F	6	20	-18	19	No
North Anna	2	PWR	WNA201	W	3	26	-23	36	No
Oconee	1	PWR	POC102	P	6	21	5	20	No
Oconee	1	PWR	SHSS02	SRM	64	21	-14	6	No
Oconee	1	PWR	WOC101	W	3	26	5	36	No
Oconee	2	PWR	FOC201	F	5	19	-3	19	No
Oconee	2	PWR	WOC201	W	3	26	-23	36	No
Oconee	3	PWR	FOC301	F	4	19	2	22	No
Oconee	3	PWR	FOC302	F	3	19	21	25	No

General Information							Type A Deviation (Mean Test)		
Plant Name	Unit	Reactor Type	Heat	Product Form	n	σ [°F]	r_{mean} [°F]	r_{max} [°F]	Fails Test?
Oconee	3	PWR	WOC301	W	4	26	-28	31	No
Oyster Creek		BWR	PGG_01	P	4	19	2	22	No
Oyster Creek		BWR	PCPR02	P	4	21	-3	25	No
Oyster Creek		BWR	PEP2JP	P	5	19	-3	19	No
Oyster Creek		BWR	WGG_01	W	4	19	-8	22	No
Oyster Creek		BWR	WML101	W	6	26	-23	25	No
Oyster Creek		BWR	WQC102_1	W	4	26	26	31	No
Oyster Creek		BWR	WQC201_1	W	4	26	17	31	No
Oyster Creek		BWR	WRB_01	W	3	19	34.6	25.0	Yes
Palisades		PWR	PPAL01	P	7	21	-33	19	No
Palisades		PWR	WPAL01	W	4	26	-5	31	No
Point Beach	2	PWR	FPB202	F	4	20	19	23	No
Point Beach	1	PWR	PPB102	P	4	21	-28	25	No
Point Beach	1	PWR	PPB101	P	4	21	9	25	No
Point Beach	1	PWR	WPB101	W	4	26	-42	31	No
Point Beach	2	PWR	FPB201	F	4	19	16	22	No
Point Beach	2	PWR	WPB201	W	4	26	6	31	No
Prarie Island	1	PWR	FPI101	F	8	19	-2	15	No
Prarie Island	1	PWR	WPI101	W	4	26	-19	31	No
Prarie Island	2	PWR	FPI201	F	8	20	-4	16	No
Prarie Island	2	PWR	WPI201	W	4	26	-11	31	No
Quad Cities	1	BWR	PQC101	P	6	21	1	20	No
Quad Cities	1	BWR	WQC101	W	4	26	-16	31	No
Quad Cities	2	BWR	PQC201	P	4	21	-18	25	No
Quad Cities	2	BWR	WQC201	W	4	26	18	31	No
Saint Lucie	1	PWR	PSL101	P	5	21	-19	22	No
Saint Lucie	1	PWR	WSL101	W	3	26	-18	36	No
Saint Lucie	2	PWR	PSL201	P	3	21	14	29	No
Salem	1	PWR	PSA103	P	3	21	-30	29	No
Salem	1	PWR	PSA101	P	3	21	6	29	No
Salem	2	PWR	PSA201	P	8	21	10	17	No
Salem	2	PWR	WSA201	W	4	26	-18	31	No

General Information							Type A Deviation (Mean Test)		
Plant Name	Unit	Reactor Type	Heat	Product Form	n	σ [^oF]	r_{mean} [^oF]	r_{max} [^oF]	Fails Test?
San Onofre	2	PWR	PSO201	P	3	21	-7	29	No
San Onofre	3	PWR	PSO301	P	3	19	40.1	25.0	Yes
Seabrook	1	PWR	PSB101	P	4	19	19	22	No
Sequoyah	1	PWR	FSQ101	F	8	20	18.3	16.1	Yes
Sequoyah	1	PWR	WSQ101	W	4	26	32.4	30.8	Yes
Sequoyah	2	PWR	FSQ201	F	8	20	7	16	No
Sequoyah	2	PWR	WSQ201	W	4	26	23	31	No
South Texas	1	PWR	PST101	P	4	19	3	22	No
South Texas	2	PWR	PST201	P	4	19	4	22	No
Surry	1	PWR	PSU101	P	3	21	5	29	No
Surry	1	PWR	WSU101	W	3	26	43.5	35.5	Yes
Surry	2	PWR	PSU201	P	6	21	0	20	No
Surry	2	PWR	WSU201	W	3	26	-14	36	No
Three Mile Island	1	PWR	PTM101	P	3	21	-17	29	No
Trojan		ex-PWR	PTRO01	P	6	21	1	20	No
Trojan		ex-PWR	WTRO01	W	3	19	8	25	No
Turkey Point	3	PWR	FTP302	F	3	20	10	26	No
Turkey Point	3	PWR	SASTM	SRM	26	21	5	10	No
Turkey Point	3	PWR	WTP301	W	4	26	13	31	No
Virgil Summer	1	PWR	PVS101	P	8	21	-20	17	No
Virgil Summer	1	PWR	WVS101	W	4	19	0	22	No
Votgle	1	PWR	PVO101	P	6	19	-1	18	No
Votgle	1	PWR	WVO101	W	3	19	-4	25	No
Votgle	2	PWR	PVO201	P	6	19	-14	18	No
Votgle	2	PWR	WVO201	W	3	19	-13	25	No
Waterford	3	PWR	PWF301	P	3	19	-13	25	No
Watts Bar	1	PWR	FWB101	F	4	20	-6	23	No
Wolf Creek	1	PWR	PWC101	P	8	19	8	15	No
Wolf Creek	1	PWR	WWC101	W	4	19	17	22	No
Zion	1	ex-PWR	PZN101	P	8	21	-2	17	No
Zion	1	ex-PWR	WZN101	W	5	26	-6	28	No
Zion	2	ex-PWR	PZN201	P	6	21	3	20	No

General Information							Type A Deviation (Mean Test)		
Plant Name	Unit	Reactor Type	Heat	Product Form	n	σ [°F]	r_{mean} [°F]	r_{max} [°F]	Fails Test?
Zion	2	ex-PWR	WZN201	W	3	26	3	36	No

Table B-2. Type B Deviations (Slope Test)

General Information							Type B Deviation (Slope Test)				
Plant Name	Unit	Reactor Type	Heat	Product Form	n	σ [°F]	m	se(m)	T_m	$T_{crit(\alpha)}$	Fails Test?
Arkansas Nuclear	1	PWR	PAN101	P	6	21	-26.06	10.09	-2.58	3.75	No
Arkansas Nuclear	1	PWR	WAN101	W	3	26	-37.69	19.02	-1.98	31.82	No
Arkansas Nuclear	2	PWR	PAN201	P	3	21	-5.72	16.85	-0.34	31.82	No
Beaver Valley	1	PWR	PBV101	P	8	21	-37.91	21.46	-1.77	3.14	No
Beaver Valley	1	PWR	WBV101	W	4	26	-56.91	15.54	-3.66	6.96	No
Beaver Valley	2	PWR	PBV201	P	6	19	4.78	6.63	0.72	3.75	No
Beaver Valley	2	PWR	WBV201	W	3	26	-50.14	20.08	-2.50	31.82	No
Braidwood	1	PWR	FBD101	F	6	19	26.30	21.44	1.23	3.75	No
Braidwood	1	PWR	WBD101	W	3	19	8.25	8.49	0.97	31.82	No
Braidwood	2	PWR	FBD201	F	6	19	14.24	22.91	0.62	3.75	No
Braidwood	2	PWR	WBD201	W	3	19	6.66	19.20	0.35	31.82	No
Brunswick	1	BWR	PBR_01	P	5	21	67.73	13.28	5.10	4.54	Yes
Brunswick	1	BWR	WBR_01	W	3	26	41.69	45.09	0.92	31.82	No
Byron	1	PWR	FBY101	F	6	19	7.34	15.79	0.46	3.75	No
Byron	1	PWR	WBY101	W	3	19	26.54	8.12	3.27	31.82	No
Byron	2	PWR	FBY201	F	6	19	0.03	19.60	0.00	3.75	No
Byron	2	PWR	WBY201	W	3	19	27.60	8.32	3.32	31.82	No
Callaway		PWR	PCL101	P	8	19	-8.04	14.97	-0.54	3.14	No
Callaway		PWR	WCL101	W	4	19	-41.68	12.80	-3.26	6.96	No
Calvert Cliffs	1	PWR	PCC103	P	3	21	13.74	2.75	4.99	31.82	No
Calvert Cliffs	1	PWR	WCC101	W	3	26	37.90	2.00	18.95	31.82	No
Calvert Cliffs	2	PWR	PCC202	P	3	21	11.27	12.00	0.94	31.82	No
Catawba	1	PWR	FCB101	F	6	20	24.31	20.63	1.18	3.75	No
Catawba	1	PWR	WCB101	W	3	19	7.91	2.47	3.20	31.82	No
Catawba	2	PWR	PCB201	P	6	21	0.93	10.27	0.09	3.75	No
Catawba	2	PWR	WCB201	W	3	19	91.48	9.59	9.54	31.82	No
Commanche Peak	1	PWR	PCP101	P	4	19	-19.21	15.89	-1.21	6.96	No
Connecticut Yankee		ex-PWR	PCTY04	P	3	21	-63.22	2.55	-24.79	31.82	No
Connecticut Yankee		ex-PWR	PCTY02	P	3	21	-47.44	1.52	-31.24	31.82	No

General Information							Type B Deviation (Slope Test)				
Plant Name	Unit	Reactor Type	Heat	Product Form	n	σ [°F]	m	se(m)	T_m	$T_{crit(\alpha)}$	Fails Test?
Crystal River	3	PWR	PCR301	P	4	21	22.02	11.98	1.84	6.96	No
Crystal River	3	PWR	WCR301	W	4	26	46.92	13.65	3.44	6.96	No
Crystal River	3	PWR	WHSS66	W	4	26	-110.03	117.85	-0.93	6.96	No
Crystal River	3	PWR	WHSSCR	W	3	26	-116.65	31.01	-3.76	31.82	No
Crystal River & Surry	3 & 2	PWR	WHSS65	W	3	26	2.10	14.59	0.14	31.82	No
D.C. Cook	1	PWR	PCK101	P	8	21	-8.31	11.44	-0.73	3.14	No
D.C. Cook	1	PWR	WCK101	W	3	26	-27.17	98.72	-0.28	31.82	No
D.C. Cook	2	PWR	PCK201	P	8	21	1.58	17.98	0.09	3.14	No
D.C. Cook	2	PWR	WCK201	W	4	19	-14.88	17.64	-0.84	6.96	No
Davis Besse		PWR	FDB102	F	4	19	33.72	23.70	1.42	6.96	No
Davis Besse		PWR	WDB101	W	5	26	10.23	58.55	0.17	4.54	No
Davis Besse		PWR	PRS101	P	3	21	19.87	18.23	1.09	31.82	No
Davis Besse		PWR	WRS101	W	3	26	24.78	24.12	1.03	31.82	No
Diablo Canyon	1	PWR	PDC103	P	3	21	-2.29	33.31	-0.07	31.82	No
Diablo Canyon	1	PWR	WDC101	W	3	26	23.50	74.96	0.31	31.82	No
Diablo Canyon	2	PWR	PDC201	P	8	21	-1.49	7.64	-0.19	3.14	No
Diablo Canyon	2	PWR	WDC201	W	4	26	-34.17	7.34	-4.66	6.96	No
Dresden	3	BWR	WDR302	W	3	26	-25.60	231.23	-0.11	31.82	No
Dresden	2	BWR	PDR201	P	5	21	2.15	5.51	0.39	4.54	No
Dresden	3	BWR	PDR301	P	6	21	-2.52	4.90	-0.51	3.75	No
Dresden	3	BWR	WDR301	W	5	26	7.60	7.66	0.99	4.54	No
Duane Arnold		BWR	PDAC01	P	3	21	-2.02	13.71	-0.15	31.82	No
Duane Arnold		BWR	WDAC01	W	3	19	20.21	6.54	3.09	31.82	No
Farley	1	PWR	PFA101	P	8	21	21.46	8.51	2.52	3.14	No
Farley	1	PWR	WFA101	W	4	26	-27.48	10.40	-2.64	6.96	No
Farley	2	PWR	PFA201	P	8	21	20.33	15.54	1.31	3.14	No
Farley	2	PWR	WFA201	W	4	19	-25.24	19.69	-1.28	6.96	No
FitzPatrick		BWR	PFTZ01	P	6	21	8.83	10.75	0.82	3.75	No
Fort Calhoun		PWR	PFC101	P	5	21	-22.33	33.89	-0.66	4.54	No
Fort Calhoun		PWR	WFC101	W	4	26	-73.25	49.46	-1.48	6.96	No
Ginna		PWR	FGIN02	F	4	19	39.26	74.20	0.53	6.96	No
Ginna		PWR	FGIN01	F	4	19	-33.49	29.11	-1.15	6.96	No

General Information							Type B Deviation (Slope Test)				
Plant Name	Unit	Reactor Type	Heat	Product Form	n	σ [°F]	m	se(m)	T_m	$T_{crit(\alpha)}$	Fails Test?
Ginna		PWR	WGIN01	W	4	26	13.77	24.57	0.56	6.96	No
H.B. Robinson	2	PWR	WHB201	W	3	26	7.86	33.97	0.23	31.82	No
Indian Point	2	PWR	PIP202	P	3	21	-59.41	46.88	-1.27	31.82	No
Indian Point	2	PWR	PIP203	P	3	21	-17.19	2.14	-8.05	31.82	No
Indian Point	3	PWR	PIP304	P	5	21	2.30	29.72	0.08	4.54	No
Indian Point	3	PWR	WIP301	W	3	26	-0.18	79.92	0.00	31.82	No
Kewaunee		PWR	FKWE02	F	4	19	5.09	6.32	0.81	6.96	No
Kewaunee		PWR	FKWE01	F	4	19	-3.54	28.08	-0.13	6.96	No
Kewaunee		PWR	WKWE01	W	4	26	-15.96	19.26	-0.83	6.96	No
Maine Yankee		ex-PWR	PMY_01	P	6	21	-6.49	15.82	-0.41	3.75	No
Maine Yankee		ex-PWR	SHSS01	SRM	17	21	-4.95	15.22	-0.33	2.60	No
Maine Yankee		ex-PWR	WMY_01	W	4	26	10.14	12.08	0.84	6.96	No
McGuire	1	PWR	PMC101	P	8	21	24.92	19.19	1.30	3.14	No
McGuire	1	PWR	WMC101	W	4	26	-43.26	13.24	-3.27	6.96	No
McGuire	2	PWR	FMC201	F	8	20	4.68	13.50	0.35	3.14	No
McGuire	2	PWR	WMC201	W	4	19	-34.72	13.01	-2.67	6.96	No
Millstone	1	ex-BWR	PML101	P	4	21	-46.63	28.45	-1.64	6.96	No
Millstone	2	PWR	PML201	P	5	21	23.17	31.56	0.73	4.54	No
Millstone	2	PWR	WML201	W	3	26	-56.09	3.80	-14.77	31.82	No
Nine Mile Point	1	BWR	PNM101	P	5	21	41.45	22.11	1.87	4.54	No
North Anna	1	PWR	FNA101	F	6	20	8.37	20.75	0.40	3.75	No
North Anna	1	PWR	WNA101	W	3	26	-40.22	70.03	-0.57	31.82	No
North Anna	2	PWR	FNA201	F	6	20	18.17	12.92	1.41	3.75	No
North Anna	2	PWR	WNA201	W	3	26	-5.18	23.10	-0.22	31.82	No
Oconee	1	PWR	POC102	P	6	21	-19.62	25.32	-0.77	3.75	No
Oconee	1	PWR	SHSS02	SRM	64	21	1.87	4.39	0.43	2.39	No
Oconee	1	PWR	WOC101	W	3	26	41.08	14.09	2.92	31.82	No
Oconee	2	PWR	FOC201	F	5	19	-15.62	13.86	-1.13	4.54	No
Oconee	2	PWR	WOC201	W	3	26	30.52	12.69	2.41	31.82	No
Oconee	3	PWR	FOC301	F	4	19	-2.79	5.78	-0.48	6.96	No
Oconee	3	PWR	FOC302	F	3	19	-21.76	32.80	-0.66	31.82	No
Oconee	3	PWR	WOC301	W	4	26	41.81	33.82	1.24	6.96	No

General Information							Type B Deviation (Slope Test)				
Plant Name	Unit	Reactor Type	Heat	Product Form	n	σ [°F]	m	se(m)	T_m	$T_{crit(\alpha)}$	Fails Test?
Oyster Creek		BWR	PGG_01	P	4	19	21.14	22.39	0.94	6.96	No
Oyster Creek		BWR	PCPR02	P	4	21	-8.62	42.21	-0.20	6.96	No
Oyster Creek		BWR	PEP2JP	P	5	19	-32.14	8.29	-3.88	4.54	No
Oyster Creek		BWR	WGG_01	W	4	19	39.71	61.15	0.65	6.96	No
Oyster Creek		BWR	WML101	W	6	26	10.03	20.07	0.50	3.75	No
Oyster Creek		BWR	WQC102_1	W	4	26	6.48	11.60	0.56	6.96	No
Oyster Creek		BWR	WQC201_1	W	4	26	57.46	59.89	0.96	6.96	No
Oyster Creek		BWR	WRB_01	W	3	19	20.94	63.55	0.33	31.82	No
Palisades		PWR	PPAL01	P	7	21	-77.49	15.02	-5.16	3.36	No
Palisades		PWR	WPAL01	W	4	26	-42.23	5.32	-7.93	6.96	No
Point Beach	2	PWR	FPB202	F	4	20	41.30	12.36	3.34	6.96	No
Point Beach	1	PWR	PPB102	P	4	21	-76.91	8.77	-8.77	6.96	No
Point Beach	1	PWR	PPB101	P	4	21	-55.54	23.06	-2.41	6.96	No
Point Beach	1	PWR	WPB101	W	4	26	-12.46	53.53	-0.23	6.96	No
Point Beach	2	PWR	FPB201	F	4	19	-0.70	8.03	-0.09	6.96	No
Point Beach	2	PWR	WPB201	W	4	26	38.35	27.60	1.39	6.96	No
Prarie Island	1	PWR	FPI101	F	8	19	-0.54	17.08	-0.03	3.14	No
Prarie Island	1	PWR	WPI101	W	4	26	57.84	38.91	1.49	6.96	No
Prarie Island	2	PWR	FPI201	F	8	20	8.36	9.37	0.89	3.14	No
Prarie Island	2	PWR	WPI201	W	4	26	-40.19	12.22	-3.29	6.96	No
Quad Cities	1	BWR	PQC101	P	6	21	7.70	2.14	3.59	3.75	No
Quad Cities	1	BWR	WQC101	W	4	26	10.12	7.81	1.30	6.96	No
Quad Cities	2	BWR	PQC201	P	4	21	-10.04	3.17	-3.17	6.96	No
Quad Cities	2	BWR	WQC201	W	4	26	-3.89	4.21	-0.92	6.96	No
Saint Lucie	1	PWR	PSL101	P	5	21	-5.59	16.17	-0.35	4.54	No
Saint Lucie	1	PWR	WSL101	W	3	26	-46.07	12.84	-3.59	31.82	No
Saint Lucie	2	PWR	PSL201	P	3	21	49.57	1.95	25.45	31.82	No
Salem	1	PWR	PSA103	P	3	21	-6.76	19.49	-0.35	31.82	No
Salem	1	PWR	PSA101	P	3	21	5.06	24.98	0.20	31.82	No
Salem	2	PWR	PSA201	P	8	21	-3.87	21.39	-0.18	3.14	No
Salem	2	PWR	WSA201	W	4	26	-45.51	9.34	-4.87	6.96	No
San Onofre	2	PWR	PSO201	P	3	21	11.38	26.39	0.43	31.82	No

General Information							Type B Deviation (Slope Test)				
Plant Name	**Unit**	**Reactor Type**	**Heat**	**Product Form**	**n**	**σ [°F]**	**m**	**se(m)**	**T_m**	**$T_{crit(\alpha)}$**	**Fails Test?**
San Onofre	3	PWR	PSO301	P	3	19	15.75	21.22	0.74	31.82	No
Seabrook	1	PWR	PSB101	P	4	19	-6.15	14.03	-0.44	6.96	No
Sequoyah	1	PWR	FSQ101	F	8	20	31.83	17.01	1.87	3.14	No
Sequoyah	1	PWR	WSQ101	W	4	26	-8.36	4.54	-1.84	6.96	No
Sequoyah	2	PWR	FSQ201	F	8	20	12.09	14.40	0.84	3.14	No
Sequoyah	2	PWR	WSQ201	W	4	26	-71.71	89.12	-0.80	6.96	No
South Texas	1	PWR	PST101	P	4	19	-9.15	21.18	-0.43	6.96	No
South Texas	2	PWR	PST201	P	4	19	16.33	4.60	3.55	6.96	No
Surry	1	PWR	PSU101	P	3	21	10.46	20.36	0.51	31.82	No
Surry	1	PWR	WSU101	W	3	26	9.51	7.62	1.25	31.82	No
Surry	2	PWR	PSU201	P	6	21	-2.98	13.63	-0.22	3.75	No
Surry	2	PWR	WSU201	W	3	26	7.37	24.69	0.30	31.82	No
Three Mile Island	1	PWR	PTM101	P	3	21	-41.07	2.89	-14.23	31.82	No
Trojan		ex-PWR	PTRO01	P	6	21	-2.31	12.00	-0.19	3.75	No
Trojan		ex-PWR	WTRO01	W	3	19	-14.97	10.82	-1.38	31.82	No
Turkey Point	3	PWR	FTP302	F	3	20	52.36	70.45	0.74	31.82	No
Turkey Point	3	PWR	SASTM	SRM	26	21	10.59	8.87	1.19	2.49	No
Turkey Point	3	PWR	WTP301	W	4	26	15.55	35.61	0.44	6.96	No
Virgil Summer	1	PWR	PVS101	P	8	21	-12.14	16.33	-0.74	3.14	No
Virgil Summer	1	PWR	WVS101	W	4	19	-20.29	23.75	-0.85	6.96	No
Votgle	1	PWR	PVO101	P	6	19	20.85	19.05	1.09	3.75	No
Votgle	1	PWR	WVO101	W	3	19	-41.81	19.81	-2.11	31.82	No
Votgle	2	PWR	PVO201	P	6	19	15.57	10.12	1.54	3.75	No
Votgle	2	PWR	WVO201	W	3	19	25.29	19.30	1.31	31.82	No
Waterford	3	PWR	PWF301	P	3	19	-87.52	64.25	-1.36	31.82	No
Watts Bar	1	PWR	FWB101	F	4	20	41.28	90.57	0.46	6.96	No
Wolf Creek	1	PWR	PWC101	P	8	19	-8.38	9.54	-0.88	3.14	No
Wolf Creek	1	PWR	WWC101	W	4	19	4.70	8.95	0.53	6.96	No
Zion	1	ex-PWR	PZN101	P	8	21	14.89	14.97	0.99	3.14	No
Zion	1	ex-PWR	WZN101	W	5	26	43.23	8.52	5.07	4.54	Yes
Zion	2	ex-PWR	PZN201	P	6	21	19.41	15.57	1.25	3.75	No
Zion	2	ex-PWR	WZN201	W	3	26	17.59	31.94	0.55	31.82	No

Table B-3. Type D Deviations (Outlier Test)

General Information							Type D Deviation (Outlier Test)				
Plant Name	Unit	Reactor Type	Heat	Product Form	n	σ [°F]	$r_{i(max1)}$	$r_{i(max2)}$	C_1	C_2	Fails Test?
Arkansas Nuclear	1	PWR	PAN101	P	6	21	0.98	-0.13	1.93	2.93	No
Arkansas Nuclear	1	PWR	WAN101	W	3	26	1.47	0.03	1.55	2.71	No
Arkansas Nuclear	2	PWR	PAN201	P	3	21	0.36	-0.32	1.55	2.71	No
Beaver Valley	1	PWR	PBV101	P	8	21	2.52	2.26	2.05	3.02	No
Beaver Valley	1	PWR	WBV101	W	4	26	0.83	0.14	1.73	2.81	No
Beaver Valley	2	PWR	PBV201	P	6	19	-0.04	-0.06	1.93	2.93	No
Beaver Valley	2	PWR	WBV201	W	3	26	-0.61	-1.39	1.55	2.71	No
Braidwood	1	PWR	FBD101	F	6	19	0.41	0.23	1.93	2.93	No
Braidwood	1	PWR	WBD101	W	3	19	0.42	0.03	1.55	2.71	No
Braidwood	2	PWR	FBD201	F	6	19	0.85	0.41	1.93	2.93	No
Braidwood	2	PWR	WBD201	W	3	19	0.04	-0.59	1.55	2.71	No
Brunswick	1	BWR	PBR_01	P	5	21	4.09	2.99	1.84	2.88	No
Brunswick	1	BWR	WBR_01	W	3	26	2.56	1.53	1.55	2.71	No
Byron	1	PWR	FBY101	F	6	19	1.67	1.58	1.93	2.93	No
Byron	1	PWR	WBY101	W	3	19	0.38	0.37	1.55	2.71	No
Byron	2	PWR	FBY201	F	6	19	0.46	0.36	1.93	2.93	No
Byron	2	PWR	WBY201	W	3	19	0.59	-0.10	1.55	2.71	No
Callaway		PWR	PCL101	P	8	19	1.06	0.70	2.05	3.02	No
Callaway		PWR	WCL101	W	4	19	3.03	0.98	1.73	2.81	No
Calvert Cliffs	1	PWR	PCC103	P	3	21	-0.10	-0.19	1.55	2.71	No
Calvert Cliffs	1	PWR	WCC101	W	3	26	-0.14	-0.71	1.55	2.71	No
Calvert Cliffs	2	PWR	PCC202	P	3	21	-0.14	-0.38	1.55	2.71	No
Catawba	1	PWR	FCB101	F	6	20	0.14	0.05	1.93	2.93	No
Catawba	1	PWR	WCB101	W	3	19	-0.27	-0.46	1.55	2.71	No
Catawba	2	PWR	PCB201	P	6	21	0.30	0.26	1.93	2.93	No
Catawba	2	PWR	WCB201	W	3	19	1.75	0.74	1.55	2.71	No
Commanche Peak	1	PWR	PCP101	P	4	19	0.38	-0.15	1.73	2.81	No
Connecticut Yankee		ex-PWR	PCTY04	P	3	21	1.02	-0.60	1.55	2.71	No
Connecticut Yankee		ex-PWR	PCTY02	P	3	21	0.17	-0.45	1.55	2.71	No
Crystal River	3	PWR	PCR301	P	4	21	1.46	1.03	1.73	2.81	No

General Information							Type D Deviation (Outlier Test)				
Plant Name	**Unit**	**Reactor Type**	**Heat**	**Product Form**	**n**	**σ [°F]**	**$r_{i(max1)}$**	**$r_{i(max2)}$**	**C_1**	**C_2**	**Fails Test?**
Crystal River	3	PWR	WCR301	W	4	26	1.12	1.00	1.73	2.81	No
Crystal River	3	PWR	WHSS66	W	4	26	0.71	-0.78	1.73	2.81	No
Crystal River	3	PWR	WHSSCR	W	3	26	0.77	0.06	1.55	2.71	No
Crystal River & Surry	3 & 2	PWR	WHSS65	W	3	26	0.23	0.18	1.55	2.71	No
D.C. Cook	1	PWR	PCK101	P	8	21	0.57	0.28	2.05	3.02	No
D.C. Cook	1	PWR	WCK101	W	3	26	-2.30	-3.73	1.55	2.71	No
D.C. Cook	2	PWR	PCK201	P	8	21	2.27	1.68	2.05	3.02	No
D.C. Cook	2	PWR	WCK201	W	4	19	1.47	1.28	1.73	2.81	No
Davis Besse		PWR	FDB102	F	4	19	0.98	-0.60	1.73	2.81	No
Davis Besse		PWR	WDB101	W	5	26	2.01	0.32	1.84	2.88	No
Davis Besse		PWR	PRS101	P	3	21	-0.05	-0.12	1.55	2.71	No
Davis Besse		PWR	WRS101	W	3	26	-0.26	-0.36	1.55	2.71	No
Diablo Canyon	1	PWR	PDC103	P	3	21	-0.53	-1.24	1.55	2.71	No
Diablo Canyon	1	PWR	WDC101	W	3	26	1.14	-0.69	1.55	2.71	No
Diablo Canyon	2	PWR	PDC201	P	8	21	0.21	-0.04	2.05	3.02	No
Diablo Canyon	2	PWR	WDC201	W	4	26	0.54	-0.15	1.73	2.81	No
Dresden	3	BWR	WDR302	W	3	26	0.74	-1.02	1.55	2.71	No
Dresden	2	BWR	PDR201	P	5	21	-0.23	-1.56	1.84	2.88	No
Dresden	3	BWR	PDR301	P	6	21	0.49	-0.20	1.93	2.93	No
Dresden	3	BWR	WDR301	W	5	26	1.01	0.43	1.84	2.88	No
Duane Arnold		BWR	PDAC01	P	3	21	0.66	0.39	1.55	2.71	No
Duane Arnold		BWR	WDAC01	W	3	19	0.14	-0.32	1.55	2.71	No
Farley	1	PWR	PFA101	P	8	21	1.39	1.20	2.05	3.02	No
Farley	1	PWR	WFA101	W	4	26	0.38	-0.46	1.73	2.81	No
Farley	2	PWR	PFA201	P	8	21	1.92	1.22	2.05	3.02	No
Farley	2	PWR	WFA201	W	4	19	-2.12	-2.13	1.73	2.81	No
FitzPatrick		BWR	PFTZ01	P	6	21	-0.03	-0.16	1.93	2.93	No
Fort Calhoun		PWR	PFC101	P	5	21	0.03	-0.11	1.84	2.88	No
Fort Calhoun		PWR	WFC101	W	4	26	0.59	0.32	1.73	2.81	No
Ginna		PWR	FGIN02	F	4	19	1.35	-0.34	1.73	2.81	No
Ginna		PWR	FGIN01	F	4	19	2.19	1.10	1.73	2.81	No
Ginna		PWR	WGIN01	W	4	26	1.17	0.58	1.73	2.81	No

General Information							Type D Deviation (Outlier Test)				
Plant Name	Unit	Reactor Type	Heat	Product Form	n	σ [°F]	$r_{i(max1)}$	$r_{i(max2)}$	C_1	C_2	Fails Test?
H.B. Robinson	2	PWR	WHB201	W	3	26	0.96	0.05	1.55	2.71	No
Indian Point	2	PWR	PIP202	P	3	21	1.26	-0.57	1.55	2.71	No
Indian Point	2	PWR	PIP203	P	3	21	1.81	1.53	1.55	2.71	No
Indian Point	3	PWR	PIP304	P	5	21	1.41	1.11	1.84	2.88	No
Indian Point	3	PWR	WIP301	W	3	26	1.90	1.54	1.55	2.71	No
Kewaunee		PWR	FKWE02	F	4	19	-0.08	-0.43	1.73	2.81	No
Kewaunee		PWR	FKWE01	F	4	19	-0.04	-0.05	1.73	2.81	No
Kewaunee		PWR	WKWE01	W	4	26	1.10	0.74	1.73	2.81	No
Maine Yankee		ex-PWR	PMY_01	P	6	21	2.36	1.58	1.93	2.93	No
Maine Yankee		ex-PWR	SHSS01	SRM	17	21	1.48	0.96	2.37	3.24	No
Maine Yankee		ex-PWR	WMY_01	W	4	26	0.05	-0.12	1.73	2.81	No
McGuire	1	PWR	PMC101	P	8	21	1.98	1.16	2.05	3.02	No
McGuire	1	PWR	WMC101	W	4	26	0.54	-0.68	1.73	2.81	No
McGuire	2	PWR	FMC201	F	8	20	1.52	0.13	2.05	3.02	No
McGuire	2	PWR	WMC201	W	4	19	1.32	0.14	1.73	2.81	No
Millstone	1	ex-BWR	PML101	P	4	21	0.43	0.18	1.73	2.81	No
Millstone	2	PWR	PML201	P	5	21	1.94	1.09	1.84	2.88	No
Millstone	2	PWR	WML201	W	3	26	-0.27	-1.13	1.55	2.71	No
Nine Mile Point	1	BWR	PNM101	P	5	21	0.05	-0.24	1.84	2.88	No
North Anna	1	PWR	FNA101	F	6	20	0.88	-0.65	1.93	2.93	No
North Anna	1	PWR	WNA101	W	3	26	2.07	0.94	1.55	2.71	No
North Anna	2	PWR	FNA201	F	6	20	-0.12	-0.17	1.93	2.93	No
North Anna	2	PWR	WNA201	W	3	26	-0.59	-0.63	1.55	2.71	No
Oconee	1	PWR	POC102	P	6	21	1.53	1.41	1.93	2.93	No
Oconee	1	PWR	SHSS02	SRM	64	21	1.47	1.40	2.83	3.62	No
Oconee	1	PWR	WOC101	W	3	26	0.87	0.31	1.55	2.71	No
Oconee	2	PWR	FOC201	F	5	19	0.94	0.00	1.84	2.88	No
Oconee	2	PWR	WOC201	W	3	26	-0.09	-1.17	1.55	2.71	No
Oconee	3	PWR	FOC301	F	4	19	0.37	0.16	1.73	2.81	No
Oconee	3	PWR	FOC302	F	3	19	2.53	0.98	1.55	2.71	No
Oconee	3	PWR	WOC301	W	4	26	0.89	-1.03	1.73	2.81	No
Oyster Creek		BWR	PGG_01	P	4	19	0.23	-0.05	1.73	2.81	No

General Information							Type D Deviation (Outlier Test)				
Plant Name	Unit	Reactor Type	Heat	Product Form	n	σ [°F]	$r_{i(max1)}$	$r_{i(max2)}$	C_1	C_2	Fails Test?
Oyster Creek		BWR	PCPR02	P	4	21	0.48	-0.17	1.73	2.81	No
Oyster Creek		BWR	PEP2JP	P	5	19	0.86	0.12	1.84	2.88	No
Oyster Creek		BWR	WGG_01	W	4	19	0.62	-0.32	1.73	2.81	No
Oyster Creek		BWR	WML101	W	6	26	0.07	-0.70	1.93	2.93	No
Oyster Creek		BWR	WQC102_1	W	4	26	1.14	1.02	1.73	2.81	No
Oyster Creek		BWR	WQC201_1	W	4	26	1.16	1.03	1.73	2.81	No
Oyster Creek		BWR	WRB_01	W	3	19	2.27	1.87	1.55	2.71	No
Palisades		PWR	PPAL01	P	7	21	0.11	-0.48	2	2.98	No
Palisades		PWR	WPAL01	W	4	26	0.21	0.07	1.73	2.81	No
Point Beach	2	PWR	FPB202	F	4	20	1.64	1.35	1.73	2.81	No
Point Beach	1	PWR	PPB102	P	4	21	-0.37	-0.52	1.73	2.81	No
Point Beach	1	PWR	PPB101	P	4	21	1.08	1.03	1.73	2.81	No
Point Beach	1	PWR	WPB101	W	4	26	-0.46	-1.58	1.73	2.81	No
Point Beach	2	PWR	FPB201	F	4	19	1.06	0.94	1.73	2.81	No
Point Beach	2	PWR	WPB201	W	4	26	0.00	0.00	1.73	2.81	No
Prarie Island	1	PWR	FPI101	F	8	19	0.77	0.77	2.05	3.02	No
Prarie Island	1	PWR	WPI101	W	4	26	0.89	-0.43	1.73	2.81	No
Prarie Island	2	PWR	FPI201	F	8	20	0.56	0.11	2.05	3.02	No
Prarie Island	2	PWR	WPI201	W	4	26	0.57	-0.47	1.73	2.81	No
Quad Cities	1	BWR	PQC101	P	6	21	0.74	0.60	1.93	2.93	No
Quad Cities	1	BWR	WQC101	W	4	26	0.63	-0.63	1.73	2.81	No
Quad Cities	2	BWR	PQC201	P	4	21	-0.11	-0.38	1.73	2.81	No
Quad Cities	2	BWR	WQC201	W	4	26	1.07	0.81	1.73	2.81	No
Saint Lucie	1	PWR	PSL101	P	5	21	-0.55	-0.72	1.84	2.88	No
Saint Lucie	1	PWR	WSL101	W	3	26	-0.28	-0.68	1.55	2.71	No
Saint Lucie	2	PWR	PSL201	P	3	21	2.02	-0.01	1.55	2.71	No
Salem	1	PWR	PSA103	P	3	21	-1.09	-1.33	1.55	2.71	No
Salem	1	PWR	PSA101	P	3	21	0.91	0.01	1.55	2.71	No
Salem	2	PWR	PSA201	P	8	21	1.58	1.20	2.05	3.02	No
Salem	2	PWR	WSA201	W	4	26	-0.12	-0.24	1.73	2.81	No
San Onofre	2	PWR	PSO201	P	3	21	0.02	-0.10	1.55	2.71	No
San Onofre	3	PWR	PSO301	P	3	19	2.43	2.34	1.55	2.71	No

General Information							Type D Deviation (Outlier Test)				
Plant Name	**Unit**	**Reactor Type**	**Heat**	**Product Form**	**n**	**σ [°F]**	$r_{i(max1)}$	$r_{i(max2)}$	C_1	C_2	**Fails Test?**
Seabrook	1	PWR	PSB101	P	4	19	1.39	1.19	1.73	2.81	No
Sequoyah	1	PWR	FSQ101	F	8	20	2.37	1.73	2.05	3.02	No
Sequoyah	1	PWR	WSQ101	W	4	26	1.39	1.31	1.73	2.81	No
Sequoyah	2	PWR	FSQ201	F	8	20	1.57	1.36	2.05	3.02	No
Sequoyah	2	PWR	WSQ201	W	4	26	3.62	1.44	1.73	2.81	No
South Texas	1	PWR	PST101	P	4	19	0.71	0.59	1.73	2.81	No
South Texas	2	PWR	PST201	P	4	19	0.67	0.39	1.73	2.81	No
Surry	1	PWR	PSU101	P	3	21	0.80	0.02	1.55	2.71	No
Surry	1	PWR	WSU101	W	3	26	1.88	1.58	1.55	2.71	No
Surry	2	PWR	PSU201	P	6	21	0.55	0.47	1.93	2.93	No
Surry	2	PWR	WSU201	W	3	26	0.00	-0.58	1.55	2.71	No
Three Mile Island	1	PWR	PTM101	P	3	21	0.38	-1.29	1.55	2.71	No
Trojan		ex-PWR	PTRO01	P	6	21	0.74	0.14	1.93	2.93	No
Trojan		ex-PWR	WTRO01	W	3	19	0.77	0.55	1.55	2.71	No
Turkey Point	3	PWR	FTP302	F	3	20	1.05	0.67	1.55	2.71	No
Turkey Point	3	PWR	SASTM	SRM	26	21	1.98	1.94	2.53	3.36	No
Turkey Point	3	PWR	WTP301	W	4	26	1.30	0.36	1.73	2.81	No
Virgil Summer	1	PWR	PVS101	P	8	21	0.12	-0.15	2.05	3.02	No
Virgil Summer	1	PWR	WVS101	W	4	19	0.95	0.16	1.73	2.81	No
Votgle	1	PWR	PVO101	P	6	19	0.70	0.56	1.93	2.93	No
Votgle	1	PWR	WVO101	W	3	19	0.67	-0.02	1.55	2.71	No
Votgle	2	PWR	PVO201	P	6	19	-0.17	-0.23	1.93	2.93	No
Votgle	2	PWR	WVO201	W	3	19	-0.17	-0.49	1.55	2.71	No
Waterford	3	PWR	PWF301	P	3	19	0.53	-0.87	1.55	2.71	No
Watts Bar	1	PWR	FWB101	F	4	20	0.94	0.85	1.73	2.81	No
Wolf Creek	1	PWR	PWC101	P	8	19	1.10	0.88	2.05	3.02	No
Wolf Creek	1	PWR	WWC101	W	4	19	1.20	1.20	1.73	2.81	No
Zion	1	ex-PWR	PZN101	P	8	21	0.43	0.33	2.05	3.02	No
Zion	1	ex-PWR	WZN101	W	5	26	0.31	0.02	1.84	2.88	No
Zion	2	ex-PWR	PZN201	P	6	21	1.20	0.27	1.93	2.93	No
Zion	2	ex-PWR	WZN201	W	3	26	0.66	0.04	1.55	2.71	No

APPENDIX C: FLAW DEPTH AND DENSITY DISTRIBUTIONS CONSIDERING PROBABILITY OF DETECTION AND BIAS IN NDE DATA WITH APPLICATIONS

Prepared for the U.S. Nuclear Regulatory Commission under Subcontract 4000099247with UT-Battelle, LLC (Oak Ridge National Laboratory)

Mohammad Modarres
University of Maryland

October 2011

Table of Contents

List of Tables

List of Figures

Abbreviations

Abbreviation	Definition
PDF	Probability Density Function
CDF	Cumulative Density Function
ISI	In-Service Inspection
NDE	Nondestructive Evaluation
POD	Probability of Detection
PTS	Pressurized Thermal Shock
RPV	Reactor Pressure Vessel
SAW	Submerged Arc Weld
SMAW	Shielded Metal Arc Weld
UT	Ultrasonic Test

Symbols and Expressions

Symbol	Definition
a	True flaw depth (inches)
A	Random variable representing flaw depth
$\hat{a}$	Logarithm of signal-response amplitude in flaw-detection NDE
a*	NDE measured (or observed) flaw depth (inches)
a_{th}	Threshold flaw depth for detection below which flaw detection is beyond the capability of the NDE technology used
D	The event that a flaw is detected
$\overline{D}$	The event that a flaw is not detected
E_M	Model error of the NDE measurement error, represented by a normal distribution with mean of zero and known standard deviation
$f_a(a^*\text{-}M_\varepsilon\|\Phi)$	PDF of the true flaw depth, given the vector of PDF parameters represented in terms of observed flaw depth a* but corrected for the measurement error M_ε
$f_l(a \mid \Phi, a \geq t_{tr})$	Conditional PDF of large flaw depth
$f_s(a \mid \Phi, a < t_{tr})$	Conditional PDF of small flaw depth
f(.), g(.), h(.), l(.), m(.), x(.), g'(.). k(.), γ(.)	PDF functions of model parameters, flaw depth, or flaw density
$g(M_\varepsilon)$	PDF of the measurement error (in terms of a*)
$L(a\|\Phi)$	Likelihood of true flaw depth given the vector of parameters Φ
L(Data|θ)	Likelihood of observed NDE data conditioned on (given) the unknown parameter θ
$L(n^* \mid n_j)$	Likelihood of observing n* flaws given there are a total of n_j true flaws
M_ε	NDE measurement error (combined random and systematic errors)
m^*_i	Number of flaw depths observed (reported in NDE) in the interval i
n	Number of flaw-depth intervals (reported in NDE)
n*	Number of exact flaw depths observed (reported in NDE)
$\binom{n_j}{n^*}$	Combination of n* observed flaws out of total flaws n_j (observed or detected, and unobserved or not detected flaws)
N	Mean of the PDF of the number of flaws in volume v
N(0;σ)	Normal PDF with mean zero and standard deviation of σ
POD(a)	Probability of detection of a flaw of depth a
$POD(a^*\text{-}M_\varepsilon)$	POD of true flaw depth represented in terms of observed flaw depth a* by correcting for the measurement error M_ε
Pr(.)	Probability
Pr(D)	POD independent of flaw depth
$Pr(\overline{D})$	Probability of no detection regardless of size
$Pr(n_j \mid n^*)$	Probability of total flaws n_j conditioned on observing n* flaws in NDE
$Pr(\Phi, t_{tr})$	POD independent of flaw size (i.e., Pr(D))
t_{tr}	Transition flaw depth which separates large flaw depth from small flaw depth
v	Volume of inspected weld
β_i	Parameter i of the POD model
Δ	Weld bead thickness

Symbol	Definition
ε	Random error of the model
λ	Flaw-depth intensity parameter (inch^{-1}) of the exponential distribution $f(a) = \lambda e^{-\lambda a}$ representing flaw-depth distribution, also flaw intensity (flaws/ft^3) representing Poisson flaw density distribution: $Pr(N) = e^{-\lambda v} \frac{(\lambda v)^N}{N!}$
$\pi_0(\theta)$	Prior PDF of an unknown parameter θ
$\pi_1(\theta \vert Data)$	Posterior PDF of an unknown parameter θ given observed NDE data
Φ	Vector of parameters of the flaw-depth PDF
θ	An unknown parameter of a model
Θ	Vector of parameters of the POD model
ρ	Poisson distribution parameter representing the volumetric intensity of flaws (flaws per unit volume)
$\sigma_{POD}(a)$	Standard deviation of PDF of the POD model error vs. flaw depth
$\gamma(. \vert \alpha_1, \alpha_2)$	Gamma PDF with parameters α_1 and α_2

C.1 Introduction and Background

In 2010, the NRC amended its regulations to provide alternative screening methods for protection against Pressurized Thermal Shock (PTS) events that could affect the Reactor Pressure Vessels (RPVs) of the operating Pressurized-Water Reactors (PWRs). The new rule, 10 CFR 50.61a [C-1], provides a means for determining whether the flaws found through In-Service Inspection (ISI) of a particular RPV are consistent with the assumptions regarding the number and size of flaws used in the PTS analyses that provided the technical basis for the new rule. To address this requirement, 10 CFR 50.61a includes two tables (one table for weld material and one table for plate/forging material) that express the maximum flaw density and flaw depths that are allowed in the beltline of an RPV.

The new rule relies on flaw characteristics (flaw depth and density) that were simulated and used by the probabilistic fracture mechanics computer code FAVOR [C-2] to develop the 10 CFR 50.61a flaw tables. These flaw characteristics were proposed by Simonen et al. in NUREG/CR-6817 [C-3] and are used by the VFLAW code to generate the input flaws for FAVOR. The data include distribution functions that represent the initial fabrication flaws in some RPVs. The FAVOR computer code fully incorporates these distributions by sampling from each using Monte Carlo techniques.

The flaw distributions reported in NUREG/CR-6817 are based on information obtained from destructive and very precise techniques used to experimentally detect and size the flaws. These tables have been viewed as the permissible limit for distribution of the “true” flaw depths and flaw densities. These depth and densities may be contrasted with those “observed” in an ISI using Non-Destructive Evaluation (NDE) techniques such as the Ultrasonic Test (UT). The NDE results used to assess compliance with the 10 CFR 50.61a tables would be more representative of the specific vessel inspected than the flaw distributions in NUREG/CR-6817 and could be used to support development of vessel-specific flaw-size and -density distributions. However, the NDE results are influenced by detection limits, detection errors, and sizing and measurement errors. Development of the vessel-specific distribution of the true flaw density and depth should account for such uncertainties.

This report describes the development and application of a methodology to account for uncertainties in NDE data and to analyze such data for the purpose of developing more realistic vessel-specific flaw-depth and -density distributions for comparison to the 10 CFR 50.61a screening tables, as well as for use as an input to FAVOR analysis. The methodology considers detection probability, flaw-measurement error, and flaw-detection threshold in its application. Application of the methodology is demonstrated using the ultrasonic NDE data obtained from an ISI of the Beaver Valley 2 RPV.

Flaw distributions developed and reported in NUREG/CR-6817 are based on destructive evaluation of two cancelled RPVs supplemented by expert judgment data. In contrast, the vessel-specific inspection data come from NDE inspections using, for example, UT methods. The variability in both the characteristics of the data (size, range, and number of flaws measured) and the UT system performance (probability of detection and measurement/sizing errors) highlighted a need for analyzing the inspection results on a vessel-specific or data-set-specific basis. For this purpose, traditional methods were inadequate, and therefore a new methodology that could accept a very small number of flaws (typical of vessel-specific NDE results), including inspection-system flaw-detection reliability, flaw-sizing accuracy (measurement error), and flaw-detection threshold, was developed.

The methodology is demonstrated here through an application using the UT data reported for the Beaver Valley 2 RPV [C-13]. The objective was to provide a probabilistic description (in terms of the probability density function) of the actual flaw depth and flaw density of the welds based on the detected flaws from NDE examinations of this RPV using UT. Because the NDE data are uncertain and contain measurement errors, data developed as part of the PTS study (the so-called VFLAW data) were specialized to the Beaver Valley 2 RPV and used as the prior flaw information. Combination of the prior information and the NDE results of the Beaver Valley 2 RPV led to the development of the posterior flaw information, which represents the distribution of the true flaw depth and flaw density of the Beaver Valley 2 RPV welds. See Figure C-1 for an illustration of the Bayesian updating process. It is important to note that the VFLAW data, while representing generic values of flaw characteristics (based on expert judgment and on the PVRUF and Shoreham RPVs), may be specialized to a specific RPV, for example by using RPV-specific weld length, bead thickness, geometry and other weld characteristics of (in this case) Beaver Valley 2. Therefore, the specialized VFLAW data would be the most representative information that can be used to describe prior flaw-depth and flaw-density distributions and characteristics. If other prior information is available, such information may also be used instead of or in addition to the specialized VFLAW data.

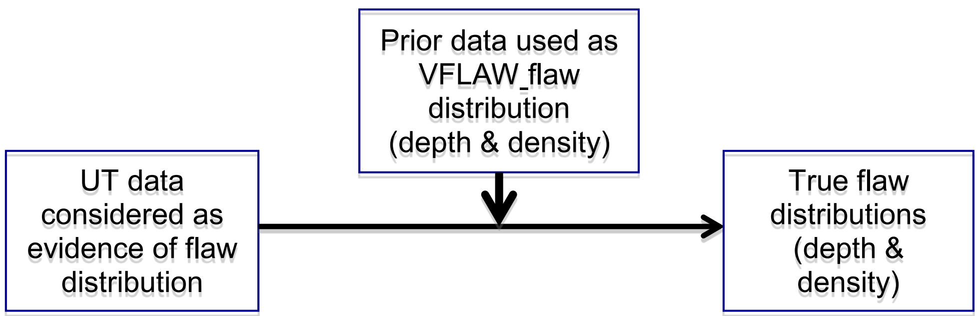

Figure C-1. A simple description of the Bayesian updating process.

In the remainder of this report, the methodology is described first, followed by the application to the Beaver Valley 2 ISI data. The results are used to compare the Beaver Valley 2 RPV to the 10 CFR 50.61a screening tables. As such, the VFLAW-based flaw models are updated to more realistically represent this RPV.

C.2 Probabilistic Approach to Combine Uncertain NDE Flaw Data with Prior Flaw Distributions

In this section, a Bayesian updating methodology is proposed to combine the observed NDE data with the available flaw data and models used as part of the PTS re-evaluation effort. First, the Bayesian framework in general will be discussed, followed by the NDE data uncertainties (i.e., probability of detection and measurement/sizing error), and finally the developed Bayesian updating procedure will be discussed.

C.2.1 The Bayesian Framework

Suppose that background (prior) information is available about a model (e.g., the probability density functions representing flaw depth and flaw density). If new evidence becomes available, for example vessel-specific NDE data, it is possible to update the prior information (e.g., distribution models) in light of the new NDE-based evidence. The process of updating prior distribution models may be formally done through Bayesian inference. Bayesian inference is conceptually simple and logically consistent. It provides a powerful approach to combine observed or measured data with background (prior) information.

In Bayesian inference, the state of knowledge (uncertainty) of a random variable of unknown value that is of interest is quantified by assigning a probability distribution or Probability Density Function (PDF) to its possible values. Bayesian inference provides the mathematical formalism by which this uncertainty can be updated in light of any new evidence.

In the framework of the Bayesian approach, the parameters of the model of interest (e.g., the intensity parameter, λ, of an exponential distribution representing flaw depth) are treated as random variables, the true values of which are unknown. Thus, a PDF can be assigned to represent the parameter values. In practice, however, some prior information about the parameters may be known, including any prior data and subjective judgments regarding the parameter values that may be available. For example, the intensity parameter, λ, of an exponential distribution representing the variable flaw depth (e.g., in $inch^{-1}$) may be known from related observations and data of similar vessels. If new NDE observations provide limited but more specific data about a particular RPV, it is possible to update any prior PDF of the flaw-depth intensity parameter by combining the NDE data with the prior PDF. In this case, the prior knowledge is combined with the specific NDE data to build a posterior PDF that is more representative of the true intensity parameter and thus the true flaw-depth distribution that accounts for the uncertainties in the observed NDE data.

Let θ be a parameter of interest (for example the flaw intensity parameter). Assume that θ is a continuous random variable, such that the prior and posterior PDFs of θ are likewise continuous. Also, let L(Data|θ) express how likely is it to observe the data (e.g., the NDE data measured) in light of given values of parameter θ. Certain values of θ show that the data observed are more likely to support the PDF whose parameter is θ. Then, according to Bayesian inference [C-4], the posterior PDF that represents a properly weighted combination of the prior PDF and the likelihood of the parameter θ will be:

$$\pi_1(\theta|\text{Data}) = \frac{\pi_0(\theta)L(\text{Data}|\theta)}{\int_\theta \pi_0(\theta)L(\text{Data}|\theta)d\theta} \qquad \text{Eqn. (C-1)}$$

The posterior PDF, $\pi_1(\theta|\text{Data})$, represents the updated prior PDF of θ, $\pi_0(\theta)$, in light of the observed data (shown by its likelihood function L(Data|θ)). The denominator of Eqn. (C-1) is called the marginal density of the data or the normalization constant. The most difficult part of a Bayesian analysis, besides describing the likelihood function, is the computational challenge of determining the normalizing constant that often requires multidimensional numerical integration. The prior PDF $\pi_0(\theta)$ reveals knowledge of parameter θ before data are used. The posterior PDF $\pi_1(\theta|\text{Data})$ is called posterior because it reflects the PDF of θ after the data are used.

Certain prior PDFs are called "conjugate" [C-4]. This is the class of prior PDFs that yields the same functional form for the posterior distribution. For example, if flaw-depth distribution is represented by an exponential distribution, a gamma PDF representing the intensity parameter, λ, of the exponential distribution is a conjugate distribution. This means that when updated by new NDE flaw data, the posterior PDF of λ will also be a gamma distribution. Hamada et al. [C-5] present a comprehensive overview of the mathematical steps for updating the conjugate distributions used in the Bayesian analyses. In simple problems, the conjugate distribution makes posterior PDF calculations simple because it eliminates the complex, computationally challenging integrations in Eqn. (C-1).

For example, consider NDE flaw observations (data). In this case, the likelihood of all such data, given a parameter θ of the flaw-depth PDF L(Data| θ), would be expressed as the probability of the intersections of the individual flaw measurements; that is, the probability of an event consisting of *flaw-measurement-1* $\cap$ *flaw-measurement-2* $\cap$ *flaw-measurement-3* $\cap$ *...* . The likelihood, therefore, would be the product of the probability of observing each flaw depth, a_i, as shown by Eqn. (C-2). The likelihood function is independent of the order of each data point and is given by:

$$L(\text{Data} \mid \theta) = c\prod_i L_i(a_i \mid \theta) \qquad \text{Eqn. (C-2)}$$

where c is a combinatorial constant that quantifies the number of combinations in which the observed NDE data points, a_i, could have occurred. The constant c cancels from the numerator and denominator of Eqn. (C-1), and therefore is usually not included in the expressions of the likelihood function. Table C-1 summarizes the likelihood functions for different types of flaw data observations, if the PDF of the variable of interest (flaw depth in this case) is described by f(a|θ) with the corresponding Cumulative Density Function (CDF) of $F(a \mid \theta) = \int_0^a f(x \mid \theta)dx$.

Table C-1. Summary of Likelihood Functions

Type of Observation	Likelihood Function	Example Description
Exact Flaw Depth	$f(a_i\|\theta)$	Exact flaw depth a_i is reported
Right Censored Flaw	$1-F(a_R\|\theta)$	Flaw depth exceeds a_R
Left Censored Flaw	$F(a_L\|\theta)$	Flaw depth is less than a_L
Interval Censored	$F(a_R\|\theta) - F(a_L\|\theta)$	Flaw depth is between a_L and a_R
Left Truncated	$f(a_i\|\theta) / [1-F(a_C\|\theta)]$	Flaw depth is a_i where flaw observations are not possible below a_C

C.2.2 Probability of Detection and Measurement Error

Interpretation of NDE data requires an understanding of the associated uncertainties. For example, one inspector may miss a specific flaw found by another. For this reason, the reliability of an inspection is customarily expressed in terms of the Probability of Detection (POD) of a given flaw size and expressed by curves of POD vs. flaw size. Determining detailed POD curves can also be difficult. Flaw detection depends on several factors and it can be difficult to produce statistical data to estimate the POD considering variations in material types, inspection methods, skill levels, equipment imprecision, and other factors.

Additionally, sizing or measurement errors occur and measurement model uncertainties exist. The measurement errors are generally composed of some combination of stochastic (random) errors and systematic errors. Random errors are intrinsic to any measurement and are caused by instrumentation imprecision and variability, among other sources. Systematic errors are biases in NDE measurement resulting in the mean of many separate measurements differing consistently and appreciably from the true value of the measured flaw. Biases or systematic errors are often significant contributors to flaw data uncertainties. For example, in UT application to RPVs, there is a general trend toward overestimating the size of small flaws while underestimating the size of larger flaws [C-6].

C.2.2.1 Probability of Detection

Formally, the POD can be defined as the probability that the NDE system detects a flaw of specific depth a, if it exists, and is denoted by POD(a) [C-6]. POD is generally modeled as a function of through-wall extent of the flaw. The POD also depends on other factors such as material test equipment, measurement method, and geometry. For example, POD generated for a particular material thickness might not be true for the same material with a different thickness. The POD should also consider appropriate adjustments for shallow surface flaws adjacent to the clad.

Consider a binary random variable D indicating a flaw detected (or $\overline{D}$ indicating a flaw not detected). Probability of detection of a flaw of depth a_i is:

$$\mathrm{POD}(a_i) = \Pr(D \mid a = a_i) \qquad \text{Eqn. (C-3)}$$

The data from which POD(a) functions are generated can be categorized into two types: hit/miss and signal-response amplitude. The hit/miss data type shows whether a flaw is detected or not. This type of data is subjective in nature depending on the operator experience. In this method, the smallest and largest flaw sizes detected should be identified. Any size below the smallest size is never detected, whereas a size above the largest size is always detected. The POD is then calculated as the ratio of the number of successful detections over the total number of inspections performed for a particular flaw size and is called the averaged POD.

Different forms of POD curves have been used in the literature (see References [C-7], [C-8], and [C-9]). The logistic POD model for hit/miss data is a common model and is represented as:

$$\mathrm{POD}(a \mid \beta_1, \beta_2, a_{th}) = \begin{cases} \mathrm{logistics}(a \mid \beta_1, \beta_2, a_{th}) & \text{for } a > a_{th} \\ 0 & \text{otherwise} \end{cases} \qquad \text{Eqn. (C-4)}$$

where a is the flaw depth and $N(0;\sigma(a))$ is the random error represented by a normal distribution with a constant standard deviation σ or a deviation which may be a function of flaw depth (that is, $\sigma(a)$). The random error accounts for the POD model error. Model parameters β_1 and β_2 may be uncertain (epistemic) and would be represented by the bivariate PDF $k(\Theta)$, where Θ is the vector of the parameters, $\Theta = \{\beta_1, \beta_2\}$. The PDF function $m(\sigma(a))$ may also be used to express any epistemic uncertainties by treating $\sigma(a)$ as a random variable. The parameter a_{th} in Eqn. (C-4) represents the threshold (the flaw size below which detection is not possible).

The other type of POD data represents measurements of the amplitude of signal response recorded by the NDE system, such as in a UT system. For signal-response data, much more information is supplied in the signal for further analyses than is in the hit/miss data. In the signal-response approach, the most important parameters are the inspection threshold (noise level) and the decision threshold. All responses less than the inspection threshold are ignored.

In the signal-response approach, it is generally assumed that the logarithm of the signal-response amplitude, $\hat{\mathbf{a}}$, is linearly correlated to the logarithm of the flaw depth, a, as shown in Eqn. (C-5):

$$\log(\hat{a}) = \beta_3 + \beta_4 \log(a) + \varepsilon \qquad \text{Eqn. (C-5)}$$

where ε is the random error and β_3 and β_4 are the regression parameters. The random error can be assumed to have a normal distribution with mean zero and a constant or variable standard deviation. Based on this assumption, it can be shown that the POD curve can be modeled using a lognormal CDF. The corresponding POD is shown as:

$$POD(a) = \Pr(\hat{a} > \hat{a}_{th}) = \Pr(\log(\hat{a}) > \log(\hat{a}_{th})) \qquad \text{Eqn. (C-6)}$$

where a_{th} is the decision (detection) threshold signal. The decision threshold is chosen to be a bit higher than the inspection threshold in order to minimize the probability of a false call (for cases in which the decision threshold is not intentionally chosen to allow a certain probability of a false call) in the POD estimates. The â vs. a data can also be converted into hit/miss data by using the decision threshold, and an averaged POD can be determined.

C.2.2.2 Measurement (Sizing) Error

Measurement results are always associated with errors of varying magnitudes. Measurement error is defined as the difference between the measured and the true flaw depth. Measurement error is defined by Eqn. (C-7), where M_ε is the measurement error, a^* is the measured value of flaw depth, and a is the true value of flaw depth:

$$M_\varepsilon = a^* - a \qquad \text{Eqn. (C-7)}$$

The measurement error has two components: systematic error (bias) and random error. Random error may be represented by a normal distribution with zero mean and constant standard deviation. Systematic error in most cases is a major contribution to flaw measurements and cannot be ignored. In its simplest form, the measurement error can be represented by a linear function of true size as shown in Eqn. (C-8), where m is the slope and c is the intercept of the line representing measurement error, M_ε, versus true flaw depth, a. If available, PDFs of m and c can be expressed to represent the epistemic uncertainty in these parameters. Also, M_ε, may be represented as a linear function of measured flaw depth a^* because all data available are in terms of a^*.

$$
\begin{aligned}
&M_\varepsilon = ma + c + E_M \\
&\text{where, } a = \text{true flaw depth and } E_M = N_M(0,\sigma_M), \\
&\text{or based on Eqn. (7):} \\
&M_\varepsilon = m(a^* - M_\varepsilon) + c + E_M;\ \text{or} \\
&M_\varepsilon = \frac{m}{m+1}a^* + \frac{c}{m+1} + \frac{E_M}{m+1} = m'a^* + c' + E'_M \qquad \text{Eqn. (C-8)} \\
&\text{where, } a^* = \text{measured depth, } m' = \text{slope, } c' = \text{intercept,} \\
&\text{and } E'_M = N_M(0,\sigma'_M) \text{ of } M_\varepsilon \text{ vs. } a^*
\end{aligned}
$$

The aleatory random measurement error E'_M is shown by the normal distribution $N_M(0; \sigma'_M)$ in Eqn. (C-8). As such, the total measurement error may be represented as the normal distribution $g(M_\varepsilon) = N(m'a^*+c'; \sigma'_M)$. Figure C-2 shows a conceptual example of the measurement error as a function of true flaw size (one can also show M_ε vs. a*). According to Eqn. (C-7), the relationship between the true flaw depth, a, and measured depth, a^*, is $a = a^* - M_\varepsilon$.

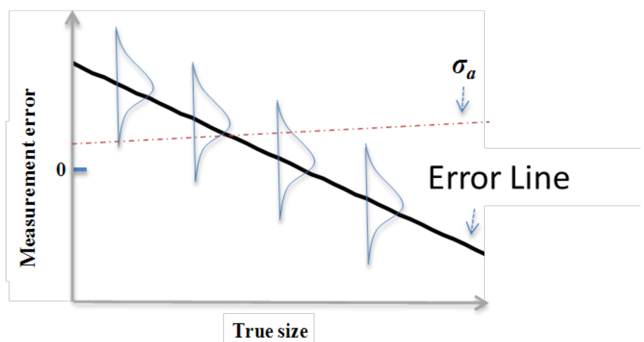

Figure C-2. Measurement-error distribution

If the measurement error's given flaw depth, a, is M_ε, E_M describes the PDF of random or stochastic error. Clearly, Figure C-2 depicts a case in which the standard deviation of the PDF of E_M is not constant; rather, it is a monotonically increasing line.

C.2.3 The Methodology for Updating the NDE Data

This section discusses the details of the Bayesian updating approach, which combines UT data (including their uncertainties) with the prior PDF models of flaw depth and density (used in VFLAW to generated FAVOR input) to arrive at posterior distributions of flaw characteristics.

C.2.3.1 Updating Flaw-Depth Distribution Models

The ultimate objective of this analysis is to describe PDFs of the flaw depth and density considering UT measurement of flaws (which contain modeling uncertainty and stochastic variability in form of the POD and measurement error). We start with the Bayesian estimation of the (large and small) flaw depths, followed by the same estimation for flaw density.

In the Bayesian framework described by Eqn. (C-1), prior information on the flaw depth PDF (for example, data and expert elicitation described in NUREG/CR-6817) may be combined with the uncertain measurement data from NDE to assess a posterior distribution of the flaw depths. Consider the PDF of the flaw depth, a, as *f(a | Φ)*, where Φ is a vector of all the PDF parameters.

The data reported in NUREG/CR-6817 show that the small and large flaw depths are represented using different distributions. For example, the models proposed and used in VFLAW rely on the exponential distribution for large flaw depths but use the multinomial distribution to model small flaw depths. The flaw depth that separates the two distributions is defined as the transition flaw depth. Therefore, a given PDF may only be true up to a limit from which it transitions to another distribution. For the transition flaw depth t_{tr}, the PDF that describes the flaw depth should be conditioned on exceeding or falling below the transition limit. Therefore:

$$f_l(a \mid \Phi, a \geq t_{tr}) = \frac{f(a \mid \Phi)}{\Pr(a \geq t_{tr})}$$
$$f_s(a \mid \Phi, a < t_{tr}) = \frac{f(a \mid \Phi)}{\Pr(a < t_{tr})} \qquad \text{Eqn. (C-9)}$$

In VFLAW, for example, t_{tr} for the weld regions was selected as the flaw depth of about the bead thickness, Δ, of the corresponding weld. Further, in VFLAW the flaw depth is normalized to the dimensionless random variable a/Δ instead of to a. The approach discussed herein applies to PDFs of both a and a/Δ, but the respective equations of the approach are only shown in terms of the PDF similar to Eqn. (C-9).

Consider the PDF of NDE measurement error M_ε (represented by Eqn. (C-8)) of a measured flaw depth a^* with stochastic random variable *E*. The flaw-depth distribution corrected for the measurement error, M_ε, by assuming that true flaw depth, a, may be represented by correcting the measured depth a^* using the relationship $a = a^* - M_\varepsilon$ [C-10]. As stated earlier in Eqn. (C-8), the PDF of M_ε will be $g(M_\varepsilon) = N(m'a^* + c'; \sigma'_M)$. If there are epistemic uncertainties about parameters m' and c', they may be represented by the bivariate PDF x(Ω), where Ω is the vector of the parameters m' and c'. The expected distribution of measurement error would be:

$$g'(M_\varepsilon) = \int_\Omega g(M_\varepsilon) x(\Omega) d\Omega \qquad \text{Eqn. (C-10)}$$

While the measurement-error-corrected PDF adjusts the flaw depths to true values, the flaws missed, as characterized by the POD, should also be accounted for. That is, for every measured flaw a^*, a corresponding probability (including uncertainties) that additional flaw(s) may be missed should be accounted for.

If the POD is represented as a mathematical function of the flaw size, a, the vector of parameters Θ of the POD function may be associated with a known multivariate PDF k(Θ) in order to account for the uncertainties. It is also possible to add a stochastic model error term, represented by a normal distribution with the mean zero and the standard deviation $\sigma_{POD}(a)$. For simplicity, it is also possible to assume that the error term is absorbed in the PDF of the POD model parameters (i.e., k(Θ)). The marginal POD independent of the random variables Θ and $\sigma_{POD}(a)$ would be:

$$\mathrm{POD}(a) = \iint_{\sigma_{POD},\Theta} \mathrm{POD}(a \mid \Theta, \sigma_{POD}(a)) k(\Theta) m(\sigma_{POD}(a)) d\Theta d\sigma_{POD} \qquad \text{Eqn. (C-11)}$$

Marginal POD, independent of flaw depth conditional on Φ (see Eqn. (C-9)) and t_{tr}, is then expressed as:

$$\begin{aligned} \Pr_s(D) &= \mathrm{POD}(\Phi, a < t_{tr}) = \int_0^{t_{tr}} \mathrm{POD}(a) f_s(a \mid \Phi, a < t_{tr}) da \\ \Pr_l(D) &= \mathrm{POD}(\Phi, a \geq t_{tr}) = \int_{t_{tr}}^{\infty} \mathrm{POD}(a) f_l(a \mid \Phi, a \geq t_{tr}) da \end{aligned} \qquad \text{Eqn. (C-12)}$$

where Pr(D) expresses the probability that a small or large flaw is detected regardless of size, which in general is a function of Φ and t_{tr}; that is, POD(Φ, t_{tr}). The probability of not detecting a flaw would be $\Pr(\overline{D}) = 1 - \Pr(D)$.$\Pr(\overline{D})=1\text{-}\Pr(D)$. Let the random variable A represent the true flaw depth. Then, according to the Bayesian formulation by Celeux et al. [C-11], the probability that a detected flaw has a depth in the vicinity of a, inside an interval Δa, may be expressed as:

$$\begin{aligned} \Pr(a < A < a + \Delta a \mid D) &= \frac{\Pr[a < A < a + \Delta a \cap D]}{\Pr(D)} \\ &= \frac{\Pr(a < A < a + \Delta a) \cdot \Pr(D \mid a < A < a + \Delta a)}{\Pr(D)} \end{aligned} \qquad \text{Eqn. (C-13)}$$

where D is the event that a flaw is detected. The limit of Eqn. (C-13) as the flaw depth interval Δa approaches zero may be found after dividing Eqn. (C-13) by Δa. The left term limit represents the likelihood that a detected flaw will have the depth a. Further, by rearranging the right side, the PDF of flaw depth independent of detection and POD, given a flaw of depth a, may be found:

$$\begin{aligned} &\lim_{\Delta a \to 0} \frac{\Pr(a < A < a + \Delta a \mid D)}{\Delta a} = L(a \mid D) = \lim_{\Delta a \to 0} \frac{\Pr(a < A < a + \Delta a).\Pr(D \mid a < A < a + \Delta a)}{\Pr(D)\Delta a} = \\ &\underbrace{\lim_{\Delta a \to 0} \frac{\Pr(a < A < a + \Delta a)}{\Delta a}}_{f(a \mid \Phi, t_{tr})} . \underbrace{\lim_{\Delta a \to 0} \Pr(D \mid a < A < a + \Delta a)}_{\mathrm{POD}(a)} . \frac{1}{\Pr(D)} \end{aligned} \qquad \text{Eqn. (C-14)}$$

Using Eqn. (C-14), the corresponding likelihood that a detected flaw is of depth a may be expressed as:

$$L(a \mid \Phi) = \frac{f(a \mid \Phi, t_{tr}).\mathrm{POD}(a)}{\mathrm{POD}(\Phi, t_{tr})} \qquad \text{Eqn. (C-15)}$$

Eqn. (C-15) forms the basis for development of the likelihood function, which would be necessary in the Bayesian framework (as discussed in Section C.2.1) to estimate the posterior PDF of flaw depth given the observed NDE flaw data and the prior information about the characteristics of flaw PDF.

C.2.3.1.1 Likelihood Function of Exact Flaw-Depth Measurements

Suppose that the NDE reports exact flaw depths. Based on Eqn. (C-2), the likelihood function of n^* flaws of known depth (containing measurement errors) $a_1^*, a_2^*, a_3^*, \ldots$ would be $L(\text{Data} \mid \Phi) = \prod_{n^*} L(a^* \mid \Phi)$. It is important to correct for POD and the measurement error and parameter uncertainties according to Eqn. (C-10) and to represent flaw depths in terms of the measured value using Eqn. (C-7) so that $a^* = M_\varepsilon + a$ [1]. Therefore, using Eqn. (C-15), the likelihood of exact flaw measurements reported may be expressed as [C-10]:

$$L(\text{All exact measured data} \mid \Phi, t_{tr}) = \frac{1}{[POD(\Phi, t_{tr})]^{n^*}} \prod_{i=1}^{n^*} \int_{M_\varepsilon} POD(a_i^* - M_\varepsilon) f((a_i^* - M_\varepsilon) \mid \Phi, t_{tr}) g'(M_\varepsilon) dM_\varepsilon \qquad \text{Eqn. (C-16)}$$

Because NDE data are measured and have associated measurement error and other uncertainties, but the POD and measurement error discussed earlier are modeled to be relevant to the true flaw depth, a, in Eqn. (C-16) the true flaw depth is replaced with its equivalent (a^*-M_ε). The expectation of the numerator of Eqn. (C-15), independent of the measurement error, is found by multiplying the term $f(a \mid \Phi, t_{tr}).POD(a)$ by the expected PDF of the measurement error, $g'(M_\varepsilon)$, and integrating this over all values of the measurement error.

C.2.3.1.2 Likelihood Function of Interval Flaw-Depth Measurements

If in addition to or instead of the exact flaw-depth data, interval data are reported (such as the number of flaws observed less than a given depth or between an upper and lower limit), the likelihood of m_i^* flaws reported in the interval i, corrected for the measurement error but independent of the error, would be [C-12]:

$$L(\text{Interval i consisting of } m_i^* \text{ measured flaw depths} \mid \Phi, t_{tr}) = \left[\frac{1}{POD(\Phi, t_{tr})} \int_{a_{i-1}^*}^{a_i^*} \int_{M_\varepsilon} POD(a^* - M_\varepsilon) f((a^* - M_\varepsilon) \mid \Phi) g'(M_\varepsilon) dM_\varepsilon \, da^* \right]^{m_i^*}$$

Eqn. (C-17)

If n such flaw-depth intervals were reported, the corresponding likelihood function using Eqn. (C-17) would be:

$$L(n \text{ intervals of measured depths} \mid \Phi, t_{tr}) = \prod_{i=1}^{n} \left[\frac{1}{POD(\Phi, t_{tr})} \int_{a_{i-1}^*}^{a_i^*} \int_{M_\varepsilon} POD(a^* - M_\varepsilon) f((a^* - M_\varepsilon) \mid \Phi) g'(M_\varepsilon) dM_\varepsilon \, da^* \right]^{m_i^*}$$

Eqn. (C-18)

---

[1] Note that if X and Y are two continuous random variables with probability density functions f(x) and g(y), the random variable Z = X + Y will have a probability density function h(Z) such that:

$$h(z) = \int_{-\infty}^{\infty} f(z - y) g(y) dy$$

If exact and interval NDE data are both reported, the likelihood function would be a multiple of Eqn. (C-16) and Eqn. (C-18). That is:

$$\begin{aligned}&L(\text{Mix Measured Flaw Depths} \mid \Phi, t_{tr}) = \\ &L(\text{n Interval Measured Flaw Depths} \mid \Phi, t_{tr}) \times L(\text{n * Exact Measured Flaw Depths} \mid \Phi, t_{tr})\end{aligned}$$

C.2.3.1.3 Bayesian Updating of Parameters of the Flaw Depth Distribution

Regardless of the form of the data (exact flaw-depth and/or interval data), the Bayesian inference of the vector of parameters Φ of the flaw-depth PDF would be obtained (according to Eqn. (C-1)) from $\pi_1(\Phi \mid \text{Data}, t_{tr}) \propto L(\text{Data} \mid \Phi, t_{tr})\pi_0(\Phi)$, where $\pi_1(\Phi \mid \text{Data})$ is the posterior multivariate PDF of vector Φ, and $\pi_0(\Phi)$ is the prior multivariate PDF of Φ.

Determination of the posterior $\pi_1(\Phi \mid \text{Data})$ requires complex integrations. Further, integration of the denominator of the Bayesian inference in Eqn. (C-1) also requires multi-dimensional integration that in most cases can only be performed numerically.

It is also critically important to note that Eqn. (C-9) through Eqn. (C-20) are all in terms of the actual flaw depth, a, measured in English or metric units. As stated before, it is also possible to express the equations in terms of the normalized flaw depth, a/Δ, instead. This is simply done by replacing flaw depth, a, with a/Δ in all PDFs, measurement error, and POD equations. Clearly the parameters of the equations should be adjusted accordingly.

C.2.3.2 Updating the Flaw Density Model

If flaws are detected with a probability given by Eqn. (C-11) and Eqn. (C-12) as $Pr(D) = POD(\Phi, t_{tr})$ (or not detected with a probability of $Pr(\overline{D}) = 1 - Pr(D)$), the probability that a specific total number of flaws n* observed in a given volume v out of the true number of flaws n_j follows the binomial distribution (see References [C-11] and [C-12]):

$$L(n^* \mid n_j) = \binom{n_j}{n^*} \quad [Pr(D)]^{n^* n} [1 - Pr(D)]^{n_j - n^*}$$

or

$$L(n^* \mid n_j) = \binom{n_j}{n^*} \quad [POD(\Phi, t_{tr})]^{n^* n} [1 - POD(\Phi, t_{tr})]^{n_j - n^*} \qquad \text{Eqn. (C-19)}$$

where $\binom{n_j}{n^*} = \frac{n_j!}{n^*!(n_j - n^*)!}$. The best estimate of the true number of flaws would be to assume that n^* represents the mean of Eqn. (C-19). Accordingly, the mean estimate of the true number of flaws, N, would be found from:

$$N = \frac{n^*}{POD(\Phi, t_{tr})} \qquad \text{Eqn. (C-20)}$$

A more formal way to estimate the number (and thus density) of flaws would be to use the Bayesian updating of n_j, which allows the estimation of the posterior distribution of n_j to describe the true number of flaws:

$$\Pr(n_j \mid n^*) = \frac{L(n^* \mid n_j)\Pr(n_j)}{\sum_{n_j} L(n^* \mid n_j)\Pr(n_j)} \qquad \text{Eqn. (C-21)}$$

Using Eqn. (C-19) (representing the likelihood of observing n^* flaws out of the unknown n_j flaws) and a Poisson prior flaw density model, the posterior probability distribution of the number of flaws would be obtained from:

$$\Pr(n_j \mid n^*) = \frac{\binom{n_j}{n^*}\left[POD(\Phi,t_{tr})\right]^{n^{*}n}\left[1-POD(\Phi,t_{tr})\right]^{n_j-n^*}\left[\frac{e^{-\rho v}(\rho v)^{n_j}}{n_j!}\right]}{\sum_{n_j=n^*}^{\infty}\binom{n_j}{n^*}\left[POD(\Phi,t_{tr})\right]^{n^{*}n}\left[1-POD(\Phi,t_{tr})\right]^{n_j-n^*}\left[\frac{e^{-\rho v}(\rho v)^{n_j}}{n_j!}\right]} \qquad \text{Eqn. (C-22)}$$

where ρ is the volumetric flaw intensity and ρv is the expected number of true flaws in the inspected volume v. If the mean number of flaws from Eqn. (C-20) is large, the computer rounding issues associated with Eqn. (C-22) may be avoided by performing the analysis for a smaller volume (for example, 1/100th of the inspected volume) and later prorating n_j accordingly. An alternative approach that is approximate, but simpler than Eqn. (C-19) through Eqn. (C-22), would be to update the parameter ρ itself based on the mean number of flaws. For example, if the volume of the UT inspection is v, the volumetric flaw intensity ρ of the flaws associated with the mean estimated N true flaws from Eqn. (C-20) in this volume would be $\rho = \frac{N}{v}$. Assuming that the mean occurrence intensity of flaws remains constant over the volume of inspection, the Poisson distribution may be used to represent the likelihood of N flaws in volume v, given the volumetric flaw intensity ρ as shown by Eqn. (C-23):

$$L(N \mid \rho) = e^{-(\rho v)}\frac{(\rho v)^N}{N!} \qquad \text{Eqn. (C-23)}$$

where v is the inspection volume and ρ is the flaw intensity (flaws per unit volume) associated with the mean estimated number of flaws N.

If prior information about the flaw intensity, ρ, were available, it would be desirable to update the flaw intensity by using such prior information. For example, assume that the prior volumetric flaw intensity is described by the PDF, $\pi_0(\rho)$. Then, the posterior PDF, $\pi_1(\rho|N)$, can be estimated using the likelihood function in Eqn. (C-23) from:

$$\pi_1(\rho \mid N) \propto L(N \mid \rho)\pi_0(\rho)$$
$$\text{where } L(N \mid \rho) = \prod_j L(N \mid \rho_j) \qquad \text{Eqn. (C-24)}$$

If the prior PDF of the flaw intensity is expressed by the gamma distribution with parameters $\boldsymbol{\alpha_1}$ **and** $\boldsymbol{\alpha_2}$, as $\gamma_0(\rho) = \text{gamma}(\rho \mid \alpha_1,\alpha_2) = \frac{\alpha_1^{\alpha_2}\rho^{\alpha_2-1}}{\Gamma(\alpha_2)}e^{-\alpha_1\rho}$, the posterior PDF is a conjugate distribution described by $\gamma_1(\rho) = \text{gamma}(\rho \mid v+\alpha_1, n_j+\alpha_2)$. The alternative form of the gamma distribution used by the MATLAB tool (to be used later in the following example) uses parameter β instead of parameter α_1, so that $\mathrm{gamma}(\rho \mid \beta = \frac{1}{\alpha_1}, \alpha_2)$.

C.3 Application Example

As part of a cooperative effort between the Electric Power Research Institute (EPRI) and the NRC to provide guidance on evaluation of PTS, NDE analyses were performed for a PWR RPV (Beaver Valley 2). In this section, the Beaver Valley 2 NDE data will be described first. Next, the VFLAW data described in NUREG/CR-6817 will be used as prior information, followed by the application of the Bayesian updating procedure discussed in Section C.2 to determine flaw-depth and flaw-density distributions specific to Beaver Valley 2. The resulting posterior distribution of the parameters of the flaw depth and flaw density, as described in Section C.2, will be derived and discussed. The results of flaw-depth and flaw-density PDFs will be used to compare against the 10 CFR 50.61a flaw tables, and to update the distribution models in VFLAW into new flaw distributions that are representative of the Beaver Valley 2 RPV.

C.3.1 Description of the NDE Data Used as Evidence to Build the Likelihood Function

The EPRI report by Spanner [C-13] provides UT-based measured flaw data near the inner surface (~2.5 inches) of the Beaver Valley 2 RPV, including small flaw sizes. These data, while subject to POD and measurement error, provide a more vessel-specific perspective of the distribution of flaws for Beaver Valley 2 than does the VFLAW distributions used in FAVOR.

The observed Beaver Valley 2 NDE data (with detection and sizing uncertainty) are mostly in the form of interval-censored data as summarized below [C-13]:

1. 19 weld flaws were detected by the UT NDE of Beaver Valley 2 in the first inch (the inspection volume specified in Supplement 4 to Mandatory Appendix VIII to Section XI of the ASME Code) of the RPV (~0.616 ft^3), all having a flaw depth less than 0.125".
2. 103 weld flaws were detected and reported by the UT NDE of Beaver Valley 2 in the first 3/8t (2.953") (the inspection volume specified in Supplement 6 to Mandatory Appendix VIII to Section XI of the ASME Code) of the RPV were reported, all with flaw depths less than 0.125", except for one flaw that measured 0.260".

The lower limit of the detected flaw intervals described above is not stated in [C-13], but is certainly not zero. Two possible subjective lower limits were assumed, and later the sensitivities of the final (posterior) flaw-distribution results to these two choices were assessed. The two lower limits are 0.04" and 0.075".

The NDE data described above provide an incomplete depiction of the true flaws in the Beaver Valley 2 RPV because they contain uncertainties associated with the UT technology used to detect and size flaws. The associated weld bead thicknesses are not reported. However, the weld region of the observed flaws and flaw length is reported. Such results should be corrected for detection and sizing capability, particularly for the small flaws.

The Beaver Valley 2 RPV weld map is shown in Figure C-3 [C-14]. In the absence of the Beaver Valley 2 average weld bead thickness as the point of transition between large and small depths, it is assumed that all flaws reported are Submerged Arc Welds (SAWs), which form over 90% of welds in the VFLAW data, with the bead thickness of $\Delta = t_{tr} = 0.26$". Using the Beaver

Valley 2 RPV information shown in Figure C-3, the following weld characteristics were computed and used to specialize the VFLAW data to represent the prior distributions of flaw depth and density for Beaver Valley 2 RPV:

Total Weld Length = 816.18"
Total Weld Volume[2] = 4.975 ft^3
Total Weld Fusion Area = 92 ft^2
Weld Volume of 1" = 0.616 ft^3
Weld Volume of 3/8t = 1.865 ft^3

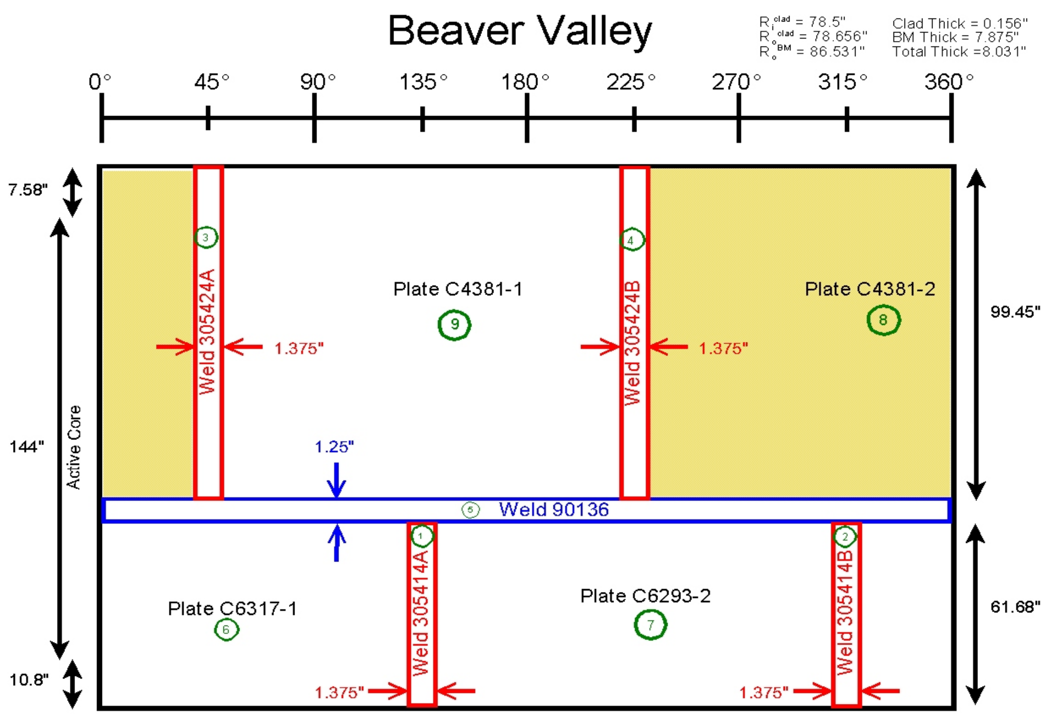

Figure C-3. Beaver Valley 2 weld map [C-14]

C.3.2 Description of Flaw-Depth and -Density Information Used in VFLAW as Prior PDFs in This Example

Smaller flaws neighboring the inner surface of the RPV that would be subjected to high thermal stresses during PTS events are dominant contributors to the risk of vessel failure posed by PTS. During the PTS re-evaluation effort in the late 1990s and early 2000s, the Marshall distribution was updated using the results of destructive tests of the Pressure Vessel Research User Facility (PVRUF) and Shoreham RPVs [C-2]. These analyses assumed that the flaws were near the inner surface of the RPV and included very small flaws of less than 0.125 inches (3 mm) in through-wall extent. The purpose of the re-evaluation was to provide an up-to-date estimate of the distribution of weld flaw density and sizes using modern NDE methods of analysis. These distributions represent the flaw-depth and flaw-density models in VFLAW [C-3].

[2] The total volume of reactor vessel weld area according to the weld dimensions shown in Figure C-3 = [1.375 × 99.45 × 2 × (86.531 - 78.656)] + [2 × 1.375 × 61.68 × (86.531 - 78.656)] + [1.25 × 3.14 × 2 × 86.531 × (86.5312 - 78.6562)] = 8,595.29 in^3 = 4.974 ft^3.

Because we need prior distributions in the Bayesian inference described earlier, the VFLAW distributions many be specialized to Beaver Valley 2. This is done by using the corresponding bead thickness and other vessel characteristics for Beaver Valley 2 to determine the prior distributions of the flaw depth and flaw density from VFLAW distributions. The prior distributions fill the gaps in the limited inspected data and uncertainties associated with the NDE results.

Analysis of flaws should consider different vessel regions and welding types. Welding types include the Submerged Arc Weld (SAW), Shielded Metal Arc Weld (SMAW), and repair weld. Depending on the known details of fabrication, NUREG/CR-6817 estimated flaw distributions for each weld type used in a particular region of the vessel. Measured flaw data showed vessel-to-vessel variability in both flaw density and depth. To supplement the limited data from the PVRUF and Shoreham flaw measurements, NUREG/CR-6817 used expert elicitation. Distribution functions to characterize the number and sizes of flaws in the various regions of the RPVs were then developed based on the measured data and insights from an expert elicitation exercise and used in VFLAW.

The prior distributions used in this example updated the PVRUF flaw models described in NUREG/CR-6817 and used in VFLAW, including the hyper-distributions that address the uncertainties associated with the parameters for the distribution functions describing flaw depth and flaw density. For example, the exponential distribution was used to represent the variability of large flaw depths. However, the parameter λ of the exponential distribution (i.e., assuming $f(a) = \lambda e^{-\lambda a}$, where a is the flaw depth) was in turn considered to be a random variable and described by the gamma distribution. The gamma distribution itself has two parameters, α_1 and α_2, that are given as constants in NUREG/CR-6817. These parameters were updated in this example based on the observed data from Beaver Valley 2. The values of the hyper-distributions used in VFLAW are shown in Table C-2. Note that the flaw-depth data in Table C-2 are in meters, whereas this example calculation is based on inches. The relationship between the flaw-depth and flaw-density PDFs and the corresponding hyper-PDFs of their parameters are illustrated in Figure C-4.

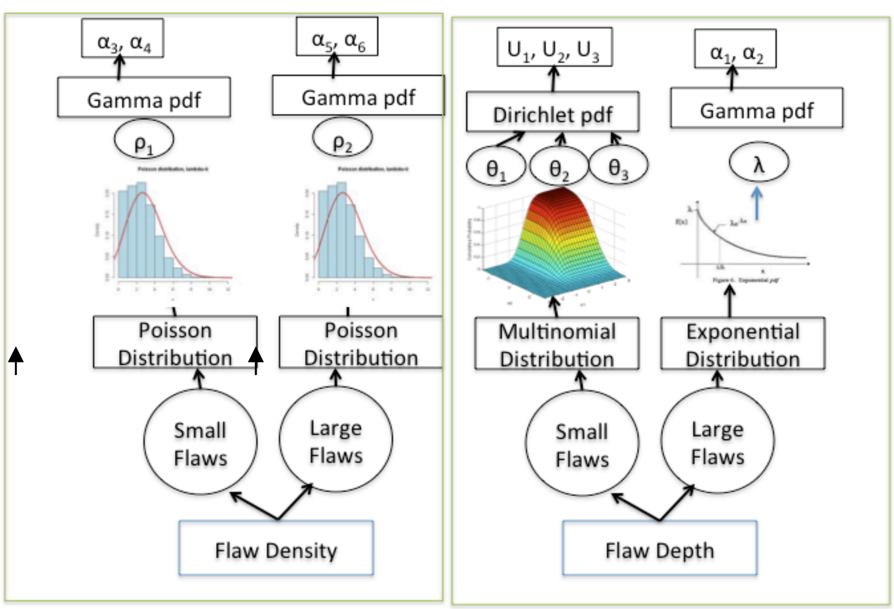

Figure C-4. Flaw-depth and flaw-density distributions used in VFLAW and their corresponding parameter hyper-PDFs.

Table C-2. Flaw-Depth (a) and Flaw-Density (b) Distributions and Hyper-PDF Parameters Used in VFLAW for PVRUF

(a) Flaw-depth characteristics (in meters) based on data from PVRUF RPV

Case	Flaw Size Category	Welding Process	Random Variable Representing Flaw Depth	PDF of Flaw Depth	Parameters of PDF	Distribution Describing Uncertainty of Parameters of PDF	Parameters of Uncertainty Distribution
1	Small ($a \le \Delta$)	SAW	a/Δ	Multinomial	P_1, P_2, P_3	Dirichlet	$U_1 = 34$ $U_2 = 8$ $U_3 = 1$
2	Small ($a \le \Delta$)	SMAW	a/Δ	Multinomial	P_1, P_2, P_3	Dirichlet	$U_1 = 34$ $U_2 = 8$ $U_3 = 1$
3	Small ($a \le \Delta$)	Repair Weld	a/Δ	Multinomial	P_1, P_2, P_3	Dirichlet	$U_1 = 34$ $U_2 = 8$ $U_3 = 1$
4	Large ($a > \Delta$)	SAW	a/Δ	Exponential	λ	Gamma	$\alpha_1 = 21.68$ $\alpha_2 = 52$
5	Large ($a > \Delta$)	SMAW	a/Δ	Exponential	λ	Gamma	$\alpha_1 = 21.68$ $\alpha_2 = 52$
6	Large ($a > \Delta$)	Repair Weld	a/Δ	Exponential	λ	Gamma	$\alpha_1 = 17.58$ $\alpha_2 = 13$

(b) Flaw-density characteristics based on data from PVRUF RPV

Case	Flaw Size Category	Welding Process	Random Variable Representing Flaw Depth	PDF of Flaw Depth	Parameters of PDF	Distribution Describing Uncertainty of Parameters of PDF	Parameters of Uncertainty Distribution
1	Small ($a \le \Delta$)	SAW	Flaws per cubic meter	Poisson	λ	Gamma	$\alpha_3 = 0.180$ $\alpha_4 = 1419$
2	Small ($a \le \Delta$)	SMAW	Flaws per cubic meter	Poisson	λ	Gamma	$\alpha_3 = 0.014$ $\alpha_4 = 197$
3	Small ($a \le \Delta$)	Repair Weld	Flaws per cubic meter	Poisson	λ	Gamma	$\alpha_3 = 0.00123$ $\alpha_4 = 12$
4	Large ($a > \Delta$)	SAW	Flaws per cubic meter	Poisson	λ	Gamma	$\alpha_3 = 0.180$ $\alpha_4 = 4$
5	Large ($a > \Delta$)	SMAW	Flaws per cubic meter	Poisson	λ	Gamma	$\alpha_3 = 0.014$ $\alpha_4 = 4$
6	Large ($a > \Delta$)	Repair Weld	Flaws per cubic meter	Poisson	λ	Gamma	$\alpha_3 = 0.00123$ $\alpha_4 = 7$

C.3.3 Detection and Sizing Error Models

Analysis of UT-detected performance data reported by EPRI [C-6] was used to identify a POD function for the purpose of this example. Currently, EPRI is updating these performance data and will supply more appropriate POD models for future consideration; the POD and flaw-sizing error functions used here are therefore intended only to illustrate this numerical method. The threshold limit of this POD function (Eqn. (C-4)) was taken as 0.00 and the epistemic uncertainties associated with the parameters of the model were not considered in this example. Accordingly, the following mean POD function based on Eqn. (C-4) was used[3]:

$$\mathrm{POD}(a) = 1 - \frac{1}{1 + e^{63.2100(a - 0.1124)}} \qquad \text{Eqn. (C-25)}$$

where a is the true, unbiased flaw size. Figure C-5 shows a plot of this POD function.

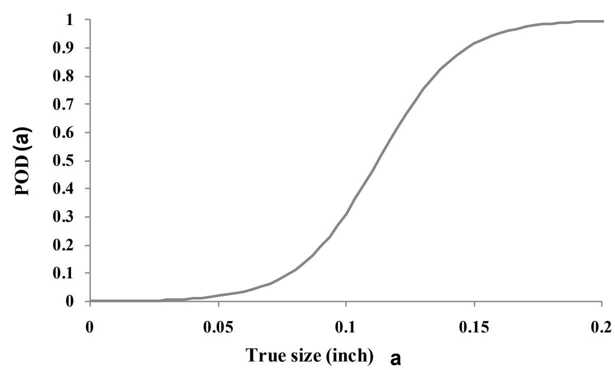

Figure C-5. POD vs. flaw depth.

The measurement error was assumed, based on some examples and measurement errors reported in EPRI report [C-6]. The measurement error is a linear function that oversizes small flaws and undersizes large flaws. Figure C-6 depicts a plot of the measurement-error model used in this example. The model itself can be described as a line with a slope of -0.1905 and an intercept of 0.0476, with the variability resulting from the model error described by a normal distribution. That is, $M_\varepsilon = -0.1905a^* + 0.0476 + N(0, 0.0298)$, where N(0, 0.0298) is a normal distribution with a mean of zero and a constant standard deviation of 0.0298. Note that in this example we are not accounting for the epistemic uncertainties of the measurement-error model. However, such uncertainties should be considered when new measurement-error models are developed. Equally, as described by Eqn. (C-10), it is possible to represent the above line by the normal PDF: $g'(M_\varepsilon) = 13.41e^{-564.55(M_\varepsilon + 0.1905a^* - 0.0476)^2}$.

[3] The model error associated with the logistic distribution was not considered.

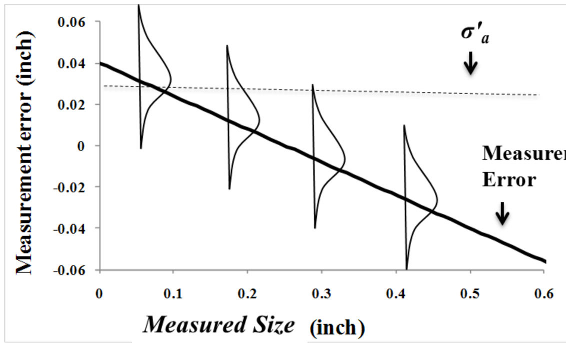

Figure C-6. Measurement error vs. flaw depth.

C.3.4 Bayesian Updating of the Parameters of the Flaw-Depth Distributions

In this section, the process of updating the prior data specialized to Beaver Valley 2 with the observed NDE data using Bayesian inference will be discussed. Figure C-7 describes the main elements of the updating process. The observed UT-based flaw data discussed in Section C.3.1 is corrected for POD and measurement error. The POD and measurement error models were discussed in Section C.3.3. In the remainder of this section, development of the likelihood functions for the two sets of observed flaw data (one for the first one inch and another for the 3/8t of the inner RPV welds) will be discussed first. Then the Bayesian inference that combines the observed data with the prior data will be considered. The analysis will be performed for each of the NDE observed data sets to determine different conclusions.

1. The observed data for the first 3/8t of the RPV welds were used to update the prior models shown in Table C-2 in order to specialize them for the Beaver Valley 2 RPV. The updated values can be used for PTS calculations specific to the Beaver Valley 2 RPV using VFLAW and FAVOR.

2. The observed data for the first inch of the vessel were used to estimate the true number of flaws in the flaw-depth ranges of the 10 CFR 50.61a tables. This information is used to assess how the estimated number of flaws of a given size in Beaver Valley 2 (estimated based on inspection data, VFLAW distributions, and Bayesian inference) compares to the number and size of flaws permitted by the 10 CFR 50.61a tables.

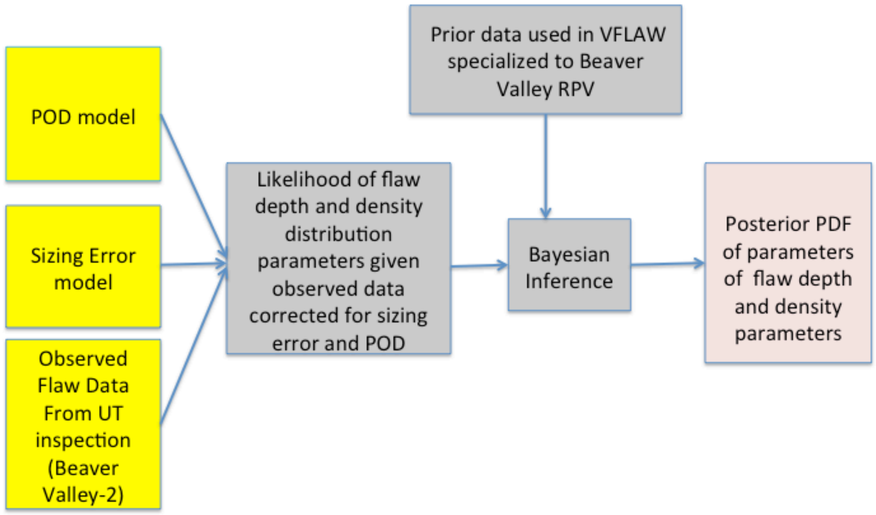

Figure C-7. Bayesian updating elements of the Beaver Valley 2 example.

C.3.4.1 Bayesian Updating of the Parameters of Large-Flaw Depth Distribution Based on the 3/8t UT Inspection Data

According to the prior data used by VFLAW as described in Section C.3.3, small-to-large flaw-size transition occurs at flaw depths exceeding the SAW weld bead thickness. According to Table C-2, large flaws will follow an exponential distribution, conditional on exceeding the transition flaw depth. Thus, the distribution of large-flaw depths corrected for the bias would be:

$$f(a \mid \lambda_l, a > t_{tr}) = \frac{f(a \mid \lambda_l)}{\Pr(a > t_{tr})} = \lambda_l e^{-\lambda_l (a - t_{tr})} = \lambda_1 e^{-\lambda_l (a^* - M_\varepsilon - t_{tr})} \qquad \text{Eqn. (C-26)}$$

where λ_l is the large-flaw depth intensity (per inch) and a_{tr} is the transition flaw depth (assumed to be 0.26"). To build the likelihood function, the flaws should be represented in terms of the measured flaw depths. Because the NDE data reported only one exact flaw depth ($n^* = 1$, $a_1^* = 0.26$) in the large-flaw region (exceeding the transition t_{tr}) for Beaver Valley 2, the likelihood function based on Eqn. (C-16) would be:

$$L(a^*_{data} \mid \lambda_l) = \frac{1}{[POD(\lambda_l)]^1} \prod_{i=1}^{1} \int_{-1}^{1} \left[1 - \frac{1}{1 + e^{63.2100(a_i^* - M_\varepsilon - 0.1124)}}\right] \left[\lambda_l \, e^{-\lambda_l (a_i^* - M_\varepsilon - 0.26)}\right] \left(13.41 e^{-564.55(M_\varepsilon + 0.1905 a_i^* - 0.0476)^2}\right) dM_\varepsilon$$

Eqn. (C-27)

where $POD(\lambda_l) = \int_{0.26}^{\infty} POD(a) \lambda_l e^{-\lambda_l (a - 0.26)} da$ would be near 1 in this case because the POD(a) reaches unity when the flaw depth exceeds 0.2 inch in Eqn. (C-25). Note that, for simplicity, the random variable M_ε is integrated over the range of -1 to 1 because these are the extreme ranges of the measurement error. The next step is finding the posterior distribution of λ_l based on Eqn. (C-1). That is:

$$\pi_1(\lambda_l \mid a^*_{data}) = \frac{L(a^*_{data} \mid \lambda_l)\pi_0(\lambda_l)}{\int_{\lambda_l} L(a^*_{data} \mid \lambda_l)\pi_0(\lambda_l)\, d\lambda_l} \qquad \text{Eqn. (C-28)}$$

Using Eqn. (C-27) as the likelihood, the Bayesian updating with the gamma PDF as the prior hyper-PDF for λ_l, $\pi_0(\lambda_l) = gamma(\lambda_l \mid \alpha_1 = 1.2, \alpha_2 = 4)$ (or the alternative form $\pi_0(\lambda_l) = gamma(\lambda_l \mid \beta = 0.8333, \alpha_2 = 4)$), from the VFLAW (SAW) information specialized to Beaver Valley 2 by using the bead thickness of 0.26" and converted to per unit inch (using the SAW data listed in Table 6.6 of NUREG/CR-6817[4]), the posterior distribution of λ_l is calculated and fitted into another gamma distribution. The posterior gamma PDF representing the Beaver Valley 2 RPV would be $\pi_1(\lambda_l) = gamma(\lambda_l \mid \alpha_1 = 1.186, \alpha_2 = 5)$ and plotted and compared to the prior PDF in Figure C-8 (see Appendix C-1). The gamma distributions used to describe flaw-depth intensity and flaw density in Table C-2 are normalized based on the bead thickness. As evident from Table C-2, VFLAW uses normalized flaw-depth distributions (i.e., based on a/Δ instead of a). Assuming a bead thickness of 0.26", the normalized gamma prior and posterior PDFs for large-flaw-depth intensity for Beaver Valley 2 would be $\pi_0(\lambda_l) = gamma(\lambda_l \mid \alpha_1 = 4.615, \alpha_2 = 4)$ and $\pi_1(\lambda_l) = gamma(\lambda_l \mid \alpha_1 = 4.563, \alpha_2 = 5)$. Note that Figure C-8 is not the normalized version. The normalized posterior would be the new hyper-distribution that reflects the measured data and can be used in the VFLAW and FAVOR runs for Beaver Valley 2 RPV.

From Figure C-8, it is evident that the prior and posterior values are very similar, because only one flaw depth data point is reported and used, so the posterior relies primarily on the prior information. The impact will, however, affect the density PDF more strongly.

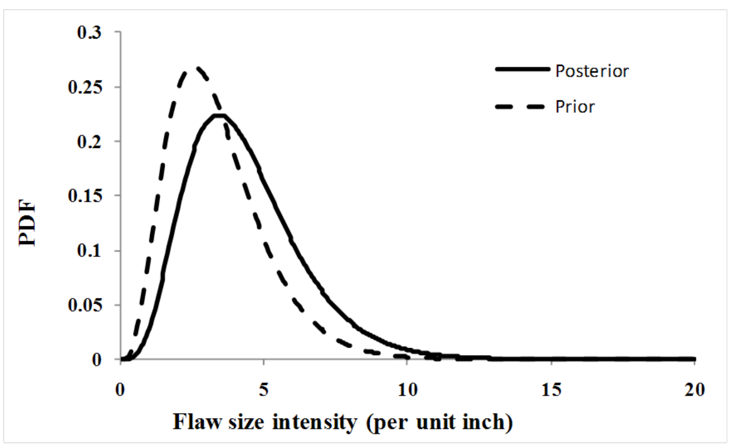

Figure C-8. Prior and posterior distributions of the flaw-depth intensity of parameter λ_l.

Appendix C-1 describes the MATLAB routine used to generate the posterior distribution and solutions to Eqn. (C-26) through Eqn. (C-28).

[4] Note that to specialize VFLAW flaw-depth distributions for Beaver Valley 2, only PVRUF large-flaw depths reported for SAW in Table 6.6 of the NUREG/CR-6817 were used instead of the distributions summarized in Table 2 of this report.

C.3.4.2 Bayesian Updating of the Parameters of Small Flaw Depth Distribution Based on the 3/8t UT Inspection Data

Flaw depths smaller than the bead thickness for PVRUF (from Table 6.4 in NUREG/CR-6817) were analyzed and appeared to best fit an exponential PDF. That is:

$$f(a \mid \lambda_s) = \frac{\lambda_s e^{-\lambda_s a}}{1 - e^{-0.26\lambda_s}}, \lambda_s > 0,\ a > 0 \qquad \text{Eqn. (C-29)}$$

where λ_s is the flaw depth (per inch) for small flaws. The hyper-distribution of λ_s was also estimated as the gamma distribution $\pi_0(\lambda_s) = gamma(\lambda_s \mid \alpha_1 = 2.854, \alpha_2 = 39)$ that was used as the prior PDF for Beaver Valley 2.

The procedure from this point on is the same as that for the large flaws with the exception that the NDE data for small flaws were given in the form of a single flaw depth interval, as discussed in Section C.3.1. Accordingly, with m = 1 and using Eqn. (C-17), the likelihood function for the evidence consisting of 103 detected (observed) flaws, all with a depth of less than 0.125" but larger than 0.04" (or 0.075" as sensitivity value), will be:

$$L(\text{Data} \mid \lambda_s) = \left[\frac{1}{POD(\lambda_s)} \int_{0.075 \text{or} 0.04}^{0.125} \int_{-1}^{1} \left[1 - \frac{1}{1 + e^{63.2100(a^* - M_\varepsilon - 0.1124)}} \right] \left(\frac{\lambda_s e^{-\lambda_s (a^* - M_\varepsilon)}}{1 - e^{-0.26\lambda_s}} \right) \left(13.41 e^{-564.55(M_\varepsilon + 0.1905 a^* - 0.0476)^2} \right) dM_\varepsilon \, da^* \right]^{103}$$

Eqn. (C-30)

The Bayesian updating for small flaws is the same as Eqn. (C-28) and the likelihood given by Eqn. (C-30) results in the posterior distributions of λ_s as shown in Figure C-9 (see Appendix C-1). Also, a plot of the POD(λ_s) as expressed by equation:

$$POD(\lambda_s) = \int_0^{0.26} \left(1 - \frac{1}{1 + e^{63.2100(a - 0.1124)}} \right) \frac{\lambda_s e^{-\lambda_s a}}{\left(1 - e^{-0.26\lambda_s a}\right)} da \qquad \text{Eqn. (C-31)}$$

is shown in Figure C-10. Clearly, because small flaws are associated with small POD and considerable measurement error, the impact of these would be significant in the posterior results shown in Figure C-9. The posterior can be expressed as the gamma PDF $\pi_1(\lambda_s) = gamma(\lambda_s \mid \alpha_1 = 1.614, \alpha_2 = 60)$. The normalized versions of the prior and posterior can be expressed by dividing α_1 by the bead thickness of 0.26". Note that Figure C-9 does not show the normalized versions of the prior and posterior distributions.

The VFLAW data for small flaw depths uses the multinomial distribution, whose parameters are described by the Dirichlet PDF. Accordingly, it is possible to find the equivalent Dirichlet PDFs that best describe the posterior PDF of λ_s expressed in form of the gamma distribution.

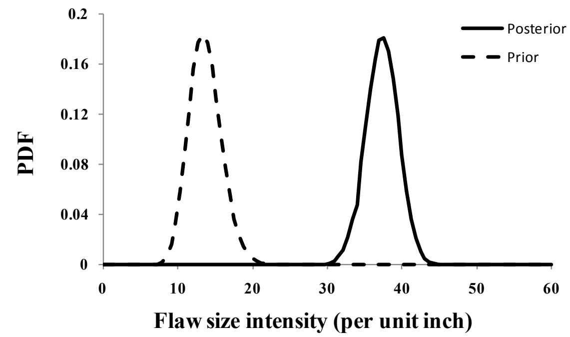

Figure C-9. Bayesian prior and posterior PDFs of λ_s (per unit inch).

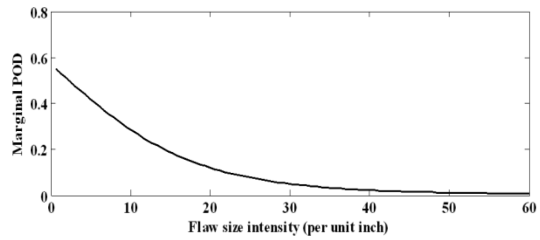

Figure C-10. Marginal POD independent of small flaw depth.

To update the Dirichlet hyper-distribution that represents uncertainties in the parameters of the multinomial distribution representing small-flaw-depth PDF used in VFLAW, the posterior PDF of λ_s shown in Figure C-9 is used to calculate the number of flaws in each of the ranges (0" to 0.072", 0.072" to 0.126", and 0.126" to 0.170") used by the multinomial distribution in VFLAW. Because the Dirichlet distribution is a conjugate distribution, the posterior number of flaws is found (see Section C.3.4.3.2 for estimating the number of posterior flaws) by adding the posterior mean number of flaws in each flaw-depth bin (see Table C-3). When added to the prior number of flaws (see Appendix A of NUREG/CR-6817 for the procedure), the updated Dirichlet values are viewed as being more representative of the distributions of true flaws in the Beaver Valley 2 RPV and are summarized in Table C-3.

Table C-3. Updated VFLAW Distribution for Small Flaws

Flaw-Depth Bins (in)	**Normalized Flaw-Depth Bins (per NUREG/ CR-6817) per Unit of Bead Thickness**	**Prior U (see Table C-2)**	**Prior Multinomial Parameter**	**Posterior U**	**Updated Mean of Multinomial Parameter**
a_1 (0 to 0.072)	0.25 (0.0 to 0.4)	$U_1 = 34$	$P_1 = 0.7907$	$U'_1 = 479.75$	$P'_1 = 0.9639$
a_2 (0.072 to 0.126)	0.55 (0.4 to 0.7)	$U_2 = 8$	$P_2 = 0.1860$	$U'_2 = 9.71$	$P'_2 = 0.0332$
a_3 (0.126 to 0.17)	0.85 (0.7 to 0.1)	$U_3 = 1$	$P_3 = 0.0233$	$U'_3 = 5.354$	$P'_3 = 0.0029$

A critical observation from this example is that the posterior results of the flaw-depth distribution in general and small depth distribution in particular are most sensitive to the POD model and measurement error model and their associated uncertainties. The lower tail of the POD model, in the ranges of small flaw depths (<0.1"), expects small probabilities of detection. When a flaw of small depth is reported, because of the corresponding small POD, it increases the likelihood that there are several flaws not detected for the one detected. This will substantially affect the results.

Appendix C-1 describes the MATLAB routine used to solve the integrals in Eqn. (C-29) through Eqn. (C-31) to estimate the posterior PDF of small flaws.

C.3.4.3 Results of Updating Parameters of Flaw Density Distribution Based on the 3/8t UT Inspection Data

In Section C.2.3.2, two methods were presented to update the flaw densities. One was based on a binomial likelihood function (Eqn. (C-19)) and one used the Poisson density and took advantage of the conjugate properties of the prior gamma PDF used as the prior distribution of the intensity, ρ, of the Poisson distribution (Eqn. (C-23)). The later method is used to update the flaw densities for this example. This method is based on the mean values only and is simpler than the former.

C.3.4.3.1 Posterior Density of Large Flaws

The number of large flaws (size > 0.26 inch), given the single UT-detected flaw, yields the posterior flaw depth intensity, λ_l, which was shown in Figure C-8. The marginal POD independent of the flaw size was almost 1 (for any value of posterior λ_l). Accordingly, using Eqn. (C-20), the number of flaws based on the posterior estimates of flaw depth would be 1.

Using the conjugate features of the prior gamma distribution for ρ_l, the posterior distribution (see Appendix A of NUREG/CR-6817) will be:

$$\begin{aligned}\pi_1(\rho_l \mid n_l) &= gamma(\rho_l \mid \alpha_1 = 6.6467 + V, \alpha_2 = 4 + n_l) = \\ &gamma(\rho_l \mid \alpha_1 = 8.5119, \alpha_2 = 5)\ \text{flaws/ ft}^3\end{aligned} \qquad \text{Eqn. (C-32)}$$

Figure C-11 compares prior and posterior distributions of the number of flaws and flaw intensity of large flaws for Beaver Valley 2 in a volume of 1.8652 ft^3. Note that VFLAW values are in cubic meter. The equivalent prior and posterior distributions in cubic meter are summarized in Table C-4.

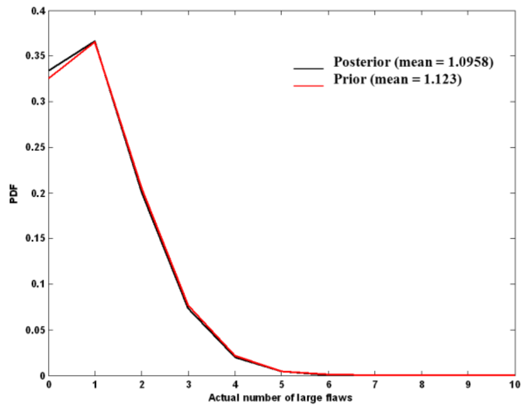

(a)

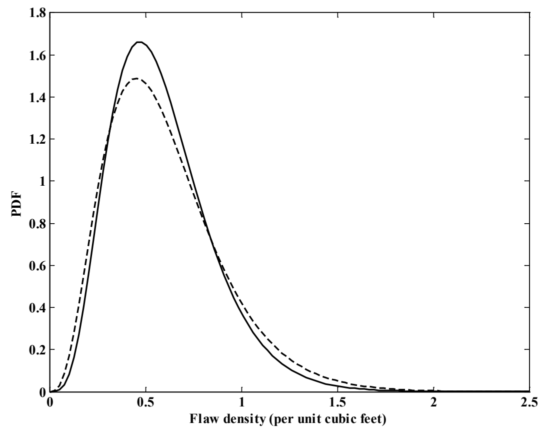

(b)

Figure C-11. Prior and posterior flaw density (a) and intensity (b) for large size flaw

C.3.4.3.2 Posterior Density of Small Flaws

Similar to the large flaw density, the prior gamma distribution representing the flaw density per unit volume, ρ_s, used in the VFLAW was updated based on the 103 UT-detected small flaws in the interval of 0.04" to 0.125". This would yield the posterior flaw depth intensity, λ_s, as was shown in Figure C-9. The mean value of the flaw depth intensity (i.e., $\lambda_s = 37.16$) estimated by the posterior shown in Figure C-9 yields a marginal probability of detection independent of flaw depth of, $POD(\lambda_s) = 0.0274$.

The likelihood of observing n_s small flaws would be expressed as:

$$\begin{aligned}
&\pi_1(\rho_s \mid n_s) = gamma(\rho_s \mid \alpha_{1,s}^{pos} = 6.6467 + V, \alpha_{2,s}^{pos} = 1419 + n_s) \\
&= gamma(\rho_s \mid \alpha_{1,s}^{pos} = 8.5119, \alpha_{2,s}^{pos} = 1909) \\
&\pi_0(\rho_s) = gamma(\rho_s \mid \alpha_{1,s} = 6.6467, \alpha_{2,s} = 1419)\,\text{flaws}/\text{ft}^3 \\
&(\text{Table 6.2 SAW} - \text{PVRUF NUREG/CR-6817})
\end{aligned} \qquad \text{Eqn. (C-33)}$$

Figure C-12 compares prior and posterior distributions of the number of flaws and volumetric flaw intensity of small flaws.

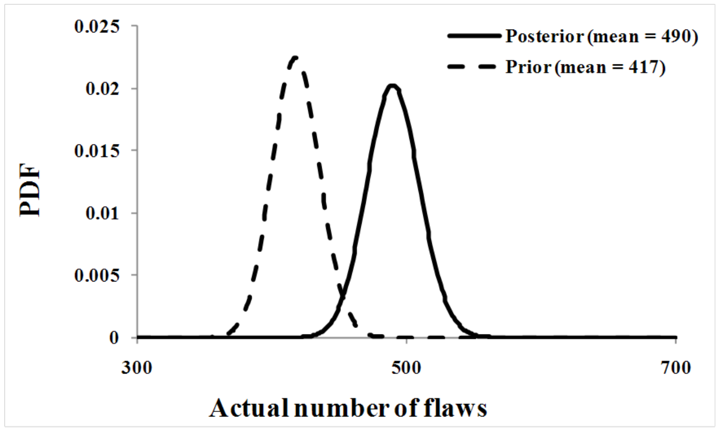

(a)

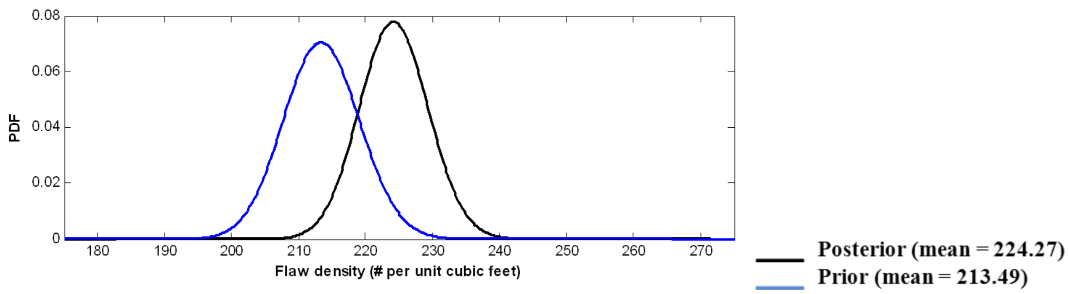

(b)

Figure C-12. Prior and posterior flaw density (a) and intensity (b) for small size flaws

Because the posterior flaw density distributions shown in Figure C-11 and Figure C-12 are based on the mean values of λ for both large and small flaws, a Monte Carlo simulation was used to select random realizations of λ from the posterior PDFs of λ for large and small flaws to develop the corresponding posterior flaw density PDFs. Figure C-13 shows the results of the spread of the number of the flaws of various depths for the Beaver Valley 2 RPV, including the epistemic uncertainties shown in the form of box plots.

Similar to the flaw-depth distribution, the posterior distribution of flaw density will be dominated by the POD and measurement error models and their uncertainties. Specifically, when a large number of small flaws are reported during the NDE inspection, the corresponding low POD value increases the number of expected undetected flaws.

Based on the results of this section, Table C-4 summarizes the posterior results to be used for Beaver Valley 2 VFLAW and FAVOR runs. The posterior results have been changed to metric units in this table, because VFLAW uses metric values.

Table C-4. Summary of the Posterior Parameter PDFs of Flaw Depth and Flaw Density to be used in VFLAW and FAVOR Runs for Beaver Valley 2

Case	Flaw Size Category	Welding Process	Random Variable Representing Flaw Depth	PDF of Flaw Depth	Parameters of PDF	Distribution Describing Uncertainty of Parameters of PDF	Original VFLAW Parameters of Uncertainty Distribution (Flaw Depth parameters are specialized to Beaver Valley 2	Posterior Parameters of Uncertainty Distribution Based on Beaver Valley 2 Specialized Prior and NDE Data
1	Small ($a \leq \Delta$)	SAW	Flaws per cubic meter	Poisson	ρ	Gamma	$\alpha_3 = 0.180$ $\alpha_4 = 1419$	$\alpha'_3 = 0.230$ $\alpha'_4 = 1909$
2	Large ($a > \Delta$)	SAW	Flaws per cubic meter	Poisson	ρ	Gamma	$\alpha_3 = 0.180$ $\alpha_4 = 4$	$\alpha'_3 = 0.230$ $\alpha'_4 = 5$
3	Small ($a \leq \Delta$)	SAW	a/Δ	Multinomial	P_1, P_2, P_3	Dirichlet	$U_1 = 34$ $U_2 = 8$ $U_3 = 1$	$U'_1 = 513.75$ $U'_2 = 17.71$ $U'_3 = 1.54$
4	Large ($a > \Delta$)	SAW	a/Δ	Exponential	λ	Gamma	$\alpha_1 = 4.615$[§§] $\alpha_2 = 4$	$\alpha'_1 = 4.563$ $\alpha'_2 = 5$

[§§] VFLAW combined all SAW and SMAW flaw data to arrive at the gamma distribution with $\alpha_1 = 21.68$ $\alpha_2 = 52$. As described in Section C.3.4.1, this example used only PVRUF SAW data for large flaw depths to build the specialized Beaver Valley prior PDF.

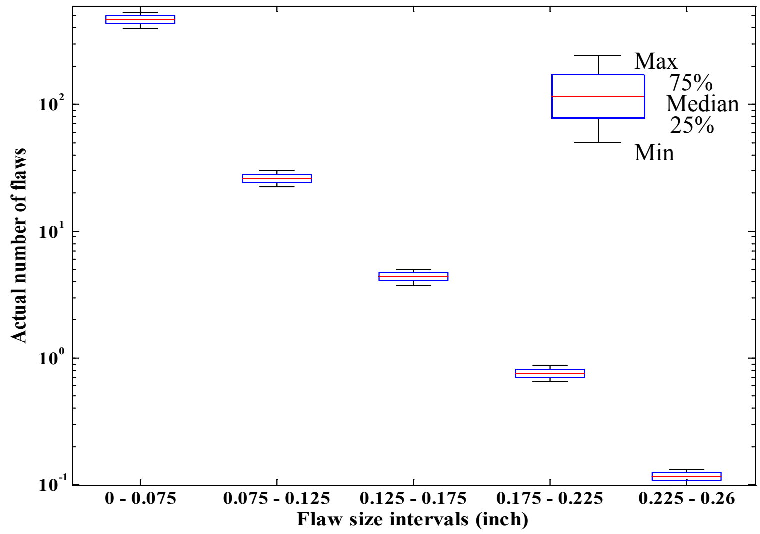

Figure C-13. Posterior number of flaws in the 3/8t region in various flaw size intervals including epistemic uncertainties

C.3.4.3.3 Sensitivity of the Flaw Density Results to a Lower Bound of 0.075" for the Interval Data Observed in the 3/8t Region

Estimations of the posterior PDFs presented in Sections C.3.4.3.1 and C.3.4.3.2 have been made by assuming that the observed interval of small flaws was 0.075" to 0.125". To assess the sensitivity of this assumption, it is assumed that the detection up to 0.075" is possible and all data would be between 0.075" and 0.125". Repeating the calculations in Section C.3.4 (including subsections) yields the posterior flaw depth and density PDFs that are very similar. Therefore, it was concluded that the results are relatively insensitive to choice for the lower bound of the data. More discussions of this topic are presented in Section C.3.5.

C.3.5 Updating the 10 CFR 50.61a Tables

The NDE data from the inspection volume specified in Supplement 4 to Mandatory Appendix VIII to Section XI of the ASME Code (the first one-inch of the weld) is used as the evidence for the Bayesian updating procedure described in the previous sections to obtain the flaw depth and density characteristics for Beaver Valley 2. The posterior characteristics are used to develop the corresponding 10 CFR50.61a flaw tables (consisting of only 19 UT-detected flaws in the interval 0.04" to 0.125"). The procedure is the same as the one used to update the UT data observed in the 3/8t region as discussed in Section C.3.4.

If the posterior distributions of the flaw density are used to estimate the mean number of flaws in the ranges of flaw sizes described in the 10 CFR 50.61a flaw tables, the results should be prorated to the number of flaws per 1,000" of weld. Because Beaver Valley 2 has a total weld length of 816.18", the prorated mean number of flaws was calculated and compared with the allowable number of flaws per length of weld, as shown in Table C-5. If the lower limit of the observed data interval is changed from 0.04" to 0.075" to line up with the smallest bin size in the 10 CFR 50.61a flaw tables, the results summarized in Table C-5 are calculated. In this case, the results of the mean number of flaws were also not too sensitive to the choice of the lower limit of the interval of NDE data.

To assess the epistemic uncertainties in the POD and measurement error uncertainties, again for the case of the Supplement 4 inspection volume (the first one inch), a Monte Carlo simulation was used to select random realizations of λ from the posterior PDFs of λ for both large and small flaws to develop the corresponding posterior flaw density PDFs. Repeating this process will result in the epistemic uncertainty for each flaw depth interval used in Table C-4. Figure C-14 shows the results of the number of the flaws of various depth intervals, by employing box and whisker plots. Epistemic uncertainties are larger (than those shown in Figure C-13), because of the smaller evidence, because there were only 19 observed flaws in the Supplement 4 inspection volume.

Table C-5. Alternate PTS Rule Flaw Table Assessment using Mean Number-of-Flaws by Size Interval for Beaver Valley 2 (Assuming a Lower Limit of 0.04**"** for Observed Data Interval)

Flaw Depth (inch)	**Observed (Detected) Number of Flaws (Biased)**	**Posterior Mean Number of Flaws (Unbiased and Corrected for POD)**	**Rule's Limits per 1,000" of Weld**
0.000 < a ≤ 0.075	19	124.98	No limit
0.075 < a ≤ 0.475		38.21	166.70
0.125 < a ≤ 0.475	0	14.13	90.80
0.175 < a ≤ 0.475	0	4.86	22.82
0.225 < a ≤ 0.475	0	1.30	8.66
0.275 < a ≤ 0.475	0	0.21	4.01
0.325 < a ≤ 0.475	0	0.13	3.01
0.375 < a ≤ 0.475	0	0.09	1.49
0.425 < a ≤ 0.475	0	0.04	1.00

Table C-6. Alternate PTS Rule Flaw Table Assessment using Mean Number-of-Flaws by Size Interval for Beaver Valley 2 (Assuming a Lower Limit of 0.075**"** for Observed Data Interval)

Flaw Depth (inch)	**Observed (Detected) Number of Flaws (Biased)**	**Posterior Mean Number of Flaws (Unbiased and Corrected for POD)**	**Rule's Limits per 1,000" of Weld**
0.000 < a ≤ 0.075	0	122.89	No limit
0.075 < a ≤ 0.475	19	39.05	166.70
0.125 < a ≤ 0.475	0	14.69	90.80
0.175 < a ≤ 0.475	0	5.12	22.82
0.225 < a ≤ 0.475	0	1.38	8.66
0.275 < a ≤ 0.475	0	0.21	4.01
0.325 < a ≤ 0.475	0	0.13	3.01
0.375 < a ≤ 0.475	0	0.08	1.49
0.425 < a ≤ 0.475	0	0.04	1.00

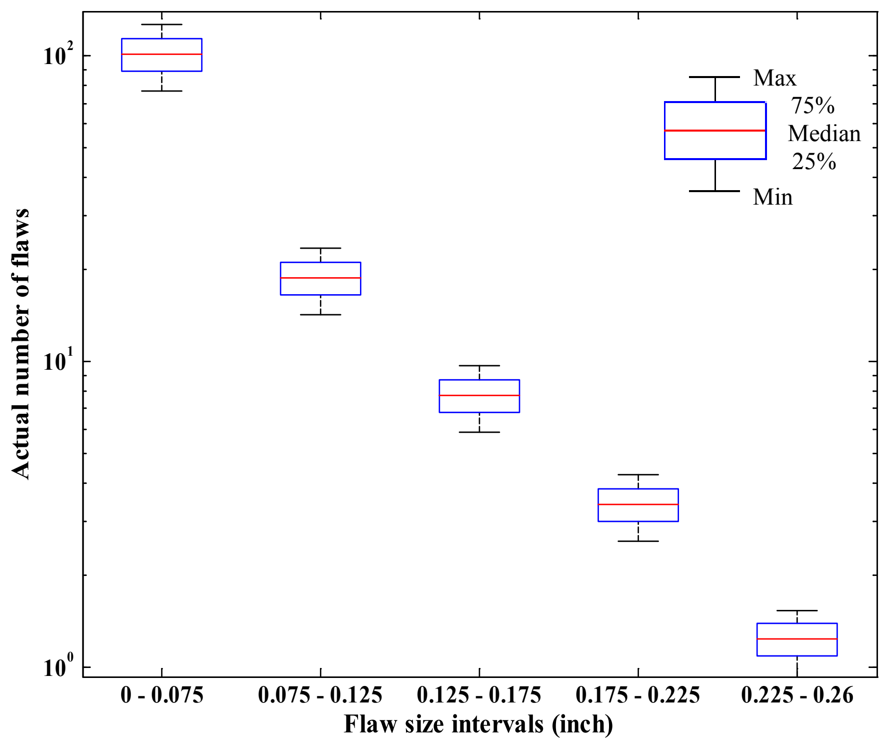

Figure C-14. Posterior number of flaws in the Supplement 4 inspection volume in various flaw size intervals including epistemic uncertainties

C.4 References

[C-1] *U.S. Code of Federal Regulations*, Title 10, "Energy," Chapter I, Section 50.61a, "Alternate Fracture Toughness Requirements for Protection Against Pressurized Thermal Shock Events" (10 CFR 50.61a).

[C-2] Williams, P.T., T.L. Dickson, and S. Yin, "Fracture Analysis of Vessels - Oak Ridge FAVOR, v09.1, Computer Code: Theory and Implementation of Algorithms, Methods, and Correlations," ORNL/TM-2010/5, January 2010, Oak Ridge National Laboratory, Oak Ridge, TN.

[C-3] U.S. Nuclear Regulatory Commission, "A Generalized Procedure for Generating Flaw-Related Inputs for the FAVOR Code," NUREG/CR-6817, March 2004, Agencywide Documents Access and Management System (ADAMS) Accession No. ML040830499.

[C-4] Gelman, A., et al., *Bayesian Data Analysis*, 2nd Ed., Chapman & Hall/CRC, Boca Raton, FL, July 2003.

[C-5] Hamada, M.S., et al., *Bayesian Reliability*, Springer Science+Business Media, LLC, New York, NY, July 2008.

[C-6] Becker, F.L., "Reactor Pressure Vessel Inspection Reliability Based on Performance Demonstrations," EPRI Report 1007984, June 2004, Electric Power Research Institute, Palo Alto, CA.

[C-7] Georgiou, G.A., "Probability of Detection (PoD) Curves: Derivation, Applications and Limitations," Research Report 454, UK Health & Safety Executive, London, UK, 2006.

[C-8] Li, M., and W. Q. Meeker, "A Noise Interference Model for Estimating Probability of Detection for Nondestructive Evaluations," *Proceedings of the Review of Progress in Quantitative Nondestructive Evaluation, July 20–25, 2008, Chicago, IL*, American Institute of Physics, College Park, MD, 2009.

[C-9] U.S. Department of Defense, "Nondestructive Evaluation System Reliability Assessment," MIL-HDBK-1823, April 30, 1999.

[C-10] Chatterjee, K., and M. Modarres, "A Bayesian Probabilistic Approach to Improved Health Management of Steam Generator Tubes," published online by the Prognostics and Health Management Society, 2011, available at https://www.phmsociety.org/sites/phmsociety.org/files/phm_submission/2011/phmc_11_012.pdf (accessed July 21, 2014).

[C-11] Celeux, G., et al., "Using Markov Chain Monte Carlo Methods to Solve Full Bayesian Modeling of PWR Vessel Flaw Distributions," *Reliability Engineering and System Safety*, 66(3):243–252, December 1999.

[C-12] Chatterjee, K., and M. Modarres, "A Probabilistic Approach for Estimating Defect Size and Density Considering Detection Uncertainties and Measurement Errors," *Journal of Risk and Reliability*, 227(1):28–40, February 2013.

[C-13] Spanner, J., "Materials Reliability Program: Reanalysis of Reactor Vessel Examination Data from the 1996 Beaver Valley 2 Vessel Examination (MRP-207), RPV Flaw Distribution," EPRI Report 1014548, November 2006, Electric Power Research Institute, Palo Alto, CA.

[C-14] U.S. Nuclear Regulatory Commission, “Probabilistic Fracture Mechanics - Models, Parameters, and Uncertainty Treatment Used in FAVOR Version 04.1,” NUREG-1807, June 2007, ADAMS Accession No. ML072010411.

Appendix C-1: Sample MATLAB Routine

```
clear
%%*******************************************************************
%%This MATLAB routine estimates posterior values of parameters of flaw-
%%depth distributions for small and large flaws in RPVs using NDE data,
%%accounting for measurement error, POD, and epistemic uncertainties. The
%%routine solves Equations 16, 17 and 18. The specific data used in this
%%routine are related to the POD of Eqn. 25 and the measurement error
%%discussed in Section C.3.3 The NDE data of Beaver Valley 2 are used. It
%%also shows the solution to the likelihood functions of Eqn. 27 and Eqn. 30.
%%Finally the routine solves the Bayesian inferences in Eqn. 28 for both
%%small and large flaws.
%%*******************************************************************
% THIS ROUTINE IS FOR DEMONSTRATION OF ONE WAY TO SOLVE THE BAYESIAN
% INFERENCE METHODS DISCUSSED IN THIS REPORT. THE RESULTS MAY BE USED TO
% CROSS-CHECK THE RESULTS IF OTHER VALUES OR OTHER SOLUTION ROUTINES ARE
% USED. THE ROUTINE DOES NOT COVER ALL E ANALYSES PERFORMED AND DISCUSSED
% IN THIS REPORT. FOR EXAMPLE, THE ROUTINE TO ESTIMATE THE FLAW-DENSITY
% DISTRIBUTIONS HAS NOT BEEN PRESENTED (ONLY FLAW-DEPTH MODEL
% DISTRIBUTIONS HAVE BEEN PRESENTED).
%%*******************************************************************
%%LIMITATIONS
% 1. THIS ROUTINE ASSUMES THE SINGLE PARAMETER EXPONENTIAL DISTRIBUTION
% FOR MODELING DISTRIBUTION OF BOTH SMALL AND LARGE FLAW DEPTHS.
% 2. THE POSTERIOR FOR SMALL FLAWS WILL GO TO INFINITY IF THE RIGHT EXTREME
% OF THE LEFT-CENSORED NDE DATA OR LEFT EXTREME OF INTERVAL DATA FOR
% SMALL FLAWS IS EXTREMELY SMALL (THAT IS, LESS THAN 0.09 INCH).
% 3. THE POSTERIOR FOR SMALL FLAWS APPROACHES INFINITY FOR LARGE SIGMA;
% THAT IS, THE RANDOM ERROR FOR THE MEASUREMENT ERROR MODEL (WHEN SIGMA
% EXCEEDS 0.035").
%%*******************************************************************
%%ASSUMPTIONS
% 1. THIS ROUTINE ASSUMES LEFT-TRUNCATED SINGLE-PARAMETER EXPONENTIAL
% DISTRIBUTION FOR FLAW DEPTH FOR SMALL FLAWS.
% 2. THIS ROUTINE ASSUMES RIGHT-TRUNCATED SINGLE-PARAMETER EXPONENTIAL
% DISTRIBUTION FOR LARGE FLAWS.
% 3. THIS ROUTINE ASSUMES TWO-PARAMETER LOGISTIC DISTRIBUTION EQN. 4 WITH
% A POD THRESHOLD OF ZERO.
% 4. SIMILARLY TO EQN. 30, INTEGRAL RANGE FOR THE MEASUREMENT IS BETWEEN
% -1 AND 1, WHICH COVERS THE EXTREME RANGES OF THE BIAS AND RANDOM ERRORS.
%%*******************************************************************
%%NOMENCLATURE:
%m & c are parameters discussed in Eqn. 8; sigma is standard deviation of
%random error associated with the measurement error model of Eqn. 8.
%beta1 & beta2 are POD function parameters in Eqn. 4; ath is the detection
%threshold of Eqn. 4.
%atr is the transition flaw depth between small and large flaws discussed
%in Eqn. 9.
%lambda1 & lambda2 are flaw-depth distribution parameters (i.e., the flaw-
% depth intensity) for small and large defects respectively.
%n1 is the total number of censored NDE data for small flaws.
%are is the right extreme of left-censored or interval of small-flaw-
%depth NDE data.
%ale is the left extreme of interval of small-flaw-depth data; ale must
% be greater than the parameter c of the measurement error model.
%a1 is a set, representing values of exact small-flaw-depth NDE data
%reported.
%n2 is the number of exact small-flaw-depth NDE data reported
%n3 is the total number of exact large-flaw-depth NDE data reported
%n4 is the total number of interval or left-censored large-flaw-depth NDE
%data reported
```

```
%a2 is set, representing exact values of large-flaw-depth NDE data
%reported
%are_large is the right extreme of the left-censored or interval large-
%flaw-depth NDE data reported
%ale_large is the left extreme of interval data of large-flaw-depth NDE
%data reported
%%*********************************************************************
%%Measurement error parameters
m=0.84;c=0.04;sigma=0.0298;
%%*********************************************************************
%%POD parameters
ath=0;beta1=63.21;beta2=0.1124;
%%*********************************************************************
%%Transition point for large flaws
atr=0.26;
%%*********************************************************************
%%*********************************************************************
%%NDE data of small flaws
n1=103;are=0.125;ale=c;a1=[0.15];n2=0;
%%*********************************************************************
%%*********************************************************************
%%NDE data of large flaws
a2=[0.26];n3=length(a2);n4=0;ale_large=0.27;are_large=0.3;
%%*********************************************************************
%BAYESIAN INFERENCE FOR ESTIMATING POSTERIOR DISTRIBUTION OF THE PARAMETER
%LAMBDA (FLAW-DEPTH INTENSITY) OF THE SMALL-FLAW-DEPTH EXPONENTIAL PDF
lambda1=linspace(0,60,100);
Norm_const=0;
for i=2:length(lambda1)
Marginal_Pod=@(a)((1-(1+exp(-beta1*beta2))./(1+exp(beta1*(a-beta2-ath)))).*(la
mbda1(i).*exp(-lambda1(i).*a)./(1-exp(-lambda1(i).*atr))));
Likeli_int=@(Ea,a)((1-(1+exp(-beta1*beta2))./(1+exp(beta1*(a-Ea-beta2-ath)))).
*(lambda1(i).*exp(-lambda1(i).*(a-Ea))./(1-exp(-lambda1(i).*atr))).*((1/sqrt
(2*pi*sigma^2)).*exp(-(1/(2*sigma^2)).*((m*Ea+(1-m)*a-c)/m).^2)));
Likeli_exact=@(Ea)((1-(1+exp(-beta1*beta2))./(1+exp(beta1*(a1-Ea-beta2-ath))))
.*(lambda1(i).*exp(-lambda1(i).*(a1-Ea))./(1-exp(-lambda1(i).*atr))).*((1/sqrt
(2*pi*sigma^2)).*exp(-(1/(2*sigma^2)).*((m*Ea+(1-m)*a1-c)/m).^2)));
Likelihood_exact(i)=((quad(Likeli_exact,-1,1))./(quad(Marginal_Pod,0,atr)))^n2
;
Likelihood_int(i)=((dblquad(Likeli_int,-1,1,ale,are))./(quad(Marginal_Pod,0,at
r)))^n1;
Prior_small(i)=(gampdf(lambda1(i),39,.3504));
Numerator(i)=Likelihood_int(i).*Likelihood_exact(i).*Prior_small(i);
Norm_const=Norm_const+Numerator(i)*(lambda1(i)-lambda1(i-1));
end
Posterior_small=Numerator/Norm_const;
Mean_Posterior_Small_Flaw_Depth_Intensity=sum(lambda1.*Posterior_small)*0.6061
Mean_Posterior_Small_Flaw_Depth=1/Mean_Posterior_Small_Flaw_Depth_Intensity
POD_of_Posterior_Mean_Small_Flaw_Depth=1-(1+exp(-beta1*beta2))./(1+exp(beta1*(
Mean_Posterior_Small_Flaw_Depth-beta2-ath)))
subplot(211)
plot(lambda1,Posterior_small,lambda1,Prior_small,'-.','LineWidth',2)
xlabel('Flaw Depth intensity (per unit
inch)','fontsize',12,'fontweight','b','FontName','Times New Roman')
ylabel('Relative Frequency','fontsize',12,'fontweight','b','FontName','Times
New Roman')
title('Posterior and prior flaw depth intensity for small
flaws','fontsize',14,'fontweight','b','FontName','Times New Roman')
h = legend('Posterior_small','Prior_small');
set(h,'Interpreter','none')
set(gca,'FontSize',12,'FontWeight','b','FontName','Times New Roman')
%%*********************************************************************
%BAYESIAN INFERENCE FOR ESTIMATING POSTERIOR DISTRIBUTION OF THE PARAMETER
%LAMBDA (FLAW-DEPTH INTENSITY) OF THE LARGE-FLAW-DEPTH EXPONENTIAL PDF
```

```
lambda2=linspace(0,10,100);
Norm_const1=0;
for i=2:length(lambda2)
Marginal_Pod1=@(a)((1-(1+exp(-beta1*beta2))./(1+exp(beta1*(a-beta2-ath)))).*(l
ambda2(i).*exp(-lambda2(i).*(a-atr))));
Likeli_exact1=@(Ea)((1-(1+exp(-beta1*beta2))./(1+exp(beta1*(a2-Ea-beta2-ath)))
).*(lambda2(i).*exp(-lambda2(i).*(a2-Ea-atr))).*((1/sqrt(2*pi*sigma^2)).*exp(-
(1/
(2*sigma^2)).*((m*Ea+(1-m)*a2-c)/m).^2)));
Likelihood_exact1(i)=((quad(Likeli_exact1,-1,1))./(quad(Marginal_Pod1,atr,10))
)^n3;
Likeli_int1=@(Ea,a)((1-(1+exp(-beta1*beta2))./(1+exp(beta1*(a-Ea-beta2-ath))))
.*(lambda2(i).*exp(-lambda2(i).*(a-Ea-atr))).*((1/sqrt(2*pi*sigma^2)).*exp(-(1
/
(2*sigma^2)).*((m*Ea+(1-m)*a-c)/m).^2)));
Likelihood_int1(i)=((dblquad(Likeli_int1,-1,1,ale_large,are_large))./(quad(Mar
ginal_Pod1,atr,10)))^n4;
Prior_large(i)=(gampdf(lambda2(i),4,0.8333));
Numerator1(i)=Likelihood_exact1(i).*Likelihood_int1(i).*Prior_large(i);
Norm_const1=Norm_const1+Numerator1(i)*(lambda2(i)-lambda2(i-1));
end
Posterior_large=Numerator1/Norm_const1;
Posterior_small=Numerator/Norm_const;
Mean_Posterior_Large_Flaw_Depth_Intensity=sum(lambda2.*Posterior_large)*0.1010
Mean_Posterior_Large_Flaw_Depth=1/Mean_Posterior_Large_Flaw_Depth_Intensity
POD_of_Posterior_Mean_Large_Flaw_Depth=1-(1+exp(-beta1*beta2))./(1+exp(beta1*(
Mean_Posterior_Large_Flaw_Depth-beta2-ath)))
subplot(212)
f1=plot(lambda2,Posterior_large,lambda2,Prior_large,'-.','LineWidth',2)
xlabel('Flaw depth intensity (per unit
inch)','fontsize',12,'fontweight','b','FontName','Times New Roman')
ylabel('Relative Frequency','fontsize',12,'fontweight','b','FontName','Times
New Roman')
title('Posterior and prior flaw depth intensity for large
flaws','fontsize',14,'fontweight','b','FontName','Times New Roman')
h = legend('Posterior_large','Prior_large');
set(h,'Interpreter','none')
set(gca,'FontSize',12,'FontWeight','b','FontName','Times New Roman')
screen_size = get(0, 'ScreenSize');
f1 = figure(1);
set(f1, 'Position', [0 0 screen_size(3) screen_size(4) ] );
%%*************************************************************************
```

Output from the above routine is displayed in Figure C-14 (also shown in Figure C-8 and Figure C-9)

```
Mean_Posterior_Small_Flaw_Depth_Intensity =
37.8118
Mean_Posterior_Small_Flaw_Depth =
0.0264
POD_of_Posterior_Mean_Small_Flaw_Depth =
0.0035
Mean_Posterior_Large_Flaw_Depth_Intensity =
5.4042
Mean_Posterior_Large_Flaw_Depth =
0.1850
POD_of_Posterior_Mean_Large_Flaw_Depth =
0.9900
f1 =
230.0087
231.0082
Published with MATLAB® 7.12
```

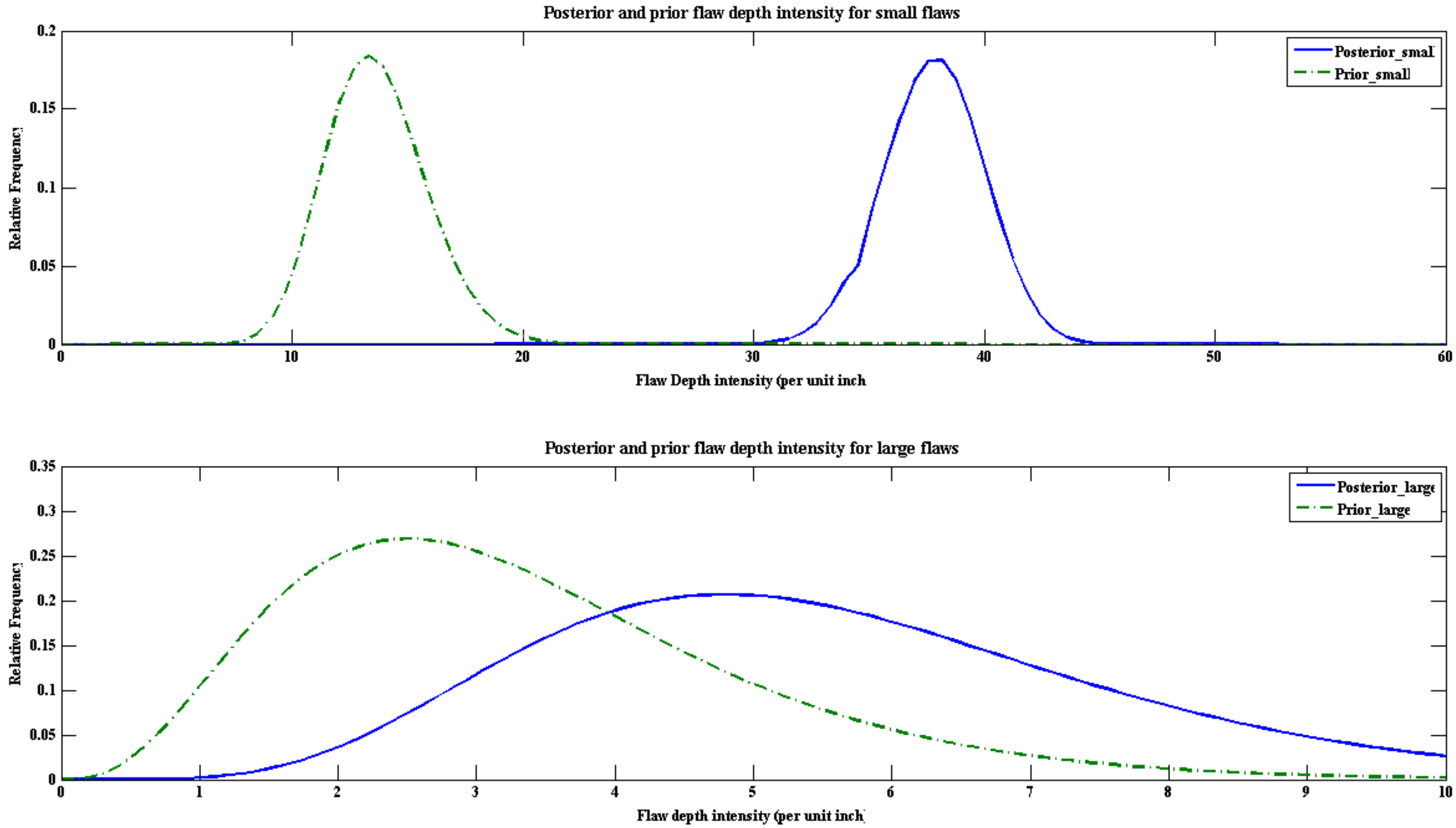

Figure C-15. MATLAB Routine Output

APPENDIX D: SENSITIVITY-STUDY RESULTS ON FLAW DISTRIBUTIONS CONSIDERING VFLAW DATA, POD, AND MEASUREMENT ERRORS IN NDE DATA

Prepared for the U.S. Nuclear Regulatory Commission under the Subcontract 4000111626 with UT-Battelle, LLC (Oak Ridge National Laboratory)

Mohammad Modarres
University of Maryland

March 2012

Table of Contents

List of Tables

List of Figures

Abbreviations

Abbreviation	Definition
PDF	Probability Density Function
NDE	Nondestructive Evaluation
POD	Probability of Detection
RPV	Reactor Pressure Vessel
SAW	Submerged Arc Weld
UT	Ultrasonic Test

Symbols and Expressions

Symbol	Definition
a	True flaw depth (inches)
a^*	NDE measured (or observed) flaw depth (inches)
a_{th}	Threshold flaw depth for detection, below which flaw detection is beyond the capability of the NDE technology used
D	The event that a flaw is detected
$\overline{D}$	The event that a flaw is not detected
E_M	Model error of the NDE measurement error, represented by a normal distribution with a mean of zero and known standard deviation
$L(a\|\Phi)$	Likelihood of true flaw depth given the vector of parameters Φ
$L(Data\|\theta)$	Likelihood of observed NDE data conditioned on (given) the unknown parameter θ
$L(n^* \| n_j)$	Likelihood of observing n^* flaws given that there are a total of n_j true flaws
M_ε	NDE measurement error (combined random and systematic errors)
n	Number of flaw-depth intervals (reported in NDE)
$\bar{n}$	Mean of the PDF of the number of flaws in volume v
n^*	Number of exact flaw depths observed (reported in NDE)
$\binom{n_j}{n^*}$	Combination of n^* observed flaws out of total flaws n_j (observed or detected, and unobserved or not detected flaws)
$POD(a)$	Probability of detection of a flaw of depth a
$Pr(.)$	Probability
$Pr(D)$	POD independent of flaw depth
$Pr(\overline{D})$	Probability of no detection regardless of size
$Pr(n_j \| n^*)$	Probability of total flaws n_j conditioned on observing n^* flaws in NDE
β_i	Parameter i of the POD model
Δ	Weld bead thickness
$\pi_0(\theta)$	Prior PDF of an unknown parameter θ
$\pi_1(\theta\|Data)$	Posterior PDF of an unknown parameter given observed NDE data
Φ	Vector of parameters of the flaw-depth PDF
θ	An unknown parameter of a model

D.1 Introduction

This report discusses the results of a sensitivity analysis by applying a Bayesian updating methodology described in Appendix C to account for probability of detection (POD) and measurement (sizing) error in the data for flaws detected through ultrasonic testing (UT). The methodology estimates vessel-specific flaw depth and density distributions for comparison to the 10 CFR 50.61a screening tables and updates the VFLAW code's distributions for further analysis with the FAVOR code. The sensitivity analysis was performed using assumed nondestructive examination (NDE) flaw data. Existing VFLAW distributions for flaw depth and density, representing welds of the Pressure Vessel Research User Facility (PVRUF) vessel, were specialized to the Beaver Valley 2 reactor pressure vessel (RPV) welds and assumed to properly describe prior flaw-depth and flaw-density distributions and characteristics.

In the remainder of this Appendix, a very brief overview of the methodology is described first, followed by the results of the sensitivity analysis. The results are compared to the 10 CFR 50.61a screening tables and conclusions are summarized.

D.2 Overview of the Bayesian Approach to Update Flaw-Depth and Flaw-Density Distributions

Finding flaws using NDE requires characterization of associated uncertainties. The reliability of an inspection is customarily expressed in terms of the POD of a given flaw size and expressed by curves of POD vs. flaw size. Additionally, sizing or measurement errors occur and model uncertainties exist. Sizes of UT-detected small flaws in RPVs tend to be overestimated while the sizes of large flaws are underestimated [D-1].

POD is generally modeled as a function of true flaw depth. Different forms of POD curves have been used in the literature (see References [D-2], [D-3], and [D-4]. The logistic POD model for hit/miss data is a common model and is represented as:

$$POD(a \mid \beta_1, \beta_2, a_{th}) = \begin{cases} 1 - \dfrac{1 + e^{-\beta_1 \beta_2}}{1 + e^{\beta_1 (a - \beta_2 - a_{th})}} & \text{for } a > a_{th} \\ 0 & \text{otherwise} \end{cases} \qquad \text{Eqn. (D-1)}$$

Measurement error is defined by Eqn. (D-2), where Mε is the measurement error, a* is the measured value of flaw depth, and a is the true value of flaw depth:

$$M_\varepsilon = a^* - a \qquad \text{Eqn. (D-2)}$$

In its simplest form, Mε can be represented by a linear function of true size, as shown in Eqn. (D-1), where m is the slope and c is the intercept of the line representing measurement error versus true flaw depth:

$$\begin{aligned} &M_\varepsilon = ma + c + E_M \\ &\text{where, } a = \text{true flaw depth and } E_M = N_M(0, \sigma_M) \end{aligned} \qquad \text{Eqn. (D-3)}$$

The likelihood of exact flaw measurements reported may be expressed as a function of POD and Mε (see Appendix C). If, in addition to or instead of the exact flaw depth data, intervals of flaw depths are reported (such as the number of flaws observed at less than a given depth or between an upper and lower limit), the likelihood may also be similarly expressed (see Appendix C).

Regardless of the form of the data (exact flaw depth and/or interval data), the Bayesian inference of the vector of parameters Φ of the flaw-depth probability density function (PDF) would be obtained from the Bayesian inference $\pi_1(\Phi \mid \text{Data}) \propto L(\text{Data} \mid \Phi)\pi_0(\Phi)$, where $\pi_1(\Phi \mid \text{Data})$ is the posterior multivariate PDF of vector Φ and $\pi_0(\Phi)$ is the prior multivariate PDF of Φ.

If flaws are detected with a probability Pr(D) (or not detected with a probability of $\Pr(\overline{D}) = 1 - \Pr(D)$), the probability that a specific total number of flaws n* observed in a given volume v out of the true number of flaws n_j follows the binomial distribution (see References [D-5] and [D-6]:

$$L(n^* \mid n_j) = \binom{n_j}{n^*} [\Pr(D)]^{n^*} [1 - \Pr(D)]^{n_j - n^*} \qquad \text{Eqn. (D-4)}$$

Accordingly, the mean estimate of the true number of flaws $\bar{n}$ would be found from:

$$\bar{n} = \frac{n^*}{POD(D)} \qquad \text{Eqn. (D-5)}$$

The Bayesian updating of n_j, which allows the estimation of the posterior distribution of n_j to describe the true number of flaws, would be:

$$\Pr(n_j \mid n^*) = \frac{L(n^* \mid n_j)\Pr(n_j)}{\sum_{n_j} L(n^* \mid n_j)\Pr(n_j)} \qquad \text{Eqn. (D-6)}$$

where the prior $\Pr(n_j)$ may be expressed by a Poisson distribution with parameter ρ (defined in VFLAW).

D.3 Application to a Base Case Example

The EPRI report by Spanner [D-7] provides UT-based measured flaw data near the inner surface (~2.5 inches) of the Beaver Valley Unit 2 RPV, including small flaw sizes. These data, while subject to POD and measurement error, provide a more vessel-specific perspective of the distribution of flaws for weld metals in the Beaver Valley 2 RPV than do the VFLAW distributions used in FAVOR.

The observed Beaver Valley 2 NDE data (with detection and sizing uncertainty) are mostly in the form of interval data as summarized below [D-7]:

19 weld flaws were detected by the UT NDE of Beaver Valley 2 in the first inch (ASME Code, Section XI, Mandatory Appendix VIII, Supplement 4 inspection volume) of the

RPV (these data are assumed normalized to 1,000" of weld length), all having a flaw depth less than 0.125". [***]

The lower limit of the detected flaw intervals described above was not stated in [D-7], but is not zero. Two possible subjective lower limits were assumed, and later the sensitivities of the final (posterior) flaw distributions to these two choices were assessed. The two lower limits selected were 0.04" and 0.075".

The associated weld bead thicknesses are not reported in [D-7]. However, the weld region of the observed flaws and flaw length is reported. Such results must be corrected for detection and sizing capability, particularly for the small flaws. The Beaver Valley 2 RPV weld map is shown in Figure D-1 [D-8]. In the absence of the Beaver Valley average weld bead thickness as the point of transition between large and small depths, it was assumed that all flaws reported are in submerged arc welds (SAWs), which form over 90% of welds in the VFLAW data, with the bead thickness of Δ = 0.26". Using the Beaver Valley 2 RPV information shown in Figure D-1, the VFLAW data were specialized to represent the prior distributions of flaw depth and density for Beaver Valley 2 RPV.

Total Weld Length = 816.18"
Total Weld Volume = 4.975 ft^3
Total Weld Fusion Area = 92 ft^2
Weld Volume of 1" = 0.616 ft^3
Weld Volume of 3/8t = 1.865 ft^3

[***] In Appendix C, the same analysis is performed, except that the analysis did not assume that the data were normalized to 1,000" of linear length of weld. Instead, it assumed that the data came from 816.18" of weld, which is the actual length of weld in the Beaver Valley 2 RPV.

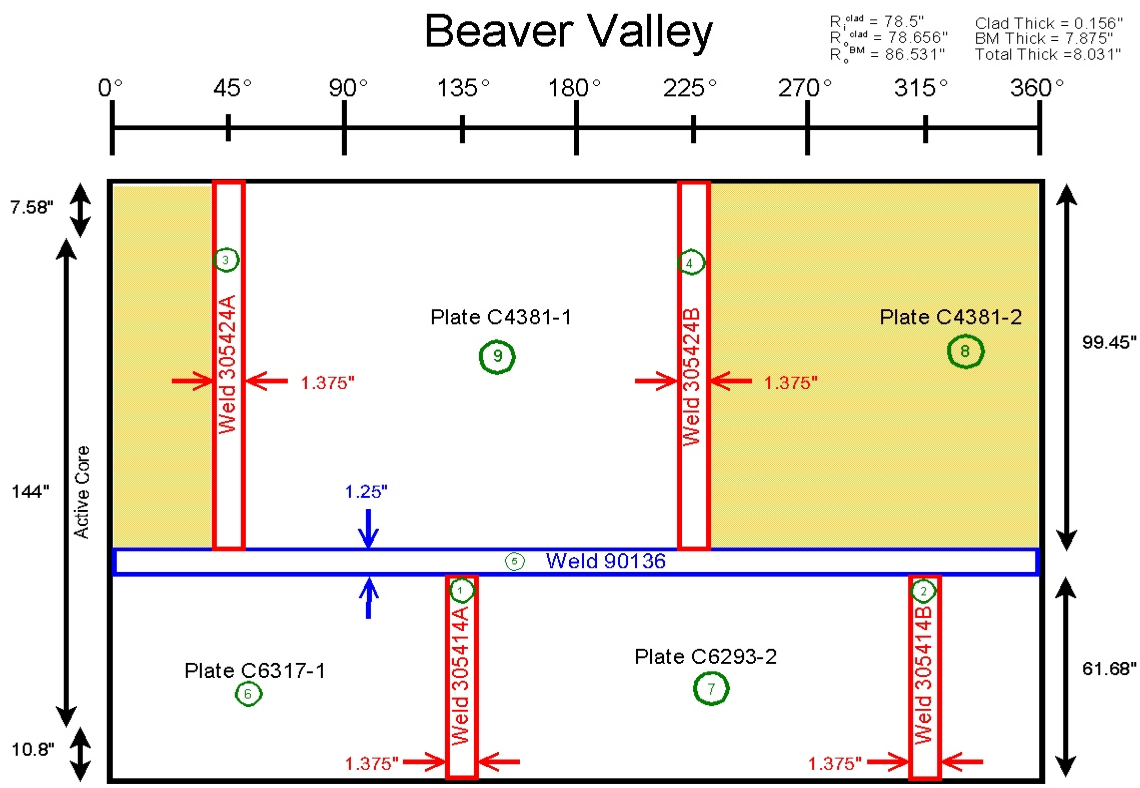

Figure D-1. Beaver Valley 2 Weld Map [D-8]

The relationship between the flaw depth and flaw density PDFs and the corresponding prior hyper-PDFs of their parameters are illustrated in Figure D-2.

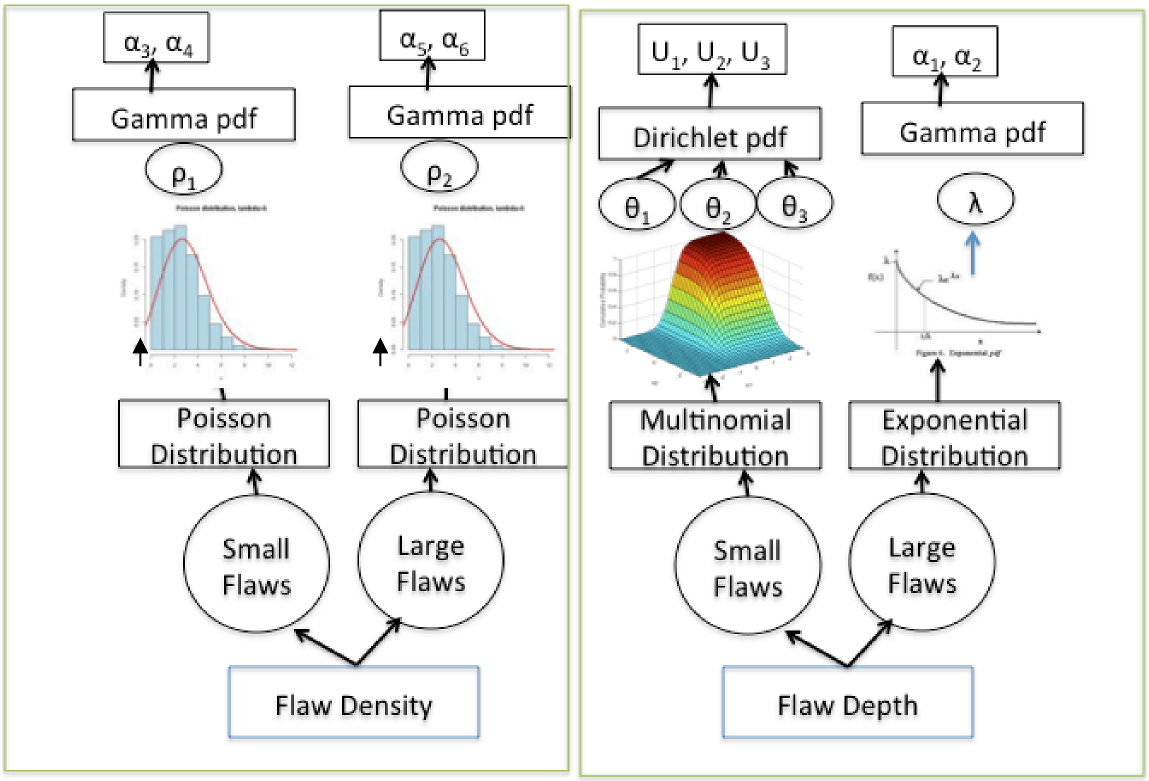

Figure D-2. Flaw-Depth and Flaw-Density Distributions Used in VFLAW and Their Corresponding Parameter Hyper-PDFs

Analysis of UT-detected performance data reported by the Electric Power Research Institute (EPRI) [D-7] was used to identify a POD function for the purpose of this example. The threshold limit of this POD function was taken as 0.00, and the epistemic uncertainties associated with the parameters of the model were not considered in this study. Accordingly, the following mean POD function was used:

$$POD(a) = 1 - \frac{1}{1 + e^{63.2100(a - 0.1124)}} \qquad \text{Eqn. (D-7)}$$

The measurement error was assumed based on some examples and measurement errors reported in Reference [D-7]. After combination of Eqn. (D-2) and Eqn. (D-3), the measurement error (a linear function that oversizes small flaws and undersizes large flaws) is:

$$M_{\varepsilon} = -0.1905a^{*} + 0.0476 + N(0, 0.0298) \qquad \text{Eqn. (D-8)}$$

where N(0, 0.0298) is a normal distribution with a mean of zero and a constant standard deviation of 0.0298. The observed data for the first inch of the vessel were used to estimate the true number of flaws in the flaw-depth ranges of the Alternate PTS Rule flaw tables. This information was used to assess how the estimated number of flaws of a given size in Beaver Valley 2 (estimated based on inspection data, VFLAW distributions, and Bayesian inference) compares to the number and size of flaws permitted by the Alternate PTS Rule flaw tables. The posterior characteristics were used to develop the corresponding Alternate PTS Rule flaw tables.

If the lower limit of the observed data interval is changed from 0.04" to 0.075" to line up with the smallest bin size in the Alternate PTS Rule flaw tables, the results summarized in Table D-1 are calculated. In this case, the results of the mean number of flaws show no sensitivity to the choice of the lower limit of the interval of NDE data. Given this flaw observation, true estimated numbers of flaws in all bins were below the Alternate PTS rule flaw limits.

Table D-1. Alternate PTS Rule Flaw Table Assessment Using Mean Number of Flaws by Size Interval for Beaver Valley 2 (assuming a Lower Limit of 0.04" vs. 0.075" for Observed Data Interval)

<table>
<tr><th rowspan="2">Bin No.</th><th rowspan="2">Flaw Depth (in)</th><th colspan="2">Base Case 1</th><th colspan="2">Base Case 2</th><th rowspan="2">Alternate PTS Rule Limit (per 1,000" of Weld)</th></tr>
<tr><th>Observed (Detected) Number of Flaws (Biased with Lower Detection Limit of 0.04")</th><th>Posterior Mean Number of Flaws (Unbiased and Corrected for POD)</th><th>Observed (Detected) Number of Flaws (Biased with Lower Detection Limit of 0.075")</th><th>Posterior Mean Number of Flaws (Unbiased and Corrected for POD)</th></tr>
<tr><td>1</td><td>0.000 < a ≤ 0.075</td><td rowspan="2">19</td><td>111.41</td><td>0</td><td>109.09</td><td>No limit</td></tr>
<tr><td>2</td><td>0.075 < a ≤ 0.475</td><td>25.73</td><td>19</td><td>27.02</td><td>166.70</td></tr>
<tr><td>3</td><td>0.125 < a ≤ 0.475</td><td>0</td><td>8.46</td><td>0</td><td>8.98</td><td>90.80</td></tr>
<tr><td>4</td><td>0.175 < a ≤ 0.475</td><td>0</td><td>2.98</td><td>0</td><td>2.88</td><td>22.82</td></tr>
<tr><td>5</td><td>0.225 < a ≤ 0.475</td><td>0</td><td>0.79</td><td>0</td><td>0.79</td><td>8.66</td></tr>
<tr><td>6</td><td>0.275 < a ≤ 0.475</td><td>0</td><td>0.29</td><td>0</td><td>0.29</td><td>4.01</td></tr>
<tr><td>7</td><td>0.325 < a ≤ 0.475</td><td>0</td><td>0.14</td><td>0</td><td>0.14</td><td>3.01</td></tr>
<tr><td>8</td><td>0.375 < a ≤ 0.475</td><td>0</td><td>0.09</td><td>0</td><td>0.09</td><td>1.49</td></tr>
<tr><td>9</td><td>0.425 < a ≤ 0.475</td><td>0</td><td>0.05</td><td>0</td><td>0.05</td><td>1.00</td></tr>
</table>

D.4 Application to Sensitivity Cases

In order to examine the effects of changes in the number of flaws observed through NDE, as well as the significance of the POD and the VFLAW prior distributions, twelve sensitivity cases were identified and examined. Methods and tools discussed in Sections D.2 and D.3 were used to carry out these sensitivity cases. The sensitivity cases examined were as follows:

1. No flaws detected, with consideration of the VFLAW prior distributions, POD, and measurement error.
2. 70% of the Alternate PTS Rule's allowed flaws in Bins 2 and 3 are detected, with consideration of the VFLAW prior distributions, POD, and measurement error.
3. 110% of the Alternate PTS Rule's allowed flaws in Bin 3 are detected, with consideration of the VFLAW prior distributions, POD, and measurement error.
4. No flaws detected, with no consideration of VFLAW priors (i.e., non-informative priors) and POD, but with consideration of flaw measurement error only (i.e., no POD or VFLAW prior).
5. 70% of the Alternate PTS Rule's allowed flaws in Bins 2 and 3 are detected, with no consideration of VFLAW priors and POD, but with consideration of flaw measurement error only.
6. 110% of the Alternate PTS Rule's allowed flaws in Bin 3 are detected, with no consideration of VFLAW priors and no consideration of POD, but with consideration of flaw measurement error only.
7. No flaws detected, no consideration of VFLAW priors, but with consideration of POD and flaw measurement error.
8. 70% of the Alternate PTS Rule's allowed flaws in Bins 2 and 3 are detected, with no consideration of VFLAW priors, but with consideration of POD and flaw measurement error.
9. 110% of the Alternate PTS Rule's allowed flaws in Bin 3 are detected, with no consideration of VFLAW priors, but with consideration of POD and flaw measurement error.
10. No flaws detected, no consideration of POD, but with consideration of VFLAW priors and flaw measurement error.
11. 70% of the Alternate PTS Rule's allowed flaws in Bins 2 and 3 are detected, with no consideration of POD, but with consideration of VFLAW priors and flaw measurement error.
12. 110% of the Alternate PTS Rule's allowed flaws in Bin 3 are detected, with no consideration of POD, but with consideration of VFLAW priors and flaw measurement error.

The results of the sensitivity studies are listed in Table D-2 through Table D-13.

Table D-2. Results of Sensitivity Case 1

Bin No.	Flaw Depth (in)	Base Case 1: Observed (Detected) No. of Flaws (Biased with Detection Limit of 0.04")	Base Case 1: Posterior Mean No. of Flaws (Unbiased and Corrected for POD)	Sensitivity Case 1: Assumed No. of Detected Flaws (with Bias)	Sensitivity Case 1: Posterior Mean No. of Flaws (Unbiased)	Alternate PTS Rule Limit (per 1,000" of Weld)
1	0.000 < a ≤ 0.075	19	111.41	0	80.13	No limit
2	0.075 < a ≤ 0.475		25.73	0	40.76	166.70
3	0.125 < a ≤ 0.475	0	8.46	0	18.79	90.80
4	0.175 < a ≤ 0.475	0	2.98	0	7.81	22.82
5	0.225 < a ≤ 0.475	0	0.79	0	2.71	8.66
6	0.275 < a ≤ 0.475	0	0.29	0	0.29	4.01
7	0.325 < a ≤ 0.475	0	0.14	0	0.14	3.01
8	0.375 < a ≤ 0.475	0	0.09	0	0.09	1.49
9	0.425 < a ≤ 0.475	0	0.05	0	0.05	1.00

Table D-3. Results of Sensitivity Case 2

Bin No.	Flaw Depth (in)	Base Case 1: Observed (Detected) No. of Flaws (Biased with Detection Limit of 0.04")	Base Case 1: Posterior Mean No. of Flaws (Unbiased and Corrected for POD)	Sensitivity Case 2: Assumed No. of Detected Flaws (with Bias)	Sensitivity Case 2: Posterior Mean No. of Flaws (Unbiased)	Alternate PTS Rule Limit (per 1,000" of Weld)
1	0.000 < a ≤ 0.075	19	111.41	0	306.12	No limit
2	0.075 < a ≤ 0.475		25.73	116.69	34.16	166.70
3	0.125 < a ≤ 0.475	0	8.46	63.56	7.71	90.80
4	0.175 < a ≤ 0.475	0	2.98	0	1.69	22.82
5	0.225 < a ≤ 0.475	0	0.79	0	0.44	8.66
6	0.275 < a ≤ 0.475	0	0.29	0	0.29	4.01
7	0.325 < a ≤ 0.475	0	0.14	0	0.14	3.01
8	0.375 < a ≤ 0.475	0	0.09	0	0.09	1.49
9	0.425 < a ≤ 0.475	0	0.05	0	0.04	1.00

Table D-4. Results of Sensitivity Case 3

Bin No.	Flaw Depth (in)	Base Case 1		Sensitivity Case 3		Alternate PTS Rule Limit (per 1,000" of Weld)
		Observed (Detected) No. of Flaws (Biased with Detection Limit of 0.04")	Posterior Mean No. of Flaws (Unbiased and Corrected for POD)	Assumed No. of Detected Flaws (with Bias)	Posterior Mean No. of Flaws (Unbiased)	
1	0.000 < a ≤ 0.075	19	111.41	0	155.03	No limit
2	0.075 < a ≤ 0.475		25.73	0	41.33	166.70
3	0.125 < a ≤ 0.475	0	8.46	99.88	15.21	90.80
4	0.175 < a ≤ 0.475	0	2.98	0	4.51	22.82
5	0.225 < a ≤ 0.475	0	0.79	0	1.21	8.66
6	0.275 < a ≤ 0.475	0	0.29	0	0.29	4.01
7	0.325 < a ≤ 0.475	0	0.14	0	0.14	3.01
8	0.375 < a ≤ 0.475	0	0.09	0	0.09	1.49
9	0.425 < a ≤ 0.475	0	0.05	0	0.05	1.00

Table D-5. Results of Sensitivity Case 4

Bin No.	Flaw Depth (in)	Base Case 1		Sensitivity Case 4		Alternate PTS Rule Limit (per 1,000" of Weld)
		Observed (Detected) No. of Flaws (Biased with Detection Limit of 0.04")	Posterior Mean No. of Flaws (Unbiased and Corrected for POD)	Assumed No. of Detected Flaws (with Bias)	Posterior Mean No. of Flaws (Unbiased)	
1	0.000 < a ≤ 0.075	19	111.41	0	0.00	No limit
2	0.075 < a ≤ 0.475		25.73	0	0.00	166.70
3	0.125 < a ≤ 0.475	0	8.46	0	0.00	90.80
4	0.175 < a ≤ 0.475	0	2.98	0	0.00	22.82
5	0.225 < a ≤ 0.475	0	0.79	0	0.00	8.66
6	0.275 < a ≤ 0.475	0	0.29	0	0.00	4.01
7	0.325 < a ≤ 0.475	0	0.14	0	0.00	3.01
8	0.375 < a ≤ 0.475	0	0.09	0	0.00	1.49
9	0.425 < a ≤ 0.475	0	0.05	0	0.00	1.00

Table D-6. Results of Sensitivity Case 5

Bin No.	Flaw Depth (in)	Base Case 1		Sensitivity Case 5		Alternate PTS Rule Limit (per 1,000" of Weld)
		Observed (Detected) No. of Flaws (Biased with Lower Detection Limit of 0.04")	Posterior Mean No. of Flaws (Unbiased and Corrected for POD)	Assumed No. of Detected Flaws (with Bias)	Posterior Mean No. of Flaws (Unbiased)	
1	0.000 < a ≤ 0.075	19	111.41	0	56.47	No limit
2	0.075 < a ≤ 0.475		25.73	116.69	60.22	166.70
3	0.125 < a ≤ 0.475	0	8.46	63.56	36.13	90.80
4	0.175 < a ≤ 0.475	0	2.98	0	18.67	22.82
5	0.225 < a ≤ 0.475	0	0.79	0	5.98	8.66
6	0.275 < a ≤ 0.475	0	0.29	0	0.00	4.01
7	0.325 < a ≤ 0.475	0	0.14	0	0.00	3.01
8	0.375 < a ≤ 0.475	0	0.09	0	0.00	1.49
9	0.425 < a ≤ 0.475	0	0.05	0	0.00	1.00

Table D-7. Results of Sensitivity Case 6

Bin No.	Flaw Depth (in)	Base Case 1		Sensitivity Case 6		Alternate PTS Rule Limit (per 1,000" of Weld)
		Observed (Detected) No. of Flaws (Biased with Detection Limit of 0.04")	Posterior Mean No. of Flaws (Unbiased and Corrected for POD)	Assumed No. of Detected Flaws (with Bias)	Posterior Mean No. of Flaws (Unbiased)	
1	0.000 < a ≤ 0.075	19	111.41	0	32.85	No limit
2	0.075 < a ≤ 0.475		25.73	0	67.03	166.70
3	0.125 < a ≤ 0.475	0	8.46	99.88	47.02	90.80
4	0.175 < a ≤ 0.475	0	2.98	0	27.19	22.82
5	0.225 < a ≤ 0.475	0	0.79	0	11.17	8.66
6	0.275 < a ≤ 0.475	0	0.29	0	0.00	4.01
7	0.325 < a ≤ 0.475	0	0.14	0	0.00	3.01
8	0.375 < a ≤ 0.475	0	0.09	0	0.00	1.49
9	0.425 < a ≤ 0.475	0	0.05	0	0.00	1.00

Table D-8. Results of Sensitivity Case 7

Bin No.	Flaw Depth (in)	Base Case 1		Sensitivity Case 7		Alternate PTS Rule Limit (per 1,000" of Weld)
		Observed (Detected) No. of Flaws (Biased with Detection Limit of 0.04")	Posterior Mean No. of Flaws (Unbiased and Corrected for POD)	Assumed No. of Detected Flaws (with Bias)	Posterior Mean No. of Flaws (Unbiased)	
1	0.000 < a ≤ 0.075	19	111.41	0	0.00	No limit
2	0.075 < a ≤ 0.475		25.73	0	0.00	166.70
3	0.125 < a ≤ 0.475	0	8.46	0	0.00	90.80
4	0.175 < a ≤ 0.475	0	2.98	0	0.00	22.82
5	0.225 < a ≤ 0.475	0	0.79	0	0.00	8.66
6	0.275 < a ≤ 0.475	0	0.29	0	0.00	4.01
7	0.325 < a ≤ 0.475	0	0.14	0	0.00	3.01
8	0.375 < a ≤ 0.475	0	0.09	0	0.00	1.49
9	0.425 < a ≤ 0.475	0	0.05	0	0.00	1.00

Table D-9. Results of Sensitivity Case 8

Bin No.	Flaw Depth (in)	Base Case 1		Sensitivity Case 8		Alternate PTS Rule Limit (per 1,000" of Weld)
		Observed (Detected) No. of Flaws (Biased with Detection Limit of 0.04")	Posterior Mean No. of Flaws (Unbiased and Corrected for POD)	Assumed No. of Detected Flaws (with Bias)	Posterior Mean No. of Flaws (Unbiased)	
1	0.000 < a ≤ 0.075	19	111.41	0	5131.91	No limit
2	0.075 < a ≤ 0.475		25.73	116.69	263.80	166.70
3	0.125 < a ≤ 0.475	0	8.46	63.56	35.54	90.80
4	0.175 < a ≤ 0.475	0	2.98	0	4.88	22.82
5	0.225 < a ≤ 0.475	0	0.79	0	0.39	8.66
6	0.275 < a ≤ 0.475	0	0.29	0	0.00	4.01
7	0.325 < a ≤ 0.475	0	0.14	0	0.00	3.01
8	0.375 < a ≤ 0.475	0	0.09	0	0.00	1.49
9	0.425 < a ≤ 0.475	0	0.05	0	0.00	1.00

Table D-10. Results of Sensitivity Case 9

Bin No.	Flaw Depth (in)	Base Case 1		Sensitivity Case 9		Alternate PTS Rule Limit (per 1,000" of Weld)
		Observed (Detected) No. of Flaws (Biased with Detection Limit of 0.04")	Posterior Mean No. of Flaws (Unbiased and Corrected for POD)	Assumed No. of Detected Flaws (with Bias)	Posterior Mean No. of Flaws (Unbiased)	
1	0.000 < a ≤ 0.075	19	111.41	0	1233.10	No limit
2	0.075 < a ≤ 0.475		25.73	0	202.01	166.70
3	0.125 < a ≤ 0.475	0	8.46	99.88	54.12	90.80
4	0.175 < a ≤ 0.475	0	2.98	0	13.13	22.82
5	0.225 < a ≤ 0.475	0	0.79	0	1.95	8.66
6	0.275 < a ≤ 0.475	0	0.29	0	0.00	4.01
7	0.325 < a ≤ 0.475	0	0.14	0	0.00	3.01
8	0.375 < a ≤ 0.475	0	0.09	0	0.00	1.49
9	0.425 < a ≤ 0.475	0	0.05	0	0.00	1.00

Table D-11. Results of Sensitivity Case 10

Bin No.	Flaw Depth (in)	Base Case 1		Sensitivity Case 10		Alternate PTS Rule Limit (per 1,000" of Weld)
		Observed (Detected) No. of Flaws (Biased with Detection Limit of 0.04")	Posterior Mean No. of Flaws (Unbiased and Corrected for POD)	Assumed No. of Detected Flaws (with Bias)	Posterior Mean No. of Flaws (Unbiased)	
1	0.000 < a ≤ 0.075	19	111.41	0	79.14	No limit
2	0.075 < a ≤ 0.475		25.73	0	41.18	166.70
3	0.125 < a ≤ 0.475	0	8.46	0	19.09	90.80
4	0.175 < a ≤ 0.475	0	2.98	0	7.93	22.82
5	0.225 < a ≤ 0.475	0	0.79	0	2.42	8.66
6	0.275 < a ≤ 0.475	0	0.29	0	0.29	4.01
7	0.325 < a ≤ 0.475	0	0.14	0	0.14	3.01
8	0.375 < a ≤ 0.475	0	0.09	0	0.09	1.49
9	0.425 < a ≤ 0.475	0	0.05	0	0.05	1.00

Table D-12. Results of Sensitivity Case 11

Bin No.	Flaw Depth (in)	Base Case 1		Sensitivity Case 11		Alternate PTS Rule Limit (per 1,000" of Weld)
		Observed (Detected) No. of Flaws (Biased with Detection Limit of 0.04")	Posterior Mean No. of Flaws (Unbiased and Corrected for POD)	Assumed No. of Detected Flaws (with Bias)	Posterior Mean No. of Flaws (Unbiased)	
1	0.000 < a ≤ 0.075	19	111.41	0	73.49	No limit
2	0.075 < a ≤ 0.475		25.73	116.69	57.04	166.70
3	0.125 < a ≤ 0.475	0	8.46	63.56	31.09	90.80
4	0.175 < a ≤ 0.475	0	2.98	0	14.66	22.82
5	0.225 < a ≤ 0.475	0	0.79	0	4.81	8.66
6	0.275 < a ≤ 0.475	0	0.29	0	0.29	4.01
7	0.325 < a ≤ 0.475	0	0.14	0	0.14	3.01
8	0.375 < a ≤ 0.475	0	0.09	0	0.09	1.49
9	0.425 < a ≤ 0.475	0	0.05	0	0.05	1.00

Table D-13. Results of Sensitivity Case 12

Bin No.	Flaw Depth (in)	Base Case 1		Sensitivity Case 12		Alternate PTS Rule Limit (per 1,000" of Weld)
		Observed (Detected) No. of Flaws (Biased with Detection Limit of 0.04")	Posterior Mean No. of Flaws (Unbiased and Corrected for POD)	Assumed No. of Detected Flaws (with Bias)	Posterior Mean No. of Flaws (Unbiased)	
1	0.000 < a ≤ 0.075	19	111.41	0	63.04	No limit
2	0.075 < a ≤ 0.475		25.73	0	66.84	166.70
3	0.125 < a ≤ 0.475	0	8.46	99.88	39.42	90.80
4	0.175 < a ≤ 0.475	0	2.98	0	20.55	22.82
5	0.225 < a ≤ 0.475	0	0.79	0	7.21	8.66
6	0.275 < a ≤ 0.475	0	0.29	0	0.29	4.01
7	0.325 < a ≤ 0.475	0	0.14	0	0.14	3.01
8	0.375 < a ≤ 0.475	0	0.09	0	0.09	1.49
9	0.425 < a ≤ 0.475	0	0.05	0	0.05	1.00

D.5 Discussion and Summary

In this study, analysis of a base case of UT-detected weld-flaw data involving measurement (sizing) error for Beaver Valley 2 was performed. The base case was evaluated for interval flaw depths detected in the inspection volume specified in Supplement 4 to Mandatory Appendix VIII to Section XI of the ASME Code. Detected flaw-depth intervals were analyzed assuming lower UT detection limits of 0.04" and 0.075". Subsequently, twelve sensitivity cases were assessed based on variations in the assumed detected flaw-depth data (in the form of intervals), choices of considering VFLAW flaw depth and flaw densities as prior information (as opposed to no prior information), and choices of considering the POD (as opposed to perfect detection; i.e., no POD) were evaluated and compared to the base case as well as the Alternate PTS Rule flaw table limits. No sensitivities to the choice of the lower UT detection limit on the observed data were found.

The results obtained from the twelve sensitivity cases were consistent and showed that small overpopulations of flaws in Bins 2 and 3 of the Alternate PTS Rule flaw tables resulting from possible oversizing of small flaws would be shifted to Bins 1 and 2 after accounting for the measurement error in the Bayesian inference. When POD is considered, the effect of the missed small flaws was clearly seen in Bins 1 and 2 with an additional number of flaws in the posterior estimates as compared to the observed flaws.

The effects of the consideration and choice of the prior distributions of flaw density and depth were significant. When no prior information was used to describe the flaw-density and flaw-depth distributions, POD and measurement error were also sensitive and significantly amplified the number of flaws in Bins 1 and 2. However, when prior VFLAW PDFs were used, the posteriors were significantly moderated by the existence of the prior PDFs, and the POD and measurement errors played less significant roles.

If the approach documented in this appendix is used to reassess actual NDE flaws, it would be advisable to use informative or semi-informative prior estimates of the flaw depth and density distributions.

D.6 References

[D-1] Becker, F.L., “Reactor Pressure Vessel Inspection Reliability Based on Performance Demonstrations,” EPRI Report 1007984, June 22, 2004, Electric Power Research Institute, Palo Alto, CA.

[D-2] Georgiou, G.A., “Probability of Detection (PoD) Curves: Derivation, Applications and Limitations,” Research Report 454, UK Health & Safety Executive, London, UK, 2006.

[D-3] Li, M., and W. Q. Meeker, “A Noise Interference Model for Estimating Probability of Detection for Nondestructive Evaluations,” *Proceedings of the Review of Progress in Quantitative Nondestructive Evaluation, July 20–25, 2008, Chicago, IL*, American Institute of Physics, College Park, MD, 2009.

[D-4] U.S. Department of Defense, “Nondestructive Evaluation System Reliability Assessment,” MIL-HDBK-1823, April 30, 1999.

[D-5] Celeux, G., et al., “Using Markov Chain Monte Carlo Methods to Solve Full Bayesian Modeling of PWR Vessel Flaw Distributions,” *Reliability Engineering and System Safety*, 66(3):243–252, December 1999.

[D-6] Chatterjee, K., and M. Modarres, “A Probabilistic Approach for Estimating Defect Size and Density Considering Detection Uncertainties and Measurement Errors,” *Journal of Risk and Reliability*, 227(1):28–40, February 2013.

[D-7] Spanner, J., “Materials Reliability Program: Reanalysis of Reactor Vessel Examination Data from the 1996 Beaver Valley 2 Vessel Examination (MRP-207), RPV Flaw Distribution,” EPRI Report 1014548, November 2006, Electric Power Research Institute, Palo Alto, CA.

[D-8] U.S. Nuclear Regulatory Commission, “Probabilistic Fracture Mechanics - Models, Parameters, and Uncertainty Treatment Used in FAVOR Version 04.1,” NUREG-1807, June 2007, Agencywide Documents Access and Management System (ADAMS) Accession No. ML072010411.

NRC FORM 335 (12-2010) NRCMD 3.7 U.S. NUCLEAR REGULATORY COMMISSION **BIBLIOGRAPHIC DATA SHEET** *(See instructions on the reverse)*	1. REPORT NUMBER (Assigned by NRC, Add Vol., Supp., Rev., and Addendum Numbers, if any.) NUREG-2163 (DRAFT)
2. TITLE AND SUBTITLE Technical Basis for Regulatory Guidance on the Alternate Pressurized Thermal Shock Rule	3. DATE REPORT PUBLISHED MONTH: February YEAR: 2015 4. FIN OR GRANT NUMBER
5. AUTHOR(S) G. L. Stevens, M. T. Kirk, and M. Modarres	6. TYPE OF REPORT Technical 7. PERIOD COVERED (Inclusive Dates)

8. PERFORMING ORGANIZATION - NAME AND ADDRESS (If NRC, provide Division, Office or Region, U. S. Nuclear Regulatory Commission, and mailing address; if contractor, provide name and mailing address.)

Office of Nuclear Regulatory Research
Division of Engineering
U.S. Nuclear Regulatory Commission
Washington, DC 20555-0001

9. SPONSORING ORGANIZATION - NAME AND ADDRESS (If NRC, type "Same as above", if contractor, provide NRC Division, Office or Region, U. S. Nuclear Regulatory Commission, and mailing address.)

Same as above

10. SUPPLEMENTARY NOTES

11. ABSTRACT (200 words or less)

During plant operation, the walls of reactor pressure vessels (RPVs) are exposed to neutron radiation, resulting in embrittlement of the vessel steel and weld materials in the area of the RPV adjacent to the core. If an embrittled RPV had a flaw of critical size and certain severe system transients were to occur, the flaw could rapidly propagate through the vessel, resulting in a through wall crack and, thereby, challenging the integrity of the RPV. The severe transients of concern, known as pressurized thermal shock (PTS), are characterized by a rapid cooling of the internal RPV surface in combination with repressurization of the RPV. Advancements in understanding and knowledge of materials behavior, the ability to realistically model plant systems and operational characteristics, and the ability to better evaluate PTS transients to estimate loads on vessel walls led the U.S. Nuclear Regulatory Commission (NRC) to develop a risk informed revision of the existing PTS Rule that was published in Section 50.61a, "Alternate Fracture Toughness Requirements for Protection against Pressurized Thermal Shock Events," of Title 10, "Energy," of the Code of Federal Regulations (10 CFR 50.61a).

This report explains the basis for the requirements that establish the entry conditions to permit use of 10 CFR 50.61a and describes methods by which the following four requirements can be met: (1) criteria relating to the date of construction and design requirements, (2) criteria relating to evaluation of plant specific surveillance data, (3) criteria relating to inservice inspection (ISI) data and non destructive examination (NDE) requirements, and (4) criteria relating to alternate limits on embrittlement.

12. KEY WORDS/DESCRIPTORS (List words or phrases that will assist researchers in locating the report)	
pressurized thermal shock, probabilistic fracture mechanics, nuclear reactor pressure vessel, pressurized water reactor	13 AVAILABILITY STATEMENT: unlimited 14 SECURITY CLASSIFICATION *(This Page)* unclassified *(This Report)* unclassified 15. NUMBER OF PAGES 16. PRICE

NRC FORM 335 (12-2010)

Printed on recycled paper

Federal Recycling Program

NUREG-2163
Draft

Technical Basis for Regulatory Guidance on the Alternate Pressurized Thermal Shock Rule

February 2015